[redacted]
(CLASSIFICATION)

DECLASSIFIED

GENERAL ELECTRIC

HANFORD ATOMIC PRODUCTS OPERATION - RICHLAND, WASHINGTON

HW-76206 RD

SERIES AND COPY NO. [redacted]

DATE January 25, 1963

[X] [redacted]STRICTED DATA

THIS DOCUMENT CONTAINS RESTRICTED DATA AS DEFINED IN THE ATOMIC ENERGY ACT OF 1954. ITS TRANSMITTAL OR THE DISCLOSURE OF ITS CONTENTS IN ANY MANNER TO AN UNAUTHORIZED PERSON IS PROHIBITED.

TITLE

DRAFT OF
PHYSICS SECTIONS
TO 100-N TECHNICAL MANUAL

[ ] OTHER OFFICIAL CLASSIFIED INFORMATION

THIS MATERIAL CONTAINS INFORMATION AFFECTING THE NATIONAL DEFENSE OF THE UNITED STATES WITHIN THE MEANING OF THE ESPIONAGE LAWS, TITLE 18, U.S.C., SECS. 793 AND 794, THE TRANSMISSION OR REVELATION OF WHICH IN ANY MANNER TO AN UNAUTHORIZED PERSON IS PROHIBITED BY LAW.

AUTHOR

COMPILED BY

R. NILSON

ISSUING FILE

CIRCULATING COPY
RECEIVED 100 D AREA
FEB 4 1963
RETURN TO
TECHNICAL INFORMATION FILES

THIS DOCUMENT [redacted] BE LEFT UNATTENDED OR [redacted] UNAUTHORIZED PERSON MAY HAVE ACCESS TO IT. WHEN NOT IN USE, IT MUST BE STORED IN AN APPROVED LOCKED REPOSITORY OR UNDER APPROVED GUARD. WHILE IT IS YOUR POSSESSION AND UNTIL YOU HAVE OBTAINED A SIGNED RECEIPT FROM OUR CENTRAL FILES, IT IS YOUR RESPONSIBILITY TO KEEP IT AND ITS CONTENTS WITHIN THE LIMITS OF THIS PROJECT AND FROM ANY UNAUTHORIZED PERSON. ITS TRANSMITTAL AND STORAGE AT YOUR PLACE OF RESIDENCE IS PROHIBITED. IT IS NOT TO BE DUPLICATED. ADDITIONAL COPIES, IF REQUIRED, OBTAIN THEM FROM THE ORIGINATED ISSUING FILE. ALL PERSONS READING THIS DOCUMENT ARE REQUESTED TO SIGN IN THE SPACE PROVIDED BELOW.

ROUTE TO:	PAYROLL NO.	LOCATION	FILES ROUTE DATE	SIGNATURE AND DATE
McLaurin	14153	100 N	FEB 5 1963	McL 8/29
R L Dickeman				
McL				
R A [redacted]	13293	326	SEP 6 1963	

DECLASSIFIED

DISCLAIMER

ument consists of
ges.

Distribution

1. R. E. Hall
2. P. F. Gast
3. P. F. Nichols
4. W. S. Nechodom
5. M. C. Leverett
6-10. R. Nilson

DRAFT OF PHYSICS SECTIONS TO 100-N TECHNICAL MANUAL

This document classified by:

DRAFT - PHYSICS SECTION OF 100-N
TECHNICAL MANUAL VOL. 1

The information presented here is a collection of most of the physics information available at this time for the New Production Reactor. The details of some of the physics information, particularly those dealing with exposure and temperature effects, are by no means to be considered the final word since there has been no experimental verification of these effects. However, the gross physics characteristics described are felt to be reasonable representations of the expected physics behavior of N Reactor and should serve as useful guides throughout the startup planning and initial operation. As actual operating transients and other operating data such as control rod calculations, etc., are obtained the information presented here should be supplanted.

The work which is presented here represents the effort of many people both indirectly and directly. The experimental physics results have been obtained in the Reactor Lattice Physics Operation under R. E. Heineman and in the Critical Mass Physics Operation under E. D. Clayton. Principal investigators have been D. E. Wood, D. L. Johnson, R. I. Smith, G. W. R. Endres, R. C. Lloyd and C. L. Brown. Analytical support has been obtained from the Theoretical Physics Operation under J. L. Carter and analog computational services have been obtained from the Systems Research Operation under R. A. Harvey. The above groups and people are in the Hanford Laboratory.

In the Irradiation Processing Department the Analytical physics work has been carried out in the Design Analysis Unit under D. L. Condotta, in the Operational Physics Subsection under G. C. Fullmer and in the Reactor Physics Unit under R. Nilson. Principle investigators have been D. E. Simpson, G. F. Bailey, C. E. Bowers, C. D. Wilkinson, C. W. Allen, W. A. Blyckert, W. S. Nechodom, R. E. Tiller, R. H. Meichle, J. C Peden, D. K. McDaniels and R. Nilson.

Indirect assistance has been obtained through the use of IBM-7090 programs of R. O. Gumprecht, R. J. Shields, C. R. Richey, D. Matsumoto, and D. L. Johnson. Also, considerable indirect assistance has been obtained from physics work at other sites. A referral to the list of references at the close of the draft will indicate the principle sources of information.

Several of the figures in this draft are not included. The reason for this is that they are identical to figures presently included in the second volume of the N-Reactor Hazards Report, HW-71408 VOL2. Where this has been done the appropriate figure is so referenced.

R Nilson
1-28-63

OUTLINE AND INDEX
PHYSICS SECTION
N-REACTOR TECHNICAL
MANUAL

	Page
1. Basic Physics Processes	6
2. Lattice Physics	7
2.1 Description of the Lattice	7
2.2 Lattice Physics (General)	7
2.3 Nuclear Properties of Reactor Materials	9
2.3.1 Material Densities and Atomic Weights	9
2.3.2 Cross Sections and Nuclear Constants	10
2.3.2.1 Thermal and Near-Thermal Cross Sections	10
2.3.2.2 Fast Neutron Cross Sections	12
2.3.2.3 Resonance Integrals	13
2.3.2.4 Other Nuclear Constants	15
2.4 Neutron Spectrum	16
2.4.1 Thermal Flux Spectrum	16
2.4.1.1 Correction for Absorbing Medium	17
2.4.1.2 Multiple Moderators	18
2.4.2 Epithermal Flux Spectrum	19
2.4.3 Fast Neutron Spectrum	21
2.5 Lattice Parameters (Theoretical)	22
2.5.1 Reproduction Factor, η	22
2.5.2 Fast Effect, ϵ	22
2.5.3 Resonance Escape Probability, p	24
2.5.4 Thermal Utilization, f	25
2.6 Lattice Parameters (Experimental)	26
2.6.1 PCTR Measurements	26
2.6.2 Exponential Pile Measurements	26
2.6.3 "Best-Value" Lattice Parameters	26
2.7 Cell Flux Distributions	31
3. Core Physics	32
3.1 Introduction	32
3.2 Description of Core and Reflector	33
3.3 Slowing Down and Diffusion of Neutrons	33
3.3.1 Fermi Age	33
3.3.2 Diffusion Area	35
3.3.3 Migration Area	36
3.4 Neutron Streaming	36
3.5 Neutron Leakage, k_{eff}	37
3.6 Core Power Distribution	38
4. Estimation of Effects of Lattice Changes	42
4.1 Changes Uniform Over the Reactor	42
4.1.1 Fuel Element Changes	42
4.1.2 Enrichment Variation	43
4.1.3 Impurities in Fuel	43
4.1.4 Reactor Atmosphere	43

4.2 Non-Uniform Changes 43
4.2.1 Reactivity Effect of Natural Uranium Fuel 45
4.2.2 Reactivity Effect of Empty Process Tubes 46
4.2.3 Reactivity Effect of Water-Filled Process Tubes 46
4.2.4 Reactivity Effect of Foreign Material in Process Tubes 46
5. Reactor Products 46
5.1 Introduction 46
5.2 Plutonium Production 46
5.3 Neptunium Production 47
5.4 Tritium Production 47
5.5 Fission Products 48
5.6 Calculation of Nuclear Reactions 48
5.6.1 Flux 48
5.6.2 Plutonium Buildup and U^{235} Burnout Calculations 49
5.6.3 Neptunium Production Calculations 52
5.6.4 Fission Products (Useful) 55
5.6.5 Tritium Production Calculations 56
5.7 Production Yields 57
5.7.1 Plutonium Buildup and U^{235} Burnout 57
5.7.2 U^{236} and Np^{237} Buildup 60
5.7.3 Useful Fission Product Yields 60
5.8 Reactor Weighting for Production 60
6. Reactivity Transients 67
6.1 Introduction 67
6.2 Temperature Coefficients of Reactivity 67
6.2.1 Graphite Temperature Coefficient of Reactivity 69
6.2.2 Coolant Temperature Coefficient of Reactivity 71
6.2.3 Doppler Coefficient of Reactivity 77
6.2.4 Operating Reactor Temperature Coefficients 78
6.3 Exposure-Dependent Effects 83
6.3.1 Long Term Gain (Cold) 83
6.3.2 Xenon Poisoning 83
6.3.3 Samarium Poisoning 83
6.3.4 Neptunium Holdup 83
6.3.5 Over-all Long Term Reactivity Effects 86
6.4 Over-all Reactivity Changes 86
6.5 Operational Reactivity Transients 88
6.5.1 Reactor Startup Transients 88
6.5.2 Normal Shutdown Transient 88
6.5.3 Scram Transient 93
6.6 Accidental Reactivity Changes 93
6.6.1 Loss-of-Coolant Reactivity Effect 93
6.6.2 Lattice Flooding 93
6.6.3 Cold Water Reactivity Effect 94
7. Reactor Control 94
7.1 Introduction 94
7.2 Control Philosophy 94
7.2.1 Operational Control Criteria 95
7.2.2 Safety Control Criteria 95
7.2.3 Backup Philosophy 95

	Page
7.3 Horizontal Control Rods	96
7.3.1 Control Strengths	96
7.3.2 Maximum Worth of Single Rods or Group of Rods	97
7.3.3 Stuck Rod Limit	97
7.4 Ball 3X System	98
7.4.1 Control Strengths	98
7.4.2 Inoperable Ball Column Limit	98
7.5 Total Control Considerations	99
7.6 Speed-of-Control Considerations	99
7.6.1 Reactivity Sources	101
7.6.1.1 Control Rod Withdrawal	102
7.6.1.2 Cold Water Addition	102
7.6.1.3 Core Flooding	102
7.6.1.4 Summary of Reactivity Ramps	103
7.6.2 Excursion With Scram	103
7.7 Ultimate Shutdown Mechanism	112
7.8 Reactor Kinetics	112
7.9 Xenon Oscillations	118
7.10 System Stability	121
8. Criticality	121
8.1 Criteria For Safe Storage	122
8.2 Basic Data	122
8.3 Procedures and Safeguards	123
9. Heat Generation	124
9.1 Equilibrium Heat Generation (Total)	124
9.1.1 Energy Sources	124
9.2 Equilibrium Heat Generation (Fractional)	125
9.2.1 Heat Generation in Fuel	125
9.2.2 Heat Generation in Process Tube	129
9.2.3 Heat Generation in Graphite Moderator	129
9.2.4 Summary of Heat Generation Fraction	129
9.3 Shutdown Heat Generation	129
9.3.1 Shutdown Heat Generation Transient	130
9.3.1.1 Assumptions on Model	130
9.3.2 Heat Generation After Shutdown (Total)	130
9.3.3 Heat Generation After Shutdown (Fractional)	134

DRAFT OF PHYSICS SECTIONS TO 100-N TECHNICAL MANUAL

N Reactor is a graphite-moderated, water-cooled thermal reactor of the Hanford type. It differs somewhat from the earlier reactors, principally in moderator-to-fuel ratio, enrichment and operating conditions. The physics discussion will be limited to the Phase I operation (plutonium production only) of N Reactor.

1. Basic Physics Processes

Like the other Hanford reactors, N Reactor is a converter – the principal nuclear processes being the transmutation of U^{238} to Pu^{239} and the fissioning of U^{235} to provide the neutron carriers of the chain reaction and the neutrons necessary for the plutonium production. These reactions are as follows:

$$U^{238} \ (n,\gamma) \ U^{239} \xrightarrow{\beta^-} Np^{239} \xrightarrow{\beta^-} Pu^{239}, \qquad (1.1)$$

$$U^{235} \ (n, f) \ FP + Q. \qquad (1.2)$$

Q is the heat of fission of about 202 Mev.

The conversion reaction (1.1) goes for all neutron energies from fission energies down to the thermal energies. The major fraction of plutonium production is by thermal neutrons with most of the remaining by resonance neutrons. (The production by fast neutrons is only on the order of one per cent.) The fission reaction in U^{235} is also possible at all neutron energies, but in N Reactor is predominantly a thermal neutron reaction.

Fission neutrons are born in the reactor fuel with an average energy of two Mev. To be useful, then, as chain carriers, they must be slowed down to thermal energies. The principal slowing down process for neutrons in a thermal reactor is by elastic scattering with the nuclei of the reactor's moderator. In N Reactor, the chief moderator is graphite with the cooling water also contributing to the moderating process.

N Reactor is a hetereogeneous reactor; that is, its fuel and moderator are separated into discrete volumes. The lumping of the uranium is necessary to overcome excessive losses of neutrons to resonance capture. The resonance capture probability in N Reactor, in spite of the lumping of the fuel, is approximately 0.17 which is higher than in the older Hanford reactors ($\sim$0.12). The principal reason for the higher resonance capture probability is the undermoderated nature of the N lattice. The C-U atom ratio, for example, is 33; this can be compared to a ratio of 75 for the K Reactors. A brief explanation of the relationship between the degree of moderation and the degree of resonance capture follows.

In an operating reactor, an equilibrium is established between the appearance and removal of neutrons at each energy over the entire energy spectrum of neutrons in the reactor. The chief processes accounting for the removal of neutrons from a particular energy interval ΔE are elastic scattering by moderator atoms (moderation effect) and absorption. Secondary processes include inelastic scattering and leakage. In a well-moderated reactor, for example the original Hanford reactors, there is an excess of moderator material over that needed for optimum reactivity. The high C-U ratio provides a highly-efficient slowing down ability for the lattice which in turn reduces the availability of the neutrons for resonance capture. On the other hand, a low C/U lattice (such as N Reactor) has less than enough moderator to be an optimum lattice insofar as reactivity is concerned, and has a much-lowered slowing down ability which in turn increases the availability of neutrons for resonance capture.

Since the predominant resonance neutron absorber in the Hanford-type reactors (including N) is U^{238}, the importance of resonance absorption is apparent. Unlike reactivity, which has a definite optimum, the absorption of neutrons in U^{238} continues to increase as the C-U ratio is decreased. As the point of optimum reactivity is passed in the lowering of the C-U ratio, a chain reaction becomes impossible in a graphite-moderated reactor fueled with natural uranium. In the case of N Reactor, uranium enriched to 0.947 w/o U^{235} is required to sustain the chain reaction. The increased amount of U^{235} present decreases the plutonium produced from thermal neutron absorption in U^{238}, but the decrease is not enough to overcome the increased resonance production.

An important feature of the undermoderated reactor, quite apart from its better over-all neutron economy, is the fact that the lattice is fail-safe upon loss of coolant. Water, which acts as both a moderator and a neutron poison, is worth more as a moderator in N Reactor and hence its removal reduces the moderating efficiency of the reactor and increases the resonance capture probability. (The resonance capture probability in the dry N lattice is ~ 0.25.)

Related to the fail-safeness of the lattice on coolant loss is the converse effect of increasing the amount of water in the reactor. Either a cold water insertion at reactor equilibrium level (which would increase the coolant density and hence the amount of water in the process tubes) or flooding of the graphite structure can add reactivity.

The relative reaction rates which go on in any nuclear reactor are functions of the concentrations present of each material, the temperatures of these materials and the average energy (temperature) of the neutrons. The dynamic equilibrium among the various competitive nuclear reactions will therefore change as new materials are formed (fission products and transuranic elements, for example) and as the reactor is brought up from a cold shutdown condition to equilibrium temperature. These temperature- and exposure-dependent effects are very important and their consideration must be taken into account in the reactor and fuel design. Sufficient reactivity must be available over all of the useful reactor operating cycle and, as well, too much reactivity must be avoided from a control standpoint. The principal operating reactivity effects are those associated with the buildup of fission products Xe^{135} and Sm^{149}, and heating of moderator, coolant and uranium. These are all discussed in later sections.

2. Lattice Physics

The physics associated with a unit lattice cell is a convenient and useful means of describing the reactor physics of a large thermal reactor. In this section, the reactor will be assumed to be infinite in extent and each lattice cell therefore is one of an infinite set of identical cells. The modifications to such a model are discussed in the next section on core physics.

2.1 Description of the Lattice

The N-Reactor lattice is rectangular; the vertical spacing is nine inches and the horizontal spacing is eight inches. The process tubes are nominal quarter-inch wall, Zircalloy-2, 2.7-inch I.D. tubes. The startup fuel elements are concentric tubes of metallic uranium enriched to 0.947 w/o U^{235}. The fuel clad is Zircalloy-2. Additional lattice dimensions are given in Table 2.1.1 and a cross sectional view of the lattice is shown in Figure 2.1.1. (See Figure C-1 of HW-71408 VOL2.)

Table 2.1.1
Lattice Dimensions

Spacing	8" horizontal x 9" vertical	
Equivalent Cell Diameter	9.575"	
Fuel Element (Inches)	Outer	Inner
O.D. Clad	2.406"	1.249"
O.D. Fuel	2.354	1.167
I.D. Clad	1.764	0.438
I.D. Fuel	1.816	0.490
Process Tubes (Inches)		
O.D.	3.258"	
I.D.	2.708	

The process tubes pierce the reactor core front-to-rear. A graphite coolant system composed of 640, Zircalloy-2 tubes runs side to side in every filler layer vertically and on 16-inch centers horizontally. These tubes are 0.75 inches O.D.

2.2 Lattice Physics (General)

The neutron spectrum in N Reactor is less thermal than in the older Hanford reactors. A question thus arises in the use of the classical Fermi picture of the neutron cycle. In spite of this, the familiar, Fermi, four-factor formula for the multiplication factor of an infinite lattice is assumed valid for N Reactor and appropriate modifications are made in the definitions to insure that all neutronic processes are properly accounted for. The Fermi formula is

Figure 2.1.1 is a cross section of an N lattice cell and is identical to Figure C-1 in HW-71408 VOL2.

$$k_{\infty} = \eta \epsilon p f, \qquad (2.2.1)$$

where k_{∞} is the infinite multiplication factor and is defined as the ratio of neutrons in the (n + 1) th generation to those in the nth generation. A k_{∞} of unity implies a constant neutron population, a $k_{\infty} > 1$ implies an increasing neutron population, and a $k_{\infty} < 1$ implies a decreasing neutron population. The lifetime of a neutron generation in a reactor is usually taken as the average time between birth in fission and death as a thermal neutron. Capture and leakage processes taking place as the neutrons slow down do not appreciably alter the lifetime in a thermal reactor.

The constant η in 2.2.1 is the reproduction factor and is defined as the number of neutrons produced by thermal fission for each neutron absorbed in the fuel (exclusive of those captured in U^{238} resonances). The constant ϵ is the fast fission factor and it accounts for fast fission in U^{238}. The fast fission factor is defined as the number of neutrons making their first collision with moderator external to the fuel element per neutron arising from thermal fission. The parameter p is the resonance escape probability and describes the probability a neutron will escape resonance capture as it slows down to thermal energies. In the formulation used, only resonance capture in U^{238} is considered in determining p and then only the true resonance captures. The 1/v-law captures are accounted for elsewhere (in f and η). The parameter f is the "thermal" utilization and is defined as the fraction of thermal and all 1/v-law absorptions (up to ~ 100 kev neutron energy) occurring in the uranium. Westcott cross sections must be used in the calculation of f and η to be consistent with these definitions. (These cross sections are described in Section 2.3.2.1).

2.3 Nuclear Properties of Reactor Materials

In a heterogeneous reactor such as N Reactor, various materials, other than fuel and moderator, are required to give structural support, transport coolant, support the fuel elements and contain the fuel. Materials are critical from both a physical standpoint (resistance to corrosion, strength, heat transfer properties, etc.) and a nuclear standpoint (neutron absorption cross section, resistance to radiation damage, etc.).

The physics of nuclear reactors deals primarily with the competitive nuclear reactions which take place in the reactor. In order to determine the important reaction rates, it is necessary to know the nuclear properties of the various reactor materials. Of importance in this regard, are 1) the neutron cross sections, 2) the material densities and atomic weights, 3) the number of neutrons released per fission, 4) the parameters describing the moderating ability of the materials (principally the moderators), 5) the angular distributions of neutrons scattered from the atoms of the various materials, etc. These properties are discussed in the following sections.

2.3.1 Material Densities and Atomic Weights

The densities, atomic or molecular weights, and nuclear densities of the principal reactor materials are listed in Table 2.3.1.1 at room temperature (20 C) and for operating reactor conditions.

Table 2.3.1.1

Physical Properties of N-Reactor Materials[a]

Material	Atomic or Mol. Wt.	Density gm/cm^3 20 C	Density gm/cm^3 Operating	Nuclear Density Nuclei/cm^3 (20 C)
H_2O	18.016	1.00	0.822 - 0.835	3.35×10^{22}[b]
C	12.011	1.71	1.71	8.58×10^{22}
Zr-2	91.22	6.4	6.4	4.23×10^{22}
U	238.07	18.9	18.66	4.783×10^{22}

a Special control materials such as Sm_2O_3, B_4C etc. are listed elsewhere
b Molecules/cm^3

2.3.2 Cross Sections and Nuclear Constants

The appropriate cross sections for the nuclear reactions taking place in a reactor are dependent on the particular neutron accounting procedure employed in the reactor physics calculations. The usual Hanford procedure is to calculate the effective multiplication factor of the reactor via the well-known Fermi four factor formula. (Section 2.2)

2.3.2.1 Thermal and Near-Thermal Cross Sections

Since most of the nuclear reactions in N Reactor occur at thermal or near-thermal neutron energies, the most important cross sections are those at these energies. The Westcott[1] formulation is particularly useful since it defines an effective cross section for a material which when multiplied by the proper flux gives the total reaction rate over the entire thermal and slowing-down neutron spectrum. The flux employed is nv_o where v_o is 2200 m/s (the velocity of neutrons corresponding to a neutron temperature of 20 C) and n is the total neutron density (integrated over all energies).

The Westcott cross section is an approximation and is most accurate for very thermal reactors – those which have a spectral index, r, of 0.1 or less. The spectral index for N Reactor is $\sim$ 0.11, hot.

The spectrum assumed in deriving the Westcott cross sections is a simple Maxwellian thermal distribution joined by an appropriate joining function to a 1/E slowing-down spectrum. The spectral index, r, is defined as the ratio of epithermal neutrons (in one logarithmic decrement) to the thermal neutrons in the Maxwellian distribution. (See Section 2.4)

The Westcott cross sections contain factors which correct for the non-1/v-ness of the cross sections both in the thermal and epithermal energy ranges. The cross section is defined by

[redacted]

$$\hat{\sigma} = \sigma_o (g + rs), \qquad (2.3.2.1.1)$$

where

σ_o = 2200 m/s value of cross section,

g = factor correcting for non-1/v behavior of the cross section where integrated over a Maxwellian distribution,

s = corresponding non-1/v correction factor for epithermal neutron spectrum.

The cross sections have been derived by Westcott for several reactor materials. Only fission and capture cross sections are considered. Scattering cross sections usually change so slowly with energy that they may be treated separately.

The non-1/v correction factors are functions of neutron energy (or temperature). Tables giving these factors are given in Reference 1. A convenient characteristic of the Westcott cross sections is that if the actual cross section is 1/v, the factors g = 1 and s = 0. Hence, for a 1/v absorber

$$\hat{\sigma} = \sigma_o . \qquad (2.3.2.1.2)$$

In reactor calculations, graphite, water, zirconium and U^{238} can be treated as 1/v absorbers. Resonance capture in U^{238} is accounted for in the calculation of p, the resonance escape probability, thus the resonances need not be considered in the determination of the Westcott cross section for U^{238}.

The Westcott cross sections can be thought of as the cross section of an equivalent 1/v-law absorber. That is multiplying the Westcott cross section, $\hat{\sigma}$, by the total neutron density times v_o gives the same reaction rate that a 1/v absorber would give with $\sigma_o = \hat{\sigma}$.

It is often convenient to have an expression for the cross section which will give the proper reaction rate in the true flux, rather than in the artificial flux nv_o.

The expression

$$\bar{\sigma} = \sqrt{\frac{\pi T_o}{4T}}\,\hat{\sigma} , \qquad (2.3.2.1.3)$$

can be used to deduce average cross section for pure thermal spectra; T_o, being the absolute neutron temperature for 2200 m/s neutrons; T, the actual neutron temperature; and $\pi/4$, the constant resulting from averaging over a Maxwellian distribution. For the actual reactor spectrum, 2.3.2.1.3 is often used, but is a poor approximation if the epithermal term σ_o rs of the cross section is large.

Theoretical spectral indices and neutron temperatures for the N Reactor fuel element are given in Table 2.3.2.1.1 for equilibrium condition

Table 2.3.2.1.1

N Reactor Spectrum Constants (Equilibrium)

	Inner Fuel Tube	Outer Fuel Tube
Spectral Index, r	~ 0.130	~0.10
Neutron Temperature (^oK)	~ 610	~ 645

2.3.2.2 Fast Neutron Cross Sections

In the neutron accounting procedure, it is useful to treat reactions above 100 kev neutron energy separately from the rest. Usually, the cross sections in this energy range are so small compared to the thermal and resonance energy cross sections that the fast reactions can be ignored insofar as any measurable effect on the neutron balance. An exception exists and this deals with the fact that fast fission (predominantly in U^{238}) occurs at a sufficient rate to materially affect the multiplication factor (see Section 2.5.2)

Fast neutron cross sections are usually important for only materials inside the fuel element or in close proximity to the fuel element. The fission neutron energy spectrum is given by[2]

$$N_f(E) = 1.096 \exp(-E/0.965) \sinh \sqrt{2.29E}, \qquad (2.3.2.2.1)$$

and the fast cross sections are usually averaged over such a spectrum.

A compilation of fast neutron cross sections from Reference 3 which are useful in calculating the fast fission factor is given in Table 2.3.2.2.1.

Table 2.3.2.2.1

Fast Three-Group Cross Sections for U^{238}[3]

5367
5528

	Group A	Group B	Group C
ν	2.845	0	0
σ_f	0.549 b	0	0
σ_{et}	1.89 b	5.91 b	5.33 b
σ_i	2.07 b	- -	- -
σ_c	0.032 b	0.138 b	0.135 b
σ_t	4.541 b	6.05 b	5.66 b

The groupings are defined in Section 2.5.2.

The cross sections are defined as follows: σ_f is the fission cross section, σ_{et} is the elastic transport cross section (the scattered neutron remains in the group), σ_i is the inelastic scattering cross section (the scattered neutron goes into group C), σ_c is the capture cross section and $\sigma_t = \sigma_f + \sigma_c + \sigma_{et} + \sigma_i$.

2.3.2.3 Resonance Integrals

The only dominant resonance absorber in a reactor such as N is U^{238}. Resonance absorption also occurs in the other heavy isotopes but their concentration is small enough that the reactions can be handled by using the Westcott cross sections. The most convenient manner of treating the resonance absorptions in U^{238} is through, p, the resonance escape probability. The calculation of p involves a knowledge of the resonance integral for U^{238}, which is a complicated function of the fuel geometry.

The resonance integral for the N-Reactor fuel geometry is based on the measured integrals of Hellstrand[4]. Although, Hellstrand's work was confined to rods and single tubes with a D_2O moderator and coolant, his results have been extended in an approximate fashion to the N Reactor case of H_2O coolant and graphite moderator.

Hellstrand's latest expression for the resonance integral of U^{238} over a S/M range of 0.07 to 0.25 (where S/M is the surface-to-mass ratio of the fuel element) is

$$RI = 2.95 + 25.8 \sqrt{S/M} \quad . \qquad (2.3.2.3.1)$$

The expression 2.3.2.3.1 can be written also in the form

$$RI = \frac{6.4}{F} + 273 \left[1 - \exp\left(-(S/M)/5.3\right) \right] , \qquad (2.3.2.3.2)$$

which converges to an infinite-dilution value of 279.4 barns when $S/M \rightarrow \infty$ and $F \rightarrow 1$. F is the disadvantage factor of the element for resonance energy neutrons.

The effective surface, S_{eff}, which is to be used in calculating the surface-to-mass ratio for the N-Reactor fuel element is complicated by the presence of moderating material (water) within the fuel element. An effective surface can be computed.

$$S_{eff} = S_o + \sum_{i=1}^{3} \gamma_i S_i, \qquad (2.3.2.3.3)$$

where S_o is the outer surface of the outer tube of the fuel and the S_i are the three inner fuel surfaces. The constants γ_i are weighting factors which give the relative worths of the inner surfaces.

A very simple set of relations for the γ i's has been derive in much the same fashion that Hellstrand used to correlate his measurements on hollow tubes filled with D_2O. If the indices 1, 2, and 3 describe the outer-tube inner surface, the inner-tube outer surface, and the inner-tube inner surface, respectively

$$\gamma_1 = 4(V/S)\Sigma_s P_1,$$

$$\gamma_2 = 4(V/S)\Sigma_s P_2, \text{ and}$$

$$\gamma_3 = 4(V_3/S_3)\Sigma_s P_3, \text{ where} \qquad (2.3.2.3.4)$$

$$S = S_1 + S_2,$$

$$V = \frac{1}{4\pi} (S_1^2 - S_2^2),$$

$$V_3 = \frac{S_3^2}{4\pi}, \text{ and}$$

Σ_s = macroscopic scattering cross section of water for resonance energy neutrons.

The P's are probabilities that resonance neutrons originating in the inner coolant regions will appear at the appropriate surfaces without suffering a collision with a water molecule. P_1 is the probability of appearing at surface S_1, P_2 at S_2, etc. These escape probabilities have been derived and appear in Reference 5. They are also built into the p-subroutine of the FLEX and MOFDA IBM-7090 programs[6].

2.3.3.4 Other Nuclear Constants

The average number of neutrons released per fission varies among fissionable isotopes and also is a function of the energy of the fission-initiating neutron. The thermal values of ν for predominantly thermal-fissioning isotopes are given in Table 2.3.2.4.1. The value given for U^{238} is averaged over a fission energy neutron spectrum (Reference 5).

Table 2.3.2.4.1

Neutrons Released Per Fission

U^{235}	2.43
Pu^{239}	2.88
Pu^{241}	3.06
U^{238}	2.85

The average logarithmic energy change of a neutron per collision can be determined for isotropic scattering in the center-of-mass coordinate system as a function of the atomic mass of scatterer, A.

$$\xi = \overline{\ln \frac{E_2}{E_1}} = \frac{2}{A + 2/3} \quad \text{for } A > 10,$$

$$\xi = 1 + \left[(A-1)^2/2A\right] \ln\left[(A-1)/(A+1)\right] \quad \text{for } A < 10. \quad (2.3.2.4.1)$$

For high energy neutrons, where p-waver or higher order scattering can occur, the above formulation for ξ is not valid. This will only be a problem in carbon or oxygen, since n-p scattering is isotropic to very high energies. Likewise, at low neutron energies, where molecular binding or lattice effects become important, the above formulas for ξ are not valid. However, for most of the neutron energy range which is of interest in reactor calculations, the simple A-dependent expressions are ξ are satisfactory.

Values of ξ for the important reactor materials are given in Table 2.3.2.4.2.

Table 2.3.2.4.2.

	ξ	μ_o
H_2O	0.948	0.324
C	0.158	0.0556
Zr	0.0218	0.0073
U	0.0084	0.0028

Although neutron scattering is isotropic in the center-of-mass coordinate system for most materials, and over most of the pertinent energy range of reactor neutrons, the scattering distribution is peaked forward in the laboratory frame of reference due to the motion of the neutron. The laboratory angle between the directions of motion of a neutron before and after scattering (for isotropic c.m. scattering) can also be expressed as a simple function of atomic mass. Of most use is the average cosine of the scattering angle.

$$\mu_o = \overline{\cos \theta} = 2/(3A). \qquad (2.3.2.4.2)$$

Values of μ_o for the reactor materials are listed in Table 2.3.2.4.2. It is seen that only for the ligher materials does the scattering have a pronounced forward peaking, i.e., $\mu_o \ll 1$.

2.4 Neutron Spectrum

The energy spectrum of reactor neutrons covers a range from fission energies (as high as 10 Mev) to thermal energies (fraction of an ev). To describe the spectrum with any accuracy in a hetereogeneous reactor is beyond present means. However, certain simplified characteristics are known with sufficient accuracy to permit useful calculations.

2.4.1 Thermal Flux Spectrum

Since most of the reactions in a thermal reactor occur at thermal or near thermal energies, a description of the energy spectrum for neutrons at these energies is of most importantance. The simplest model assumes that the neutrons reach an energy distribution in equilibrium with the moderator atoms. That is, if the moderator has an absolute temperature, T, the thermal neutrons have a speed distribution which follows Maxwell's gas law.

$$n(v) = n_o A v^2 \exp(-mv^2/2kT), \qquad (2.4.1.1)$$

where n_o is the total number of thermal neutrons per cubic centimeter and A is defined as

$$A = 4\pi \left(\frac{m}{2\pi kT}\right)^{3/2}. \qquad (2.4.1.2)$$

The mass m is the neutron mass.

The Maxwellian spectrum is not exact one for many reasons:

1) It is valid for a homogeneous non-absorbing medium,

2) It does not take into account the moderating effect of more than moderator,

3) It ignores the contribution from neutrons still slowing down.

Each of these practical aspects is discussed in turn.

2.4.1.1 Correction for Absorbing Medium

The thermal neutron distribution will be changed from the pure Maxwellian due to neutron absorption in the medium. The work of Conveyou, Bate and Osborn[7] has been useful in this respect. Using a Monte-Carlo technique, they computed thermal neutron spectra for an infinite capturing medium. The calculations were carried out for a uniform medium of unbound nuclei of constant scattering cross section and 1/v absorption cross section. It was assumed that the scattering nuclei were distributed according to a Maxwell distribution at temperature T and that neutrons were introduced into the system from a monoenergetic source. Their results indicate that the actual spectrum is peaked above that determined from Maxwell's law and the following linear relation holds.

$$T_n = T\,(1 + 1.11\,AK), \qquad (2.4.1.1.1)$$

where T_n is defined as an effective neutron temperature (the temperature which when used in 2.4.1.1 gives the best least-squares fit of a Maxwell distribution to the Monte-Carlo computed flux distribution), T is the moderator temperature in ^oK, A is the moderator mass number and K is defined as

$$K = \left(\frac{2\,T_o}{3\,T}\right)^{1/2} \left(\frac{Na}{N_s}\right) \frac{\sigma_a\,(T_o)}{\sigma_s}, \qquad (2.4.1.1.2)$$

where

T_o = 293 K,

N_a = nuclear density of absorbers,

N_s = nuclear density of scatterers,

σ_a = absorber cross section, and

σ_s = scatterer cross section.

The Conveyou etal expression for the effective neutron temperature is only an approximation in the N lattice since the lattice is far from a uniform medium.

2.4.1.2 Multiple Moderators

The moderating effect of the process cooling water in N Reactor is significant. The effective neutron temperature in the fuel is at about 200 K lower than in the graphite due to the neutron cooling effect of the water.

There is nc simple way to take into consideration the combined absorption and scattering effects of the various materials in the N lattice. A scheme used in the FLEX code considers both the absorptive effects on the neutron temperature and the moderating effects of water and graphite. A neutron temperature is thus determined for each region of the lattice cell. Typical values computed in this manner are given in Table 2.4.1.2.1 for equilibrium N-Reactor conditions. The neutron temperatures are probably accurate to within ± 50 K. (See also Table 2.7.1).

Table 2.4.1.2.1

Neutron Temperatures - N Lattice-Equilibrium

Region	Physical Temperature °C[a]	Neutron Temperature °K[a]
Graphite	550	790
Process Tube	262	675
Water	228 - 238	540 - 600
Outer Fuel	364	645
Inner Fuel	402	610

a Temperatures quoted are those which would be important from reactivity considerations - in other words flux-squared weighted, pile average values. Simple volume-average temperatures would be lower and peak temperatures higher.

[redacted]

2.4.2 Epithermal Flux Spectrum

Neutrons above thermal energies constitute a flux that is best described by a distribution function e.g., the flux per unit range of energy. The number of neutrons in a range dE at energy E (speed v) is $n(E)dE$ and the corresponding flux is $\phi(E)dE = n(E)\, v(E)dE$. In the region from about 1 ev to 100 kev, the distribution function is assumed to be inversely proportional to the energy. For the special case where all nuclei are pure scatterers,

$$\phi(E) = \frac{q_T}{\bar{\xi}\, \Sigma_s\, E}\,, \qquad (2.4.2.1)$$

where q_T is the total fission neutron emission rate per unit volume, Σ_s is the volume-weighted sum of all macroscopic scattering cross sections.

$$\Sigma_s = \frac{1}{V_T} \sum_{i=1}^{N} \Sigma_{si}\, V_i, \text{ and} \qquad (2.4.2.2)$$

$\bar{\xi}$ is the average logarithmic decrement

$$\bar{\xi} = \frac{1}{\Sigma_s} \sum_{i=1}^{N} \xi_i\, N_i\, \sigma_{si}\,, \qquad (2.4.2.3)$$

assuming all σ_s independent of energy. Actually, the scattering cross section of water is a function of energy, so 2.4.2.3 is an approximation.

The third defect mentioned in the previous section for the thermal flux distribution was the omission of the contribution of the slowing-down neutrons to the thermal spectrum. It must be recognized that the thermal and epithermal flux distributions overlap. It is here where it is most useful to combine the two distributions and again introduce the Westcott flux formulation. Westcott[8] defines a neutron-density distribution per unit speed interval as follows:

$$n(v) = n(1 - f)\, \rho_m(v) + nf\, \rho_e(v), \qquad (2.4.2.4)$$

where ρ_m and ρ_e are the Maxwellian and epithermal density distribution functions normalized so that

$$\int_0^\infty \rho_m(v)\, dv = \int_0^\infty \rho_e(v)\, dv = 1, \qquad (2.4.2.5)$$

and v is the neutron speed. The quantity f if related to the spectral index, r, by $r = f\sqrt{\pi\mu}/4$. The constant μ determines the low energy cut off energy of the epithermal component, μ kT. The numerical value of μ is $\sim$ 4-5.

The total density n is

$$n = \int_0^{\infty} n(v)\, dv. \qquad (2.4.2.6)$$

For all practical purposes, the density distributions can be cut off at $\sim$ 100 kev; no virgin fission neutrons are to be included. The quantity f is the fraction of the total density in the epithermal distribution. The thermal distribution is given by

$$\rho_m(v) = \frac{4}{\sqrt{\pi}} \frac{v^2}{v_T^3} e^{-(v/v_T)^2}, \qquad (2.4.2.7)$$

where v_T is the speed of neutrons having energy kT; $v_T = \sqrt{\frac{2\,kT}{m}}$. The epithermal distribution v_T is assumed proportional to 1/E per unit energy interval giving

$$\rho_e(v) \propto v^{-2} \qquad (2.4.2.8)$$

per unit speed interval. The epithermal distribution is assumed terminated at lower energies by a cut-off function Δ whose detailed form is discussed in Reference 8. If a simple unit step-function is used for Δ, ($\Delta = 1$ for $E > \mu kT$, $\Delta = 0$ for $E < \mu kT$), the normalized form of ρ_e is

$$\rho_e(v) = v_T \sqrt{\mu}\, \frac{\Delta}{v^2}. \qquad (2.4.2.9)$$

The flux spectrum resulting from a Maxwellian distribution joined to a 1/E slowing down distribution is useful in calculating reaction rates in a reactor. Westcott cross sections (defined earlier in Section 2.3.2.1) are defined in terms of such a flux distribution. To use Westcott cross sections in a reactor calculation the following steps must be taken:

1) Determine the spectral index for the lattice. Usually only r for the fuel is necessary since most non-1/v absorbers are found in the fuel region of the lattice. (For 1/v, $\hat{\sigma} = \sigma_0$ - See Section 2.3.2.1).

2) Determine the neutron temperature of the Maxwellian portion of the spectrum.

3) Determine the appropriate Westcott cross section for 2200 m/s neutrons (Westcott tables are available - See Reference 1, for example).

4) Determine the total neutron density n (up to $\sim$ 100 kev is sufficient) and multiply by v_o - the velocity corresponding to 273 K neutrons to determine the Westcott flux (See 5.6.1.).

The use of Westcott cross sections automatically considers the spectrum 2.4.2.4. The FLEX or MOFDA programs can be used to determine the neutron temperatures and spectral indices.

It must be remembered that, although the Westcott convention is useful, its applicability is limited to well-moderated reactors ($r < 0.1$) and the compiled Westcott cross section are limited to thin sample values, i.e., they neglect self-shielding. For s-factors this can be a very marked effect since s is deduced from "infinite-dilution" resonance integrals. In spite of these limitations, Westcott cross sections are considered a good first approximation in the N Reactor. The convetnion of including only 1/v absorption in s for U^{238} and using effective resonance integrals in the determination of s-factors in other cases where self-shielding may be important also extends the applicability of the Westcott convention.

2.4.3 Fast Neutron Spectrum

The energy distribution function for U^{235} fission neutrons has been measured[2] and follows the analytical form given in Equation 2.4.3.1

$$n(E)dE = 1.096 \exp(-E/0.965) \sinh \sqrt{2.29\,E}\, dE \qquad (2.4.3.1)$$

Here n(E) dE is the number of fission neutrons (per fission) with energies in the range E to E + dE (Mev). The normalization is based on the most recent value for ν_{25} of 2.43.[9]

$$\int_0^\infty n(E)\, dE = 2.43.$$

Actually, such a spectrum as given by Equation 2.4.3.1 does not exist anywhere in the reactor since it will be modified by neutrons which have undergone collisions and have lost some energy. Within the fuel element, the spectrum given by 2.4.3.1 should be the dominant component, at least for neutrons above 1 Mev.

The energy spectrum characterizing the neutrons during their slowing-down phase is again known only inexactly, particularly for energies close to fission energies. For neutron energies considerable below fission energies ($<$ 100 kev) the spectrum is usually assumed to follow the 1/E energy dependence given in the preceding section.

Further discussion of the fast neutron spectrum is given in Section 2.5.2.

2.5 Lattice Parameters (Theoretical)

The theoretical methods described in this section are those appearing with minor exceptions in the FLEX and MOFDA IBM 7090 programs.[6]

2.5.1 Reproduction Factor, η .

The reproduction factor is defined as the average number of therma fission neutrons released per neutron absorbed in the fuel excluding resonance capture in U^{238} and absorptions accounted for in the fast effect. The reproduction factor may be written as

$$\eta = \frac{x\ \hat{\sigma}_f^{25} \nu^{25} + y\ \hat{\sigma}_f^{49} \nu^{49} + s\hat{\sigma}_f^{41} \nu^{41}}{v\ \hat{\sigma}_a^{28} + x\ \hat{\sigma}_a^{25} + y\ \hat{\sigma}_a^{49} + z\ \hat{\sigma}_a^{40} + s\ \hat{\sigma}_a^{41} + Xe\ \hat{\sigma}_a^{Xe} + Sm\ \hat{\sigma}_a^{Sm} + FP\ \hat{\sigma}_a^{FP}}, \qquad (2.5.1.1)$$

where

ν_i = average number of neutrons released per fission by isotope i,

$\hat{\sigma}_f$ = fission cross section (Westcott) of isotope i,

$\hat{\sigma}_a$ = absorption cross section (Westcott) of isotope i, and

v, x, y, z, s, Xe, Sm, FP, are the normalized concentrations of U^{238}, U^{235}, Pu^{239}, Pu^{240}, Pu^{241}, Xe, Sm, respectively. (See Section 5).

The concentration of Pu^{239} is to be diminished by the Np^{239} concentration which has not yet decayed into Pu^{239} (See Section 7).

Usually, just the green, clean value of η is desired; this is usually the quantity derivable from measurements of the other lattice constants in the cold, clean, green lattice.

$$\eta_o = \frac{\nu^{25}\ x\ \hat{\sigma}_f^{25}}{x\ \hat{\sigma}_a^{25} + v\ \hat{\sigma}_a^{28}}. \qquad (2.5.1.2$$

2.5.2 Fast Effect, ϵ .

The fast fission factor following Spinrad's[10] model is defined as the number of neutrons making their first collision with the moderators external to the fuel element per neutron arising from thermal fission. The

calculation of ϵ is restricted to fast fission in U^{238} only and is based on a pseudo three-group calculation. The application of Spinrad's model by Fleischman and Soodak[3] is used in the FLEX and MOFDA codes. The three groups are defined as follows:

Group A consists of fission neutrons with energies above 1.4 Mev, the effective U^{238} fast fission threshold. The spectrum follows Equation 2.4.3.1.

Group B consists of fission neutrons with energies below 1.4 Mev. The spectrum also follows Equation 2.4.3.1.

Group C consists of neutrons which are scattered out of Group A. The spectrum is assumed to be Ee^{-E} resulting from the statistical model of the nucleus.

It is to be noted that all three groups refer to neutrons within the fuel. Moderated neutrons are not included except those which are scattered by moderators internal to the fuel. Thus, in the case of N Reactor each group will have a small component from neutrons scattered by water internal to the fuel. However, the component will be small.

The three-group expression for ϵ is written as

$$\epsilon = \left(1 + \frac{\nu_A \delta}{\nu_{th}}\right)\left(f_A N_A + f_B N_B + f_A J_A N_C\right), \qquad (2.5.2.1)$$

where δ is the fast-to-thermal fission ratio, ν_A is the number of fission neutrons resulting from fission by a Group A neutron (See Table 2.3.2.2.1), ν_{th} is the number of fission neutrons resulting from thermal fission (See Table 2.3.2.4.1). f_A is the fraction of fission neutrons in Group A, f_B likewise in Group B.

$$f_A = 1 - f_B = 0.561, \text{ and}$$

$$f_B = 0.439. \qquad (2.5.2.2)$$

The other constants are defined as follows. The group cross sections are given in Table 2.3.2.2.1.

$$N_A = \frac{1 - P_A}{1 - \left(\frac{\sigma_{et}}{\sigma_t}\right)_A P_A},$$

$$N_B = \frac{1 - P_B}{1 - \left(\frac{\sigma_{et} + \sigma_i}{\sigma_t}\right)_B P_B},$$

(2.5.2.3)

$$N_C = \frac{1 - P_C}{1 - \left(\frac{\sigma_{et} + \sigma_i}{\sigma_t}\right)_C P_C}, \text{ and}$$

$$J_A = \frac{\left(\frac{\sigma_i}{\sigma_t}\right)_A P_A}{1 - \left(\frac{\sigma_{et}}{\sigma_t}\right)_A P_A},$$

where P_A, P_B, and P_C are the first flight collision probabilities for neutrons in groups A, B and C, respectively. The collision probabilities can be calculated most exactly with a Monte Carlo method; however it has been shown that it is sufficiently accurate to calculate the P's by homogenizing the fuel element into a solid cylinder and then using tabulated cylindrical rod escape probabilities.

2.5.3 Resonance Escape Probability, p

The resonance escape probability is defined as the probability that a fission neutron escaping a fuel element for the first time slows down to thermal energies without resonance capture. In a predominantly U^{238} system, it is sufficient to consider resonance escape in U^{238} only. The definition further excludes any 1/v-captures in the materials considered. The following general formula may be used:[11]

$$-\ln p = \frac{N_o \, RI}{(\Sigma_s \xi)_M} \frac{V_o}{V_M} \left[\phi(x) + \frac{V_M}{V_A} \psi(y, \beta) \right], \quad (2.5.3.1)$$

where

N_o = number of U^{238} atoms per cc of fuel,

RI = effective resonance integral,

V_o = volume of fuel only,

V_M = total volume of moderator - (inside and outside of fuel), and

V_A = volume of homogenized fuel element (includes internal coolant).

x and y are dimensionless variables given by $x = A_M/(4\pi\bar{\tau}_M)$ and $y = A_A/(4\pi\bar{\tau}_M)$ where A_M and A_A are the cross sectional areas per cell of

the total moderator (including coolant) and homogenized fuel element, respectively. $\bar{\tau}_M$ is the mean value of the age of resonance neutrons in the moderator and can be related to $\bar{\tau}$, the mean value of the age of resonance neutrons in the lattice by

$$\bar{\tau}_M = \bar{\tau} \frac{V_M}{V_T} = 0.65\, \bar{\tau}. \qquad (2.5.3.2)$$

The functions ψ and ϕ characterize the absorptions in the fuel element of natal resonance-energy neutrons and resonance neutrons from other fuel elements, respectively. Expressions for these functions are given in References 5 and 11. For $x < 0.5$,

$$\phi(x) \simeq 1 - x. \qquad (2.5.3.3)$$

For N Reactor $x = 0.132$, so $\phi(x) = 0.868$.

Since the contribution to the resonance absorption in a fuel element from neutrons native to the fuel element in question is much less than the contributions from other fuel elements, the function ψ is very close to zero. In the N Reactor $\psi = .00872$.

2.5.4 Thermal Utilization, f

The "thermal" utilization is defined as the ratio of the total number of neutrons absorbed in the fuel to the total number of neutrons absorbed in all materials. In both cases, the resonance captures in U^{238} and the absorptions accounted for in the fast effect are excluded. An expression for calculating the thermal utilization is

$$f = \frac{\sum_{\text{fuel}} V\, \hat{\Sigma}_a\, \hat{\phi}}{\sum_{\text{all regions}} V\, \hat{\Sigma}_a\, \hat{\phi}}, \qquad (2.5.4.1)$$

where

V = region volume in lattice cell,

$\hat{\Sigma}_a$ = macroscopic absorption cross section (Westcott), and

$\hat{\phi} = n\, v_o$.

The term n is the total neutron density in each lattice region integrated over all energies up to $\sim$ 100 kev and v_o is 2200 m/s.

2.6 Lattice Parameters (Experimental)

The actual lattice parameters for the N Reactor (cold, clean, green) have been determined experimentally for a prototypical lattice. The descriptions of the experimental arrangements are given in Table 2.6.1.

2.6.1 PCTR Measurements

The results of the PCTR measurements are given in Table 2.6.2[12]. Actually, two lattice arrangements were studied, one was as exact a copy of the actual lattice as possible, the other was a "condensed" lattice in that the large steam vent and other voids in the stack were removed, and the lattice spacing compressed to maintain the same graphite-to-uranium ratio.

2.6.2 Exponential Pile Measurements

The material buckling of the lattice was measured for the mockup and condensed lattice in an exponential pile. The results are also given in Table 2.6.2[12]. The much higher B_m^2 determined in the condensed lattice is a result of the smaller migration area. The migration area deduced for the condensed lattice is 300 cm^2 which compares to a value of 646 cm^2 for the mockup lattice. The ratio is 2.15 which is in good agreement with the ratio predicted theoretically and which considers the effect the voids have on neutron streaming. (See Section 3.4).

Table 2.6.

Cold, Clean, Green
Experimental Lattice Parameters - Wet

	Mockup Lattice	Condensed Lattice
f	0.879	0.881
p	0.829	0.836
ϵ	1.050[a]	1.059[a]
k_∞	1.075	1.074
B_m^2	116 μb	239 μb

a Based on measurement of δ and use of one-group expression for ϵ instead of Spinrad definition (See Reference 12).

2.6.3 "Best-Value" Lattice Parameters

The availability of experimental cold, clean, green lattice parameters for a lattice almost identical to the N lattice makes it possible to normalize theoretical methods and determine best values for the lattice parameters of the actual N lattice. Features such as process tube differences, graphite purity differences, helium-vs.-air atmosphere, cross-cooling tubes,

TABLE 2.6.1 - A COMPARISON OF DIMENSIONS AND OTHER PHYSICAL PROPERTIES N-LATTICE VS. EXPERIMENTAL MOCKUP LATTICES

Property		Actual N-Lattice (Design Value)	PCTR	Exponential Pile Mockup
Lattice Pitch		8" x 9"	8" x 9"	8" x 9"
Graphite (Core)				
Solid density		1.72 ± 0.02 gm/cm^3	1.69 gm/cm^3	1.69 gm/cm^3
dih		+0.85	+0.94	+1.07
Voids		See Figure 24	See Figure 24	See Figure 24
Atmosphere		Helium	Air	Air
Gross Cooling				
Tube Material		Zr-2	None	None
Dimensions				
I.D.		0.70"		
O.D.		0.75"		
Tube Pitch		16" x 9"		
Process Tubes				
Tube Material		Zr-2	2S Aluminum	2S Aluminum
Density		6.50 gm/cm^3	2.7 gm/cm3	2.7 gm/cm^3
Dimensions				
I.D.		2.708"	2.702"	2.702"
O.D.		3.258"	3.058"	3.058"
Fuel Elements				
Clad Material		Zr-2	2S Aluminum	2S Aluminum
Clad Density		6.50 gm/cm^3	2.7 gm/cm^3	2.7 gm/cm3
Dimensions				
(Clad) O.D.		2.406"	2.394" (2.349")[a]	2.394" (2.349")[a]
(Core) O.D.		2.354"	2.336"	2.336"
Outer Tube	(Core) I.D.	1.816"	1.793"	1.793"
	(Clad) I.D.	1.764"	1.737" (1.779")[a]	1.737" (1.779")[a]
	(Clad) O.D.	1.249"	1.238" (1.196")[a]	1.238" (1.196")[a]
Inner Tube	(Core) I.D.	1.167"	1.183"	1.183"
	(Core) I.D.	0.490"	0.494"	0.494"
	(Clad) I.D.	0.438"	0.437" (0.477")[a]	0.437" (0.477")[a]
Length		23.2"	Effectively ∞	Effectively ∞
Supports		Zr-2	Effectively none[b]	Effectively None[b]
End Caps		0.250" on each end	None	None
Enrichment		(0.947" w/o)	0.947" w/o	0.947" w/o
Uranium Density		18.90 gm/cm^3	18.887 gm/cm^3	18.887 gm/cm^3
Control Element Channels				
HCR and HSR		See Figure 24	None	None
Ball 3X		See Figure 24	None	None

a. Cladding used in experiments was not bonded to fuel elements. Figures in parentheses are O.D. or I.D. of clad, whichever is appropriate.
b. Lucite spacers were used which effectively mock up water.

etc. can be taken into account in the calculations. The best-value cold, clean, green lattice parameters so derived for N Reactor are given in Table 2.6.3.

Table 2.6.3

Best-Value Cold, Clean, Green Lattice Parameters[a]

Parameter	Value
k_{∞}	1.0778
η	1.4184
ϵ	1.0411
p	0.8291
f	0.8803
B_m^2	115.6 μb

[a]No cross-cooling tube included. Effect would reduce k to 1.0752.

The agreement with experimental values is good except for ϵ, where the difference lies in the definition of ϵ. The derivation of ϵ from the measurement of δ is based on the older definition of ϵ which is the number of neutrons which slow down the U^{238} fission threshold for each neutron produced by thermal fission (See Reference 12). An average for the NPR startup element is 0.067.

2.7 Cell Flux Distributions

The 1/v-law absorber reaction rate throughout the lattice cell has been determined experimentally in the cold, wet, green N lattice by irradiating U^{235}-pins and foils at different radial positions in the lattice[12]. Plots of the measured distribution are shown in Figures 2.7.1 and 2.7.2. For all practical purposes the distributions can be assumed to be representative of the thermal flux in the cold lattice. Figure 2.7.1 is for the condensed lattice. Figure 2.7.2 is for a close mockup of the actual lattice.

FLEX-computed, region-average, thermal (1/v) fluxes in each region of the lattice cell are given in Table 2.7.1. The reactor conditions were hot, green. Other items of interest are also given in Table 2.7.1. such as physical temperatures, neutron temperatures, region areas, etc. The void regions are cylindrized void regions to mockup the actual void spaces.

A three-group flux calculation has also been made by Simpson[13] using a Fortran Code F SUPER. The exposure assumed was 700 MWD/T. The three neutron energy groups chosen for the flux calculations were a fast group ($E > 0.24$ Mev), an epithermal group (0.24 Mev $> E > 0.15$ ev) and a thermal group including all neutrons in the thermal energy Maxwellian distribution. The cell traverses are given in Figure 2.7.3.

3. Core Physics

3.1 Introduction

The preceding section was concerned with the properties of an infinite array of lattices. Consideration must be given to effects associated with a finite reactor. Also, N reactor is a reflected reactor and the effects of a reflector must be considered.

Table 2.7.1

FLEX-Computed "Thermal Flux" Traverse
(Hot, Green)

Region	Material	Phys. Temp.[a]	Neut. Temp.[a]	Area	Relative 1/v Flux[b]
1	Graphite	550 C	790 K	279.1 cm^2	2.152
2	Void	495	770	94.97	2.040
3	Graphite	470	750	33.97	1.957
4	Void	430	715	2.57	1.888
5	Zr-2	262	675	16.66	1.841
6	H_2O	228	600	7.57	1.644
7	Zr-2	249	615	1.26	1.433
8	U	364	645	11.47	1.320
9	Zr-2	261	600	1.01	1.288
10	H_2O	234	550	7.97	1.278
11	Zr-2	257	570	1.02	1.106
12	U	401	610	5.75	1.000
13	Zr-2	264	580	0.26	0.976
14	H_2O	239	540	0.99	1.036

a. Flux-squared weighted averages.
b. Region-averaged values. Normalized to unity in inner fuel region (region 12).

10,000 ppm U^{235} 400 b
1000 ppm U^{236} 944
? CF

3.2 Description of Core and Reflector

The N-Reactor core, at initial startup, will be comprised of 1004 lattice units as described previously (Figure 2.1.1). Provisions have been made to increase this number of 1072 if future operating trends justify additional irradiation volume. This core is pierced by three systems of openings in addition to the process channels and steam vents; horizontal control rod channels; the ball 3X safety system channels; and the graphite moderator cooling tubes.

These three void systems, along with the 2" x 3" rectangular steam vents running both parallel and perpendicular to the process channels, reduce the core graphite density from a nominal 1.7 gms/cm^3 to an effective 1.3 gms/cm^3.

The physical dimensions of the core are set by the lattice geometry and the charge length. There are 34 vertical rows of tubes, resulting in a core width of 34 x 0.667 feet or 22.667 feet; there are 32 horizontal rows of tubes, or a 32 x 0.75 = 24-foot core height. The corners are truncated as shown in Figure 3.2.1 (See Figure C-2, HW-71408 VOL2) resulting in a core equivalent radius of 12.64 feet. The core length is defined by the portion which contains fuel material, or 35 feet. This roughly cylindrical arrangement contains 693.0 tons of graphite (density 1.70 gms/cm^3) and 387 tons of uranium.

The core is surrounded radially by a reflector of high-purity graphite which is infinite in effect; the front and rear "reflector" is composed of graphite plus other material (e.g., process tubes, water dummies).

3.3 Slowing Down and Diffusion of Neutrons

As a consequence of the undermoderated lattice of the N-Reactor, the fast-to-thermal flux ratio is quite large relative to that of existing, overmoderated Hanford reactors. As an illustration of this difference, the ratio of fast flux to thermal flux is estimated to be 2.50 at N (compared to 1.08 at a K reactor). This enhances the production of plutonium in the reactor and also makes the lattice fail-safe (from a reactivity standpoint) upon loss of water.

The lattice migration area deduced from an exponential experiment is 646 cm^2 (see Section 2.6.2); this is separable into a Fermi age (τ) of $\sim$ 480 cm^2 and a diffusion area (L^2) of $\sim$160 cm^2 at room temperature. At operating temperature M^2 increases by $\sim$ 10%.

3.3.1 Fermi Age

The age of neutrons in a heterogeneous reactor and particularly N Reactor is not readily calculable with any precision. The complex structure of the N moderator and the large amount of water in the N lattice make the calculation of τ difficult. The Fermi age may be estimated by the equation

$$\tau = \frac{C_s \; V_T^2}{\sum_i V_i \, \xi_i \, \Sigma_{si} \left[\sum_j \frac{V_j}{\xi_j \, \Sigma_{sj} \, \tau_j} + \sum_k \frac{V_k \, \Sigma_{sk}}{15} \right]}, \qquad (3.3.1.1)$$

Figure 3.2.1 is a diagram of the core geometry of N Reactor and is identical to Figure C-2 of HW-71408 VOL2.

where C_s is a steaming correction (See Section 3.4),

V_T is the total lattice-cell volume, and the

V_i are the sub-lattice cell volumes.

The sum over i is over all lattice cell regions; the sum over j is over only moderator cell regions; and the sum k is over only non-moderator cell regions.

The quantities ξ and Σ_s have been defined previously and the τ_i's are the ages to thermal for each moderator. Inelastic scattering in the uranium fuel must be considered and the τ_i's are given by

$$\tau_i = (1 - P_2)\ \tau_{ai} + P_2\ \tau_{bi}, \qquad (3.3.1.2)$$

where

τ_a = age from fission energies to thermal, and

τ_b = age to thermal for neutrons scattered inelastically with uranium atoms.

The τ- components are given in Table 3.3.1.1 below

Table 3.3.1.1

Material	τ_a	τ_b
Graphite	$931/\rho_g^2$	$591/\rho_g^2$
Water	$33/\rho_w^2$	$20.9/\rho_w^2$

The collision probability P_2 is the fast neutron collision probability in the fuel and can be obtained from previously defined quantities.

$$P_2 = (f_A\ J_A\ N_C)\ (f_A\ N_A + f_B\ N_B + f_A\ J_A\ N_C)^{-1} \qquad (3.3.1.3)$$

from page 23 $f_A = 0.561$ $f_B = 0.439$
$= 1 - f_B$

where the constants are as defined earlier in Section 2.5.2.

DECLASSIFIED

3.3.2 Diffusion Area

The diffusion area, L^2, can be estimated from

$$L^2 = \frac{C_s \left(\sum_i V_i\ \bar{\phi}_i\right)^2}{\sum_i V_i\ \bar{\phi}_i\ \hat{\Sigma}_{ai}\ \sum_i V_i\ \bar{\phi}_i/(\hat{\Sigma}_{ai}\ L_i^2)} \qquad (3.3.2.1)$$

where again C_s is the streaming correction and the other constants are

$\hat{\Sigma}_{ai}$ = macroscopic Westcott absorption cross section of ith region,

$\bar{\phi}_i$ = volume-average 1/v flux (Westcott) in ith region,

L_i = diffusion length of ith region.

The sum over i is over all lattice cell regions.

3.3.3 Migration Area

The migration are is defined as the sum of L^2 and τ.

3.4 Neutron Streaming

The large void fraction in the reactor core allows preferential neutron passage along the void channels; this effect, called "streaming", manifests itself in various lattice parameters, in particular τ and L^2 and thus in reactor leakage and multiplication. As an illustration of the magnitude of this effect, if the graphite were "smeared" over the core (retaining the same number of graphite atoms but reducing the density and filling all void space) the over-all pile reactivity would be increased by 0.8 per cent due to decreased leakage.

The streaming correction to the age and diffusion area, C_s, can be estimated using Behren's formulas[14]. For example the effect of voids on the diffusion length of neutrons in the reactor may be calculated from the equation

$$L_1^2/L_o^2 = 1 + 2\phi\,(r\,\phi/\lambda)\left[\coth\,(r/\phi\lambda) + (Q - 1)\right], \qquad (3.4.1)$$

where

L_1 = diffusion length in the reactor with voids,

L_o = diffusion length in the reactor without voids,

ϕ = void volume/volume of solid material,

r = twice the volume of the hole divided by the surface area of the hole, 2V/S,

λ = mean free path in the moderator, and

Q = mean square chord length through the hole/square of the mean chord length.

The factor Q is dependent upon the shape of the hole and is given in Reference 14. Modifications may be made to the equation to consider voids which are not uniformly oriented; however, this is not necessary for the N Reactor because of the symmetrical distribution of the axes of the voids. The above equation may be simplified to

$$L_1^2/L_o^2 = 1 + 2\phi + r\phi Q/\lambda \qquad (3.4.2)$$

without any signficant loss in accuracy for calculations for N Reactor. This expression may be used in comparing lattices with and without voids. The second term may be thought of as a "density" correction while the third term may be considered as a "streaming" correction.

The calculated ratio of the square of the diffusion length in a normal lattice to that of a condensed lattice (i.e., without voids) is 2.01[15]. This may be compared with the experimentally determined ratio of migration areas of 2.15[12]. The calculated[15] and measured[16] values of the diffusion length of the graphite stack alone (no fuel or process tubes present) are 86.3 and 84.7 centimeters, respectively. These two examples of correlation between experiment and theory indicate that the anlaytical method of determining these values is fairly accurate for this type of reactor.

The theoretical value of the streaming term $r\phi Q/\lambda$ in 3.4.2 is 0.48,[15] hence the streaming correction C_s is equal to 1.48. The same streaming corrections can be used for correcting the age.

3.5 Neutron Leakage, k_{eff}

The neutron leakage in a reactor is a function of the reactor size and the neutron migration area; it is strongly influenced by the presence of a reflector of pure moderator material surrounding the active core. For a uniform, homogeneous loading, the effective and infinite lattice multiplication factors are related by the equation:

$$k_{eff} = \frac{k_{oo}}{1 + Bg^2L^2} e^{-Bg^2\tau} \simeq \frac{k_{oo}}{1 + Bg^2 (L^2 + \tau)}, \qquad (3.5.1)$$

where:

k_{eff} = effective pile multiplication,

k_{oo} = infinite lattice multiplication, and

Bg^2 = pile geometric buckling.

This equation may be used to calculate an effective geometric buckling for a heterogeneous reflected reactor if the various parameters are known. Both three-group calculations and modified, one-group calculations indicate a k_{eff} for the fully-loaded, green reactor of $\sim$ 1.060 at room temperature. The effective geometrical buckling may be then determined from a rearrangement of the previous equation.

$$B_g^2 = \frac{k_{oo} - k_{eff}}{k_{eff} M^2} \qquad (3.5.2)$$

Assuming "best values" of the parameters as given in Section 2.6 and a k_{eff} for the fully loaded reactor of 1.060, the total geometrical buckling is 22.1 micro-bucks ($1\ \mu b = 10^{-6}\ cm^{-2}$).

If the front and rear reflector augmentation at N Reactor is estimated from a cosine flux distribution, the longitudinal buckling component is $\sim 7.3\ \mu b$; this indicates a radial buckling component of $14.8\ \mu b$ and a radial reflector augmentation of ~ 240 centimeters (all older Hanford production reactors have radial augmentations of the order of 60 centimeters).

The rather large reflector savings is due to the predominantly "fast" neutron spectrum in the core; epithermal neutrons emerging from the core into the reflector are quickly thermalized. In the thermal state, there is a good probability that the neutrons will be transferred to the core and utilized in the fission process; in fact, there is a net gradient of thermal neutrons from the reflector inward to the core.

It should be noted that the reflector augmentation as defined by the geometrical buckling is extremely sensitive to the total pile reactivity; an error of only 0.2 per cent $\Delta k/k$ in the determination of k_{eff} can result in an error of over 60 centimeters in the estimate of δ, the reflector savings. Best estimates for the effective reactor size (in terms of neutron boundaries) are:

Effective radius = 635 centimeters,

Effective length = 1160 centimeters.

These dimensions are based upon $k_{eff} = 1.060$ at room temperature. The total leakage of NPR compares to leakage at BDF type Hanford reactor as follows:

NPR, cold, clean	.0143%	Δ k/k
NPR, hot, clean	.0151%	Δ k/k
BDF, hot, clean	.0192%	Δ k/k

3.6 Core Power Distribution

The significant reflector augmentation results in an exceptionally high flattening efficiency in N Reactor, even without the smoothing effect of control rods or other flattening agents. Theoretical flattening efficiencies of 80 - 98 per cent are calculated for routine operation, with actual efficiencies (including microscopic fine structure) of 70 - 90 per cent. The best estimate for the flattening efficiency is 90 per cent. Radial power distribution for various flattening efficiencies are plotted in Figure 3.6.1 (See Figure C-3 of HW-71408

Figure 3.6.1 is a plot of radial power distributions for various degrees of flattening and is identical to Figure C-3 of HW-71408 VOL2.

VOL2). The axial power distribution will follow an approximate cosine shape with a peaking upstream of pile center due to the lower coolant temperature towards the inlet end of the reactor. The reactivity held in flattening vs. radius of the flat zone is shown in Figure 3.6.2. Radial flux distributions are shown in Figure 3.6.3.

4. Estimation of Effects of Lattice Changes

4.1 Changes Uniform Over the Reactor

It will be useful to know some of the more probable reactivity variations caused by lattice changes which are made uniformly in each lattice cell. The simplest procedure in calculating these effects is to employ one of the IBM-7090 physics codes described earlier (MOFDA, FLEX, etc.[6]). However, it is worthwhile to discuss some general results at this time.

4.1.1 Fuel Element Changes

The initial 21.6 lb/ft fuel element for N Reactor is not the only fuel choice possible. It is a conservative choice, one designed so that the reactivity transients should be within the capacity of the horizontal rod system. A heavier fuel element is not impossible, and may well be charged after the reactor has been operated and the actual reactivity transients and effective control rod strengths determined.

Since the N Reactor is undermoderated, any further decrease in the uranium-to-moderator ratio will result in a loss in reactivity. Thus, a heavier fuel element would require a higher enrichment. Also, in general as the fuel weight is increased, the reactivity transient between cold and equilibrium reactor conditions is made more negative which further increases the enrichment requirements. The heavier the fuel element, the greater the plutonium yield. This means that important economic gains are possible if a heavier fuel element is feasible.

Since fuel redesign involves not only a change in uranium volume, but also a change in coolant volume, (assuming a fixed process tube size), any attempt to characterize the physics of the heavier fuel geometries beyond the simplest terms is impractical. Updated results of rather early calculations[17] are given in Table 4.1.1.1 to illustrate the general behavior of the required enrichment level and plutonium yield as a function of fuel gemetry and weight. Goal exposure is assumed to be 1200 MWD/T.

Table 4.1.1.1

Enrichment and Plutonium Yield as Function of Fuel Weight

Uranium Wt/Foot	gm Pu/MWD @ 1200 MWD/T	Enrichment Level[a]
24.5 lbs	0.846	1.00
23.2	0.835	0.974
22.2	0.825	0.958
21.6	0.820	0.947 ← Base
21.2	0.816	0.943

a Probably on high side. Calculated to yield a minimum equilibrium reactivity of ~ 2%.

4.1.2 Enrichment Variation

The reactivity effect of varying the enrichment level in the 21.6 lb/feet fuel element is quite linear over the range 0.92 to 1.00 w/o U^{235}. The reactivity variation is calculated to be 0.38% per 0.01% absolute change in U^{235} enrichment. For example, the difference in local reactivity between 0.947 and 0.957 w/o U^{235} fuel is 0.38%, the higher enrichment being the most reactive.

4.1.3 Impurities in Fuel

Occasionally it may be necessary to accept uranium fuel with different impurity levels than that initially specified. The presence of U^{236} in recycled fuel will also act as an impurity. For most chemical elements, the reactivity effect can be simply estimated from the change in f, the thermal utilization. For certain chemical elements whose mass is very low (so they act as moderators as well as poisons) or which may give rise to particular neutron producing reactions, such as the n,2n reaction in beryllium, other factors must be considered. But, a general rule for elements whose atomic weight is greater than about 45 can be given as follows:

$$\frac{dk}{k} = \frac{df}{f} = - f_o K_u w_p, \qquad (4.1.3.1)$$

where f_o is the thermal utilization of the uranium without the impurity, w_p is the weight fraction of the impurity and K_u is the danger coefficient of the impurity with respect to uranium.

$$K_u = \frac{\hat{\sigma}_{ap} \; A_u}{\hat{\sigma}_{au} \; A_p}, \qquad (4.1.3.2)$$

where $\hat{\sigma}_{ap}$ and $\hat{\sigma}_{au}$ are the Westcott absorption cross sections of the impurity and uranium, respectively, and the A's are the atomic weights.

4.1.4 Reactor Atmosphere

The reactivity difference between an air (nitrogen) and a helium atmosphere in the reactor has been calculated to be 0.16%. The principal effect of nitrogen in the lattice is to increase the parasitic absorptions and thus reduce the thermal utilization, f. The thermal neutron absorption cross section of helium is zero.

4.2 Non-Uniform Changes

The changes discussed in the preceding section apply for uniform changes over the entire reactor, It is also necessary to consider the problem of local lattice variations and their effect on the over-all reactor which is a much more difficult problem. The simplest method of treating these problems is the use of perturbation theory in the one-group diffusion theory model. If the perturbation involves changes which affect the thermal neutron absorption or fission cross section (impurities, nitrogen, enrichment, etc.) the appropriate statistical weight, W, is the square of the thermal flux.

$$W_{local} = \int_{local} \phi^2 \, dV \Big/ \int_{Reactor} \phi^2 \, dV. \qquad (4.2.1)$$

$$\left[\frac{dk}{k}\right]_{Reactor} = W_{local} \left[\frac{dk}{k}\right]_{local}. \qquad (4.2.2)$$

If the perturbation involves changes which affect the thermal diffusion coefficiennt (voids, density changes, etc.) the appropriate statistical weight is the square of the gradient of the flux.

$$W_{local} = \int_{local} (\nabla \phi)^2 \, dV \Big/ \int_{Reactor} (\nabla \phi)^2 \, dV. \qquad (4.2.3)$$

Perturbation theory can be extended to a two-group or multigroup model. This is necessary if the perturbation involves change in epithermal or fast neutron reaction rates (fuel element variation, for example). These problems are difficult and solutions are not described here. Some information is presented below on the effect of natural uranium columns, air columns and water columns.

4.2.1 Reactivity Effect of Natural Uranium Fuel

The possibility exists of using some natural uranium fuel elements for either flattening purposes or for reactivity tailoring (in the event that 0.947 w/o provides too much excess reactivity). The cold, clean, green material buckling for natural uranium fuel elements of the same geometry as the enriched uranium has been measured in the N-Reactor Exponential Pile.[12] The results are given in Table 4.2.1.1. The dimensions of the prototypical fuel elements used in these tests are the same as shown in Table 2.6.1 and the same corrections described in Section 2.5 whould be applied to these results. The enriched bucklings are also repeated in Table 4.2.1.1. Bowers[18] has computed the poison effect of natural uranium. This curve is given in Figure 4.2.1.

Table 4.2.1.1

Experimental Material Bucklings - Prototypical N Fuel Elements[12]

Enrichment	Wet Lattice	Dry Lattice
0.712 w/o	$-95 \pm 2\ \mu b$	$-93 \pm 4\ \mu b$
0.947 w/o	$+116 \pm 5\ \mu b$	$+24 \pm 5\ \mu b$

4.2.2 Reactivity Effect of Empty Process Tubes

An empty process tube in N Reactor is expected to result in an increase in the over-all pile reactivity due to the local increase in the C/U ratio. The magnitude of the effect must await experimental determination during the startup tests.

4.2.3 Reactivity Effect of Water-Filled Process Tubes

Again, this must be deferred to when startup test results are available.

4.2.4 Reactivity Effect of Foreign Material in Process Tubes

The reactivity effect of poison columns, target columns and other foreign materials must also await startup tests.

5. Reactor Products

5.1 Introduction

As previously stated, N Reactor is a converter – the principal nuclear processes being the transmutation of U^{238} to Pu^{239} and the fissioning of U^{235} to provide the neutron carrier of the chain reaction and the neutrons necessary for the plutonium production. The principal product is therefore Pu^{239}. However, since all the nuclei can absorb neutrons, a host of other products can and are also produced in the reactor. The other products of interest are Pu^{240}, Pu^{241} (which are higher transmutations in the plutonium chain), Np^{237} which has both U^{235} and U^{238} as precursors, and U^{236} which is a useful precursor of Np^{237} and will probably be recycled in N-Reactor fuel. Tritium may also be a product but would require a special loading including lithium targets. Po^{210} may also be a product but again could require special bismuth target elements. There are also many fission products which are useful such as Cs^{137} and Sr^{90}. Pu^{238} which has important use as an isotope power source is produced in minute amounts and could be produced in useful amounts by irradiating Np^{237} targets.

5.2 Plutonium Production

Plutonium results in the reactor when neutrons are absorbed in U^{238}. A small amount is also produced from U^{235}. The principal reactions in uranium leading to plutonium isotopes are diagrammed below.

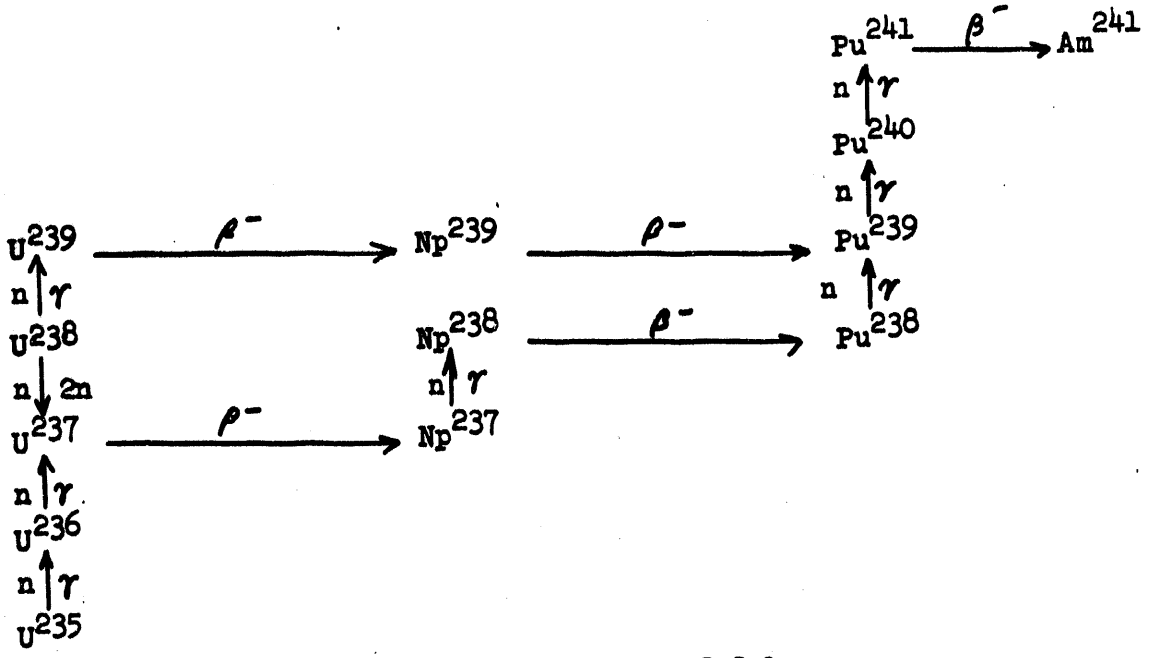

Figure 5.2.1

Principal Reactions in Uranium

The U^{238} neutron reaction to U^{239} goes at all neutron energies with the major share being in the thermal energy range. The beta decay of U^{239} has a 23.5-minute half life; the beta decay of Np^{239} has a 2.33-day half life. Pu^{239} is relatively stable with a half life of 24,300 years. Pu^{240} is an unwanted isotope in weapons grade plutonium since it is capable of spontaneous fission. Pu^{241} is beta-active with a 13-year half life and is also fissionable.

5.3 Neptunium Production

Recent interest in Pu^{238} for radioisotope power sources has stimulated a market for Np^{237}. Np^{237} can be fashioned into target elements and irradiated to yield Pu^{238}. (The Pu^{238} formed from successive transmutations in uranium is too minute to be worthwhile). The reactions leading to Np^{237} are also shown in Figure 5.2.1. It is seen that both U^{235} and U^{238} are precursors of Np^{237}. The fast neutron n,2n reaction in U^{238} contributes about 60 per cent of the Np^{237} formed from virgin uranium. Recycled uranium rich in U^{236} promises to boost Np^{237} production.

5.4 Tritium Production

Tritium (H^3) is formed by an n, α reaction in Li^6.

$$Li^6 (n,\alpha) H^3. \qquad (5.4.1)$$

The reaction is predominantly a thermal neutron reaction. To produce H^3 in N Reactor would require a special loading such as an E-N, or possibly the use of lithium control rods. Neither avenue has received serious study to date.

5.5 Fission Products

Fissioning events in the reactor lead to a host of fission products with atomic masses ranging from 72 to 161. Two isotopes with commercial interest are Cs^{137} and Sr^{90}. The fission product chains leading to these isotopes are as follows:

$$I^{137} \xrightarrow[24s]{\beta^-} Xe^{137} \xrightarrow[3.9\ m]{\beta^-} Cs^{137} \xrightarrow[29\ y]{\beta^-} Ba^{137} \qquad (5.5.1)$$

$$Kr^{90} \xrightarrow[33s]{\beta^-} Rb^{90} \xrightarrow[2.7\ m]{\beta^-} Sr^{90} \xrightarrow[28\ y]{\beta^-} Y^{90} \xrightarrow[64.3h]{\beta^-} Zr^{90}. \qquad (5.5.2)$$

The cumulative yields per thermal fission of U^{235} of Cs^{137} and Sr^{90} are 6.15% and 5.77%, respectively.

5.6 Calculation of Nuclear Reactions

5.6.1 Flux

Although most reactions of interest in a thermal reactor occur at thermal energies, sufficient epithermal events also occur that a flux defined to include both thermal and epithermal neutrons is desirable. The Westcott[1] convention is an obvious choice. This convention defines an effective cross section, $\hat{\sigma}$, by equating the reaction rate per atom, R, to the product of $\hat{\sigma}$ with nv_o where

n = neutron density, including both thermal and epithermal neutrons,

and v_o = 2200 m/s. Thus,

$$R = n\, v_o\, \hat{\sigma}\ , \text{ or}$$
$$R = \hat{\phi}\ \hat{\sigma}\ . \qquad (5.6.1.1)$$

The flux $\hat{\phi}$ is not be be confused with the conventional flux which is just the thermal neutron density times v_o. $\hat{\phi}$ is also not a true flux since it is not in terms of the true velocity of neutrons in the reactor.

The most convenient manner to determine the Westcott flux in the fuel, where most of the useful reactions take place, is to derive a relationship between the power density and the flux. The fission power generated per unit volume of fuel is given by

$$P = k \hat{\phi} \sum N_f \hat{\sigma}_f (1 + \delta), \qquad (5.6.1.2)$$

where P is the power in megawatts, k is a constant equal to the megawatts per fission per second, the $N_f \hat{\sigma}_f$ are the macroscopic fission cross sections for isotopes fissionable by thermal and epithermal neutrons, and δ is the fast-to-thermal fission ratio, usually defined for uranium only.

For a heat of fission of 202 Mev,

$$k = 3.236 \times 10^{-17} \text{ MW/fission/sec.}$$

The megawatts/ton of fuel is often a convenient unit of power density. Expressing equation 5.6.1.2 in terms of MW/T, the relationship for flux becomes

$$\hat{\phi} = \frac{6.437 \times 10^{11}}{\sum N_f \hat{\sigma}_f (1 + \delta)} \times \left(\frac{MW}{T}\right). \qquad (5.6.1.3)$$

Using representative values of the constants for N Reactor with only U^{235} and U^{238} present in the fuel the relationship between flux and MW/T is

$$\hat{\phi} = 2.44 \times 10^{12} \times \left(\frac{MW}{T}\right) \qquad (5.6.1.4)$$

For 387 tons of fuel and a power of 4000 MW, the average Westcott flux in the fuel is obtained as 2.52×10^{13}.

5.6.2 Plutonium Buildup and U^{235} Burnout Calculations

The differential equations governing the buildup of the plutonium isotopes and the burnout of U^{235} are given below.

$$\frac{dN^{25}}{dt} = -\hat{\phi} N^{25} \hat{\sigma}_a{}^{25}. \qquad (5.6.2.1)$$

$$\frac{dN^{49}}{dt} = \hat{\phi}\Big\{N^{28} \hat{\sigma}_a{}^{28} + \sum_{1} N^1 \hat{\sigma}_f^1 \nu^1 \Big[\epsilon (1 - p) e^{-\tau B g^2} + 1 - \epsilon + \frac{\delta}{\nu^{25}} (\nu^{28} - 1)\Big] - N^{49} \hat{\sigma}_a{}^{49}\Big\}. \qquad (5.6.2.2)$$

$$\frac{dN^{40}}{dt} = \hat{\phi}\ N^{49}\hat{\sigma}_c{}^{49} - \hat{\phi}\ N^{40}\hat{\sigma}_a{}^{40} \quad . \tag{5.6.2.3}$$

$$\frac{dN^{41}}{dt} = \hat{\phi}\ N^{40}\ \hat{\sigma}_c{}^{40} - \hat{\phi}\ N^{41}\hat{\sigma}_a{}^{41} \quad . \tag{5.6.2.4}$$

The sum in (5.6.2.2) is over-all thermally-fissionable isotopes.

The fission rate equation is also of importance.

$$\frac{dN^f}{dt} = \hat{\phi}\Big\{N^{25}\hat{\sigma}_f{}^{25}(1+\nu^{25}\delta') + N^{49}\hat{\sigma}_f{}^{49}(1+\nu^{49}\delta') + N^{41}\hat{\sigma}_f{}^{41}(1+\nu^{41}\delta')\Big\} \quad . \tag{5.6.2.5}$$

where $\delta' = \delta/\nu^{25}$, δ being the fast-to-thermal fission ratio for green uranium.

A convenient method of solving these equations is to introduce a new variable θ which is defined as,

$$\theta = \phi\hat{\sigma}_a{}^{25}t \ , \quad \text{and} \tag{5.6.2.6}$$

which is a measure of U^{235} burnout. Further defining

$$\begin{aligned} N^f/No^{25} &= u, \\ N^{49}/No^{25} &= y, \\ N^{40}/No^{25} &= z, \\ N^{41}/No^{25} &= s, \\ N^{25}/No^{25} &= x, \text{ and} \\ N^{28}/No^{25} &= v, \end{aligned} \tag{5.6.2.7}$$

the differential equations become

$$dx/d\theta = -x, \tag{5.6.2.8}$$

$$dy/d\theta = B + Dx + Ay + Hs \tag{5.6.2.9}$$

$$dz/d\theta = (\hat{\sigma}_a^{49} - \hat{\sigma}_f^{49})y - z\hat{\sigma}_a^{40}, \tag{5.6.2.10}$$

$$ds/d\theta = z\hat{\sigma}_a^{40} - s\hat{\sigma}_a^{41}, \tag{5.6.2.11}$$

$$du/d\theta = xE + yF + sG, \tag{5.6.2.12}$$

where

$$B = \frac{\nu\hat{\sigma}_a^{28}}{\hat{\sigma}_a^{25}},$$

$$D = \frac{\hat{\sigma}_f^{25}}{\hat{\sigma}_a^{25}}\nu^{25}\left[\epsilon(1-p)e^{-\tau B g^2} + 1 - \epsilon + \frac{\delta}{\nu^{25}}(\nu^{28}-1)\right],$$

$$A = \frac{\hat{\sigma}_f^{49}}{\hat{\sigma}_a^{25}}\nu^{49}\left[\epsilon(1-p)e^{-\tau B g^2} + 1 - \epsilon + \frac{\delta}{\nu^{25}}(\nu^{28}-1)\right] - \frac{\hat{\sigma}_a^{49}}{\hat{\sigma}_a^{25}}$$

$$H = \frac{\hat{\sigma}_f^{41}}{\hat{\sigma}_a^{25}}\nu^{41}\left[\epsilon(1-p)e^{-\tau B g^2} + 1 - \epsilon + \frac{\delta}{\nu^{25}}(\nu^{28}-1)\right],$$

$$E = \frac{\hat{\sigma}_f^{25}}{\hat{\sigma}_a^{25}}(1 + \nu^{25}\delta'),$$

$$F = \frac{\hat{\sigma}_f^{49}}{\hat{\sigma}_a^{25}}(1 + \nu^{49}\delta'), \text{ and}$$

$$G = \frac{\hat{\sigma}_f^{41}}{\hat{\sigma}_a^{25}}(1 + \nu^{41}\delta').$$

The solution of equation 5.6.2.c is

$$x = e^{-\theta} = 1 - \theta + \frac{\theta^2}{2!} - \frac{\theta^3}{3!} + \frac{\theta^4}{4!} + \cdots \tag{5.6.2.13}$$

The solution of the other equations follows the method of Cohen and etal[39]. The other quantities are expanded in power series. Writing x as a general power series also,

$$x = d_0 + d_1\theta + d_2\theta^2 + d_3\theta^3 + \ldots ,$$

$$y = a_1\theta + a_2\theta^2 + a_3\theta^3 + \ldots ,$$

$$z = g_1\theta = g_2\theta^2 + g_3\theta^3 + \ldots , \qquad (5.6.2.14)$$

$$s = h_1\theta + h_2\theta^2 + h_3\theta^3 + \ldots , \text{ and}$$

$$u = k_1\theta + k_2\theta^2 + k_3\theta^3 + \ldots .$$

The coefficients can be solved for in the usual manner and the resulting solutions are as follows:

$$y = (B + D)\theta + \sum_{i=2}^{\infty} \left(D\, d_{i-1} + A\, a_{i-1} + H\, h_{i-1} \right) \frac{1}{i}\, \theta^i ,$$

$$z = \sum_{i=2}^{\infty} \left[\left(\hat{\sigma}_a^{49} - \hat{\sigma}_a^{49} \right) a_{i-1} - \hat{\sigma}_a^{40}\, g_{i-1} \right] \frac{1}{i}\, \theta^i ,$$

$$s = \sum_{i=3}^{\infty} \left[\hat{\sigma}_a^{40}\, g_{i-1} - \hat{\sigma}_a^{41}\, h_{i-1} \right] \frac{1}{i}\, \theta^i , \qquad (5.6.2.15)$$

$$u = \sum_{i=1}^{\infty} \left[E\, d_{i-1} + F\, a_{i-1} + G\, h_{i-1} \right] \frac{1}{i}\, \theta^i .$$

Terms out to the tenth power of θ are more than sufficient to accurately determine the solutions. These equations are solved in subroutines of the FLEX and MOFDA codes[6].

5.6.3 Neptunium Production Calculations

The differential equations governing the production of Np^{237} are as follows:

$$\frac{dN^{26}}{dt} = \hat{\phi} N^{25} \hat{\sigma}_c^{25} - N^{26} \hat{\phi} \hat{\sigma}^{26} \quad , \tag{5.6.3.1}$$

$$\frac{dN^{27}}{dt} = \hat{\phi} N^{26} \hat{\sigma}^{26} + \hat{\phi} N^{28} \hat{\sigma}_{n,2n}^{*} - N^{27} \lambda^{27} \quad , \text{ and} \tag{5.6.3.2}$$

$$\frac{dN^{37}}{dt} = N^{27} \lambda^{27} - N^{37} \hat{\sigma}_a^{37} \hat{\phi} \quad . \tag{5.6.3.3}$$

Equation 5.6.3.1 represents the formation of U^{236} from U^{235}. Equation 5.6.3.2 represents the formation of U^{237} from the U^{236} formed from U^{235} or from any U^{236} initially present and also from U^{238}. The U^{238} reaction is an n,2n reaction and such only occurs at fast neutron energies. The n,2n threshold is 5.8 Mev. Thus, the n,2n cross section in 5.6.3.2 is an effective n,2n cross section defined in terms of the Westcott flux, ϕ . Equation 5.6.3.3 represents the formation of Np^{237} from U^{237} by beta decay. The half life is 6.5 days. The equations can be solved most simply by assuming instantaneous decay of U^{237} to Np^{237}, and by separating the production by precursor. The solutions are then

$$N^{37} = N_o^{25} \hat{\sigma}_c^{25} \hat{\sigma}_c^{26} \left[\frac{e^{-\hat{\phi}\hat{\sigma}_a^{25} t}}{(\hat{\sigma}_a^{26} - \hat{\sigma}_a^{25})(\hat{\sigma}_a^{37} - \hat{\sigma}_a^{25})} + \right. \tag{5.6.3.4}$$

$$\left. \frac{e^{-\hat{\phi}\hat{\sigma}_a^{26} t}}{(\hat{\sigma}_a^{25} - \hat{\sigma}_a^{26})(\hat{\sigma}_a^{37} - \hat{\sigma}_a^{26})} + \frac{e^{-\hat{\phi}\hat{\sigma}_a^{37} t}}{(\hat{\sigma}_a^{25} - \hat{\sigma}_a^{37})(\hat{\sigma}_a^{26} - \hat{\sigma}_a^{37})} \right] ,$$

$$N^{37} = \frac{N_o^{26} \hat{\sigma}_c^{26}}{\hat{\sigma}_a^{37} - \hat{\sigma}_a^{26}} \left(e^{-\hat{\phi}\hat{\sigma}_a^{26} t} - e^{-\hat{\phi}\hat{\sigma}_a^{37} t} \right) \quad . \tag{5.6.3.5}$$

$$N^{37} = \frac{N_o^{28} \hat{\sigma}_{n,2n}^{*}}{\hat{\sigma}_a^{37} - \hat{\sigma}_a^{28}} \left(e^{-\hat{\phi}\hat{\sigma}_a^{28} t} - e^{-\hat{\phi}\hat{\sigma}_a^{37} t} \right) \quad . \tag{5.6.3.6}$$

In 5.6.3.6 the absorption cross section for U^{238}, $\hat{\sigma}_a{}^{28}$, is, in contrast to earlier usage, to include the resonance absorption in U^{238} – that is the entire Westcott cross section for U^{238} is to be used (based on an effective resonance integral

Equation 5.6.3.4 can be simplified by expending the exponentials in series. Terms beyond the third power in ϕt are not necessary. In terms of the exposure variable M, MWD/T:

$$N^{37} = N_o{}^{25}\ \hat{\sigma}_c{}^{26}\hat{\sigma}_c{}^{25}\ \frac{M^2}{2}\left[(\alpha^2 B^{-1} + \beta^2 C^{-1} + \gamma^2\ D^{-1}) - \frac{M}{3}(\alpha^3\ B^{-1} + \beta^3\ C^{-1} + \gamma^3\ D^{-1})\right], \quad (5.6.3.7)$$

where

$$\alpha = \frac{1.12 \times 10^{19}\ \hat{\sigma}_a{}^{25}}{H\ N_o{}^{25}\ \hat{\sigma}_f{}^{25}\ (1+\delta)}$$

$$\beta = \frac{1.12 \times 10^{19}\ \hat{\sigma}_a{}^{26}}{H\ N_o{}^{25}\ \hat{\sigma}_f{}^{25}\ (1+\delta)},$$

$$\gamma = \frac{1.12 \times 10^{19}\ \hat{\sigma}_a{}^{37}}{H\ N_o{}^{25}\ \hat{\sigma}_f{}^{25}\ (1+\delta)},$$

$$B = (\hat{\sigma}_a{}^{26} - \hat{\sigma}_a{}^{25})\ (\hat{\sigma}_a{}^{37} - \hat{\sigma}_a{}^{25}),$$

$$C = (\hat{\sigma}_a{}^{25} - \hat{\sigma}_a{}^{26})\ (\hat{\sigma}_a{}^{37} - \hat{\sigma}_a{}^{26}),$$

$$D = (\hat{\sigma}_a{}^{25} - \hat{\sigma}_a{}^{37})\ (\hat{\sigma}_a{}^{26} - \hat{\sigma}_a{}^{37}).$$

H = Heat of fission in Mev.

Equation 5.6.3.5 can be written in terms of the exposure variable, also. Expanding the exponential terms in series and keeping terms up to M^3,

$$N^{37} = \frac{No^{26}\ \hat{\sigma}_c{}^{26}}{\hat{\sigma}_a{}^{37} - \hat{\sigma}_a{}^{26}}\left[(\gamma-\beta)\ M + (\beta^2-\gamma^2)\ \frac{M^2}{2} + (\gamma^3-\beta^3)\ \frac{M^3}{6}\right]. \quad (5.6.3.8)$$

For $\phi t < 3 \times 10^{20}$, Equation 5.6.3.6 can be simplified to

$$N^{37} = \frac{No^{28}\ \hat{\sigma}^{*}_{n,2n}\ \hat{\sigma}_{a}{}^{27}\ \hat{\phi}\ t}{\hat{\sigma}_{a}37 - \hat{\sigma}_{a}\ 28} \quad . \tag{5.6.3.9}$$

The n,2n cross section can be expressed as[20]

$$\hat{\sigma}^{*}_{n,2n} = .0477\ \delta\ \hat{\sigma}_{f}{}^{u} \quad , \tag{5.6.3.10}$$

where $\hat{\sigma}_{f}{}^{u}$ is the Westcott fission cross section for the uranium

$$\hat{\sigma}_{f}{}^{u} = \frac{N_{25}\ \hat{\sigma}_{f}{}^{25}}{N_{25} + N_{28}} \quad .$$

In terms of the exposure variable M (MWD/T)

$$N^{37} = \left(\frac{No^{28}\ 0.0477\delta}{1 + \delta}\right) \frac{1.12 \times 10^{19}\ M}{(N_{25} + N_{28})\ H} \tag{5.6.3.11}$$

5.6.4 Fission Products (Useful)

The useful fission products can be computed from the Perkins-King[21] equations using the ACTICAY[22] program for the IBM-7090.

$$MC_{i}(t) = (8.352 \times 10^{-3})\ P\ (A_{i}e^{-\lambda_{1i}t} + B_{i}e^{-\lambda_{2i}t}), \tag{5.6.4.1}$$

where P is reactor power in megawatts, MC is the megacuries of activity of isotope i at time t after reactor shutdown and λ_{1i} and λ_{2i} are the decay constants associated with the parent nuclide (or nuclides) of the isotope and of the isotope itself, respectively. The constants A_i and B_i are defined as

$$-A_{i} = \frac{Y_{2i} - Y_{1i}}{\lambda_{1i} - \lambda_{2i}} \left[\lambda_{2i}\ (1 - e^{-\lambda_{1i}T})\right] \quad , \text{ and} \tag{5.6.4.2}$$

$$B_i = -\left[\frac{(Y_{2i} - Y_{1i})}{(\lambda_{1i} - \lambda_{2i})}\lambda_{1i} + Y_{1i}\right]\left[1 - e^{-\lambda_{2i}T}\right] \quad (5.6.4.3)$$

where Y_{2i} is the cumulative yield of isotope i, Y_{1i} is the independent yield of isotope i and T is the irradiation time in the reactor in seconds.

5.6.5 Tritium Production Calculations

The differential equation governing the buildup of tritium can be expressed as:

$$\frac{dT^3}{dt} = (\hat{\phi}\ N\hat{\sigma}_a)_{Li^6} \cdot \quad (5.6.5.1)$$

Since the number of Li^6 atoms is very large compared to the number which will react to form tritium, it may be assumed to stay constant. The equation may then be integrated to give

$$N_T{}^3(t) = \left[(\hat{\phi}\ N\hat{\sigma}_a)_{Li^6}\right] t. \quad (5.6.5.2)$$

If the flux in the lithium containing target element is calculable, either absolutely or relative to the flux in the fissionable fuel elements, then the solution of the equation is straightforward.

In most cases, it is not feasible to accurately calculate the flux in the lithium-bearing target element. This is true when lithium-containing control rods are used, or when target elements are interspersed with fissionable fuel elements in the same fuel column (E-N load, for example). In these cases, another approach to the calculation of tritium buildup is necessary.

The number of neutrons absorbed in lithium-containing target elements may be measured by the effect of such absorptions on the reactivity of the reactor. The excess reactivity of the reactor without the target elements is readily calculated using conventional techniques. The reactivity of the reactor with target elements is fixed, since enough target (poison) elements will be added to reduce the excess reactivity to the required level for reactor operation. The multiplication factor, k, expresses the relative number of thermal neutrons absorbed in the fuel element in each successive generation. Since at a constant power level, this ratio must, by definition, be unity, then the number of atoms of tritium produced per thermal neutron absorbed in the fissionable fuel may be stated as Δk_{Li} where Δk_{Li} is the reactivity held in lithium.

If U^{235} is the only material in the fuel, then every neutron absorbed in the fuel destroys a U^{235} atom. Since the fission rate is directly related to the rate of U^{235} burnout, the rate of tritium buildup may thus be related to the fission rate and hence power level. If the fuel also contains U^{238}, part of the thermal neutrons are absorbed in this isotope, and furthermore U^{238} is subject to fission by fast neutrons which increases the fission rate per thermal neutron absorbed. Furthermore, plutonium is built up, which is subject to thermal neutron

absorption and fission. The exact solutions in this case require writing equations for all thermal neutron absorptions in the fissionable fuel, and for the fission rate, and integrating with respect to time as in Section 5.6.2.

A simple, but quite accurate approximation, to the T^3-buildup problem when fuel containing U^{235} and U^{238} is used is to assume that the number of fissions per thermal neutron absorption remains constant throughout the residence time of the fuel. Green fuel parameters may then be used to calculate T^3 buildup. In this case, the number of fissions per thermal absorption is simply

$$\frac{N_{25}\,\hat{\sigma}_{f25}\,(1+\delta)}{N_{25}\,\hat{\sigma}_{a25}+N_{28}\,\hat{\sigma}_{a28}}=\frac{\eta}{\nu_{25}}(1+\delta), \qquad (5.6.5.3)$$

and the number of T^3 atoms per fission is:

$$\frac{\Delta k_{Li}\,\nu_{25}}{\eta\,(1+\delta)}. \qquad (5.6.5.4)$$

Since there are 2.67×10^{21} fissions/MWD, (See Section 5.6.1) the number of T^3 atoms produced per MWD is

$$\frac{\Delta k_{Li}\,\nu_{25}}{\eta\,(1+\delta)} \times 2.67 \times 10^{21}, \qquad (5.6.5.5)$$

and the number of grams of T^3 produced per MWD is

$$\frac{\Delta k_{Li}\,\nu_{25}}{\eta\,(1+\delta)} \times 2.67 \times 10^{21} \times \frac{3.018}{6.023 \times 10^{23}}, \text{ or}$$

$$\frac{\Delta k_{Li}\,\nu_{25}}{\eta\,(1+\delta)} \times (1.338 \times 10^{-2})$$

5.7 Production Yields

5.7.1 Plutonium Buildup and U^{235} Depletion

Theoretical plutonium buildup and U^{235} depletion curves are given in Figure 5.7.1.1, and 5.7.1.2. These results are from FLEX calculations; the

FIGURE 5.7.1.1
PLUTONIUM BUILDUP AND COMPOSITION

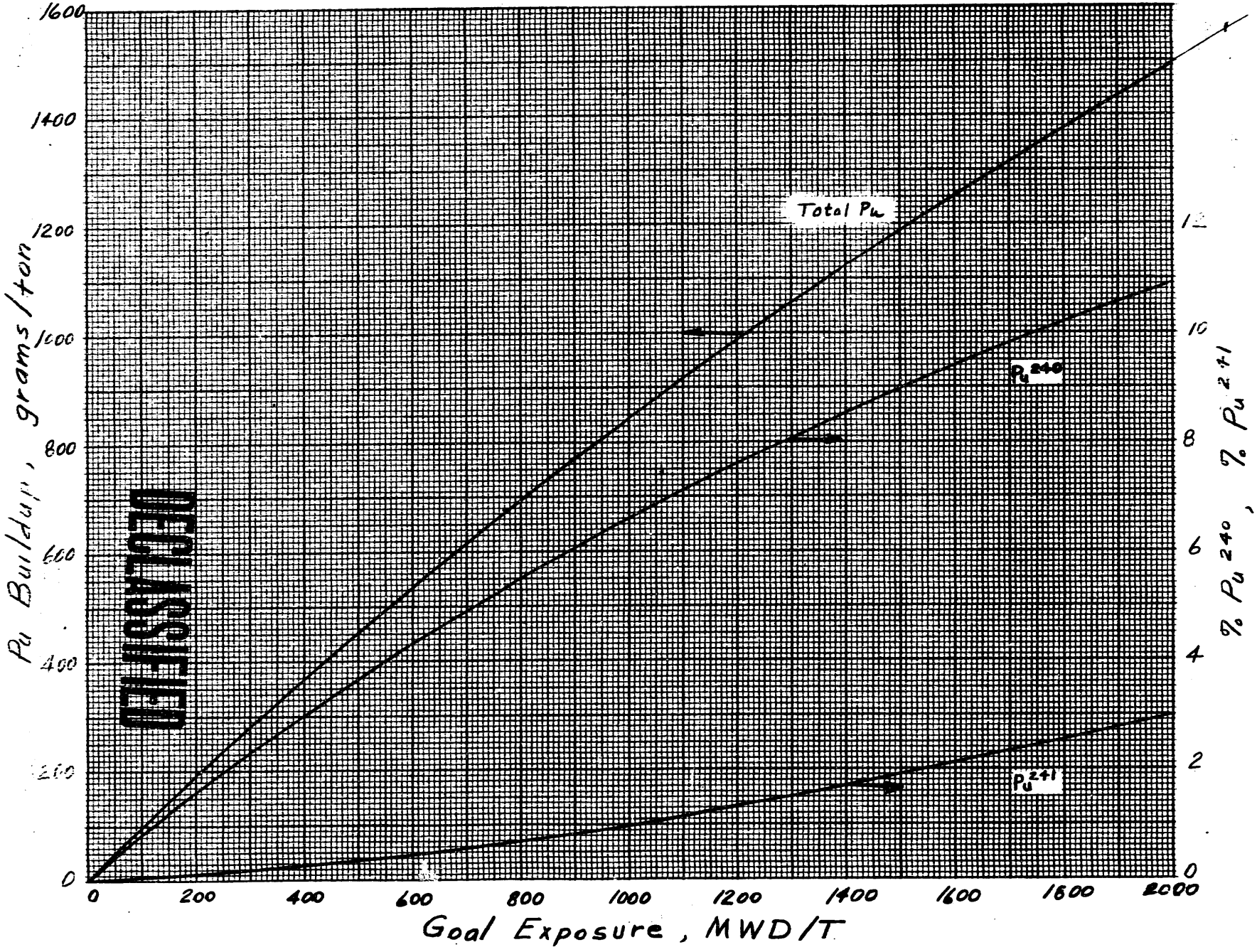

FIGURE 5.7.1.2
ENRICHMENT OF DISCHARGED FUEL

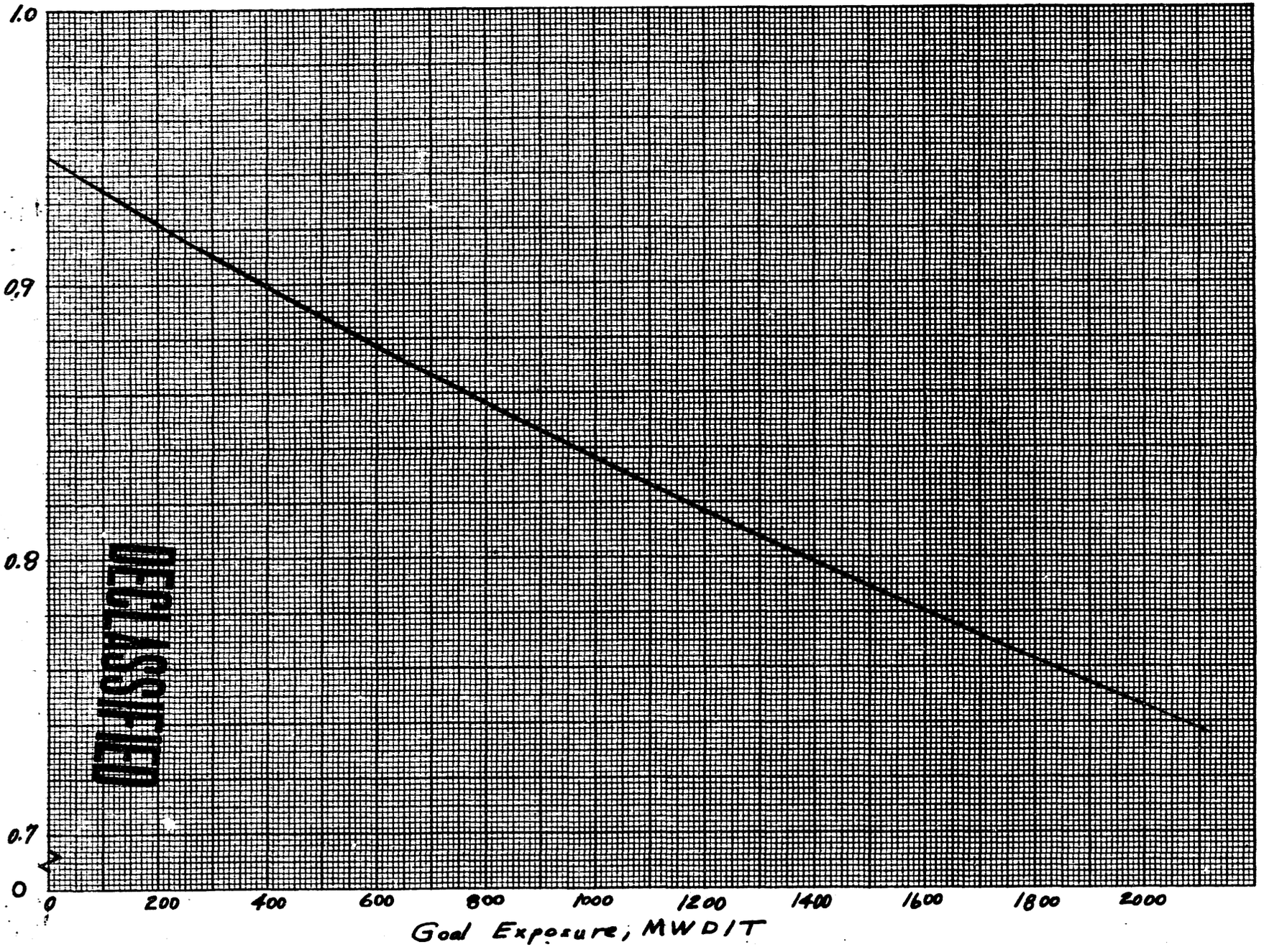

estimated uncertainty in the results is ± five per cent on a relative basis.

5.7.2 U^{236} and Np^{237} Buildup

Theoretical curves of U^{236} and Np^{237} buildup are given in Figures 5.7.2.1 and 5.7.2.2. The neptunium formation rates are given separately for U^{238} and U^{235} precursors. The formation of Np^{237} from any U^{236} initially present in the fuel (as would be the case with fuel recycle) is given in terms of gm/T per initial ppm of U^{236} in the fuel. The U^{236} produced is calculated from the U^{235} burnout of Figure 5.7.1.2 by multiplying the burnout by $\alpha/1+\alpha$, where α is the capture to fission rate of U^{235}. In the NPR hot flux spectrum, the value of α is 0.207.

The expected return of U^{236} in recycled fuel for two blending schemes, 5.0 w/o and 1.2 w/o enriched uranium blend, is shown in Figure 5.7.2.3. The degradation factors are 0.66 and 0.97, respectively for the 1.2 w/o and 5.0 w/o blend. The degradation factor is defined as U^{236} return divided by U^{236} output.

5.7.3 Useful Fission Product Yields

The yields of the fission product Cs^{137}, Sr^{90}, Pm^{147} and Ce^{144} are shown in Table 5.7.3.1 for 58 and 116 day continuous irradiations at 4000 MW. The yields are given as present per ton of fuel at one day following reactor shutdown assuming all fuel at the same exposure. The exposures corresponding to 58 and 116 days are roughly 600 and 1200 MWD/T; 387 tons of uranium are assumed in the loading.

Table 5.7.3.1

Useful Fission Products C/Ton 24 Hours After Shutdown[a]

	600 MWD/T	1200 MWD/T
Cs^{137} (30 y)	1,960	3,920
Sr^{90} (28 y)	2,000	3,990
Pm^{147} (2.6 y)	7,200	16,400
Ce^{144} (285 d)	69,000	129,000

[a]Based on 387 tons.

5.8 Reactor Weighting for Production

Since the flux varies from point to point in a reactor the concentration of products will vary and it is often necessary to define yields averaged over an appropriate reactor volume. The flux varies radially across the fuel element and longitudinally along the fuel column axis. Both variations must be taken into account to obtain a column-averaged yield. Richey's[23] formulation is used as an example in the case of the Pu^{239} concentration y.

FIGURE 5.7.2.1
U^{235} AND U^{236} CONCENTRATIONS
VS
FUEL EXPOSURE

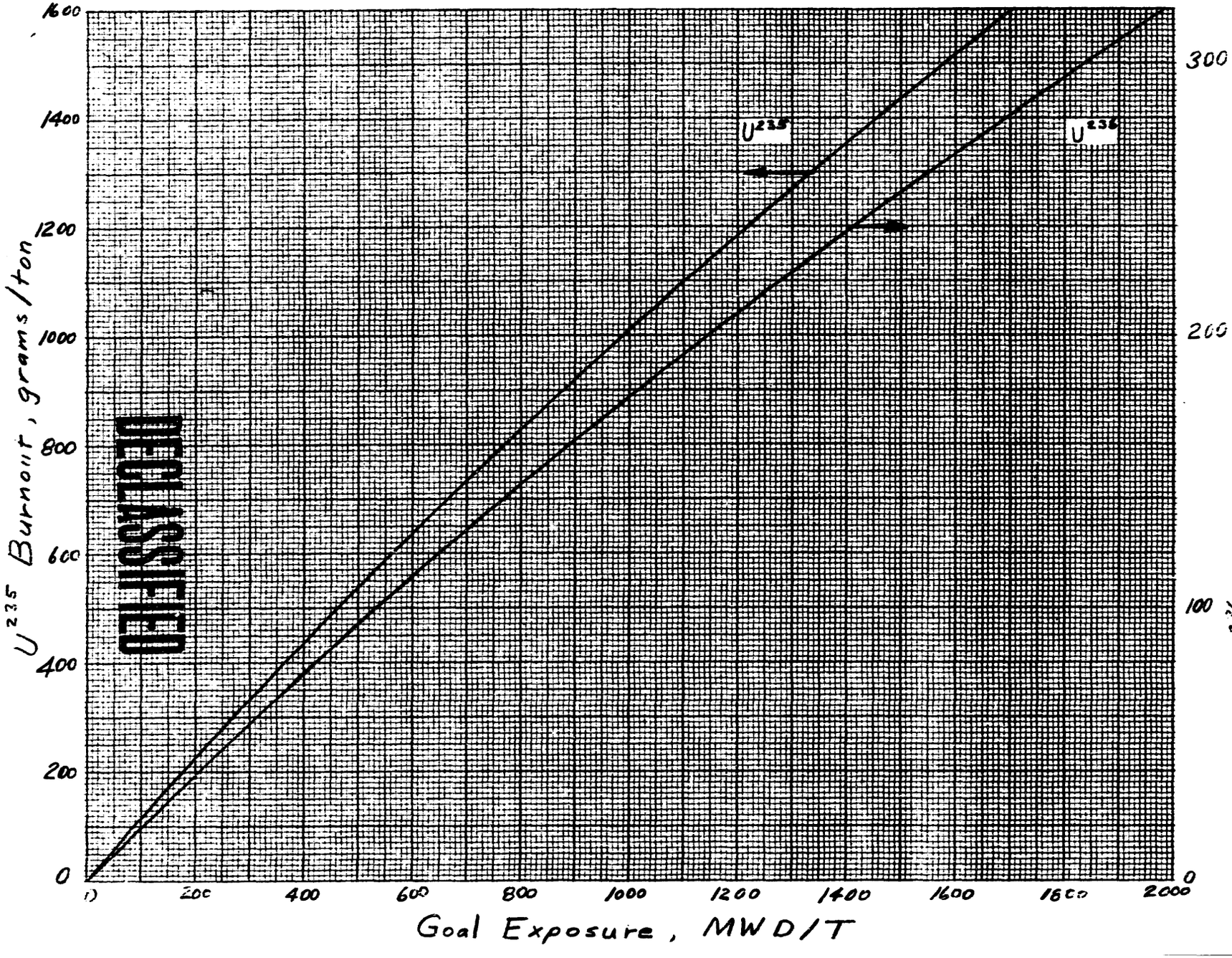

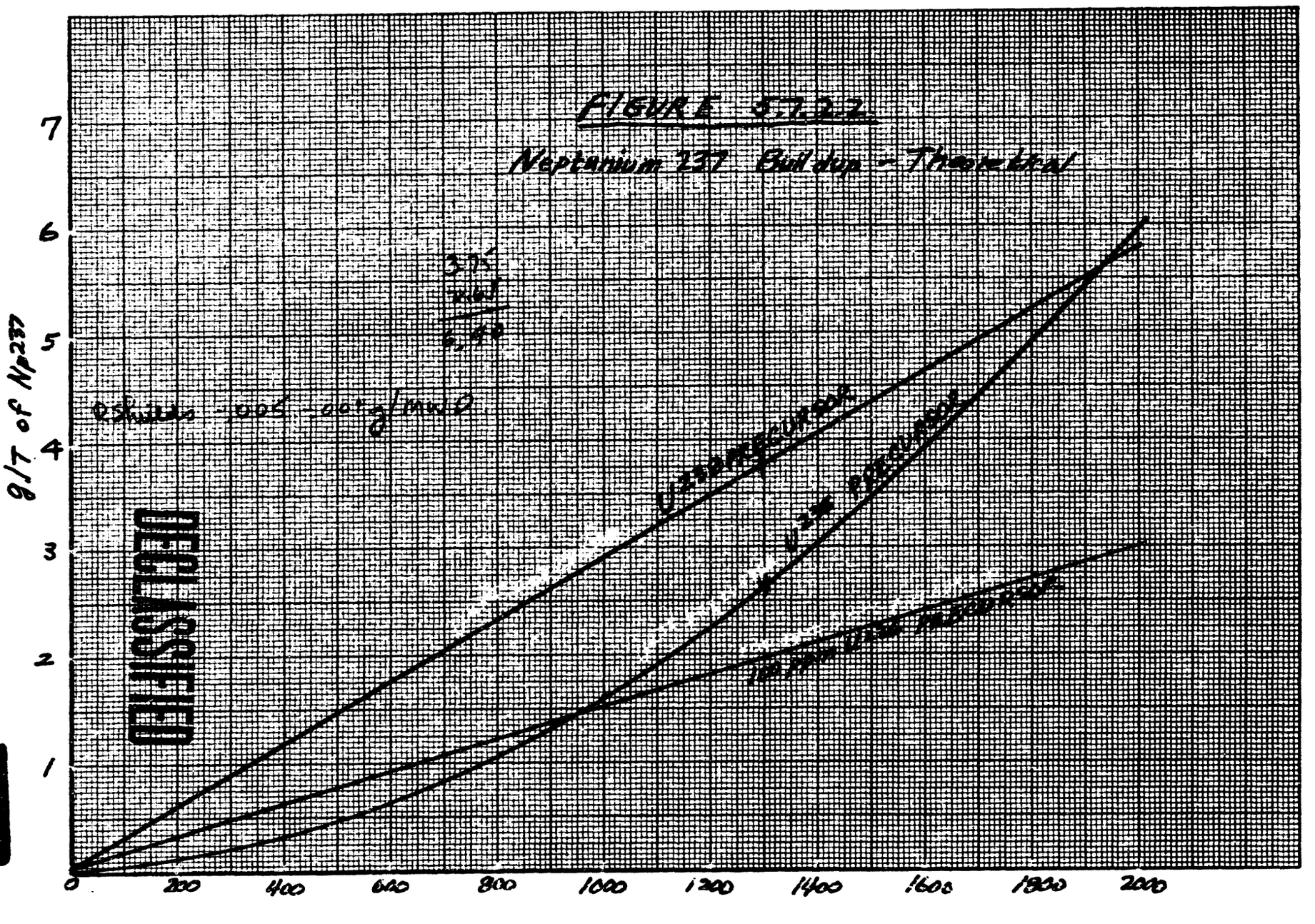
FIGURE 3.7.2.2.
Neptunium 237 Buildup - Theoretical
θ/7 of Np237
FUEL EXPOSURE
0
200
400
600
800
1000
1200
1400
1600
1800
2000
1
2
3
4
5
6
7
CLASSIFIED

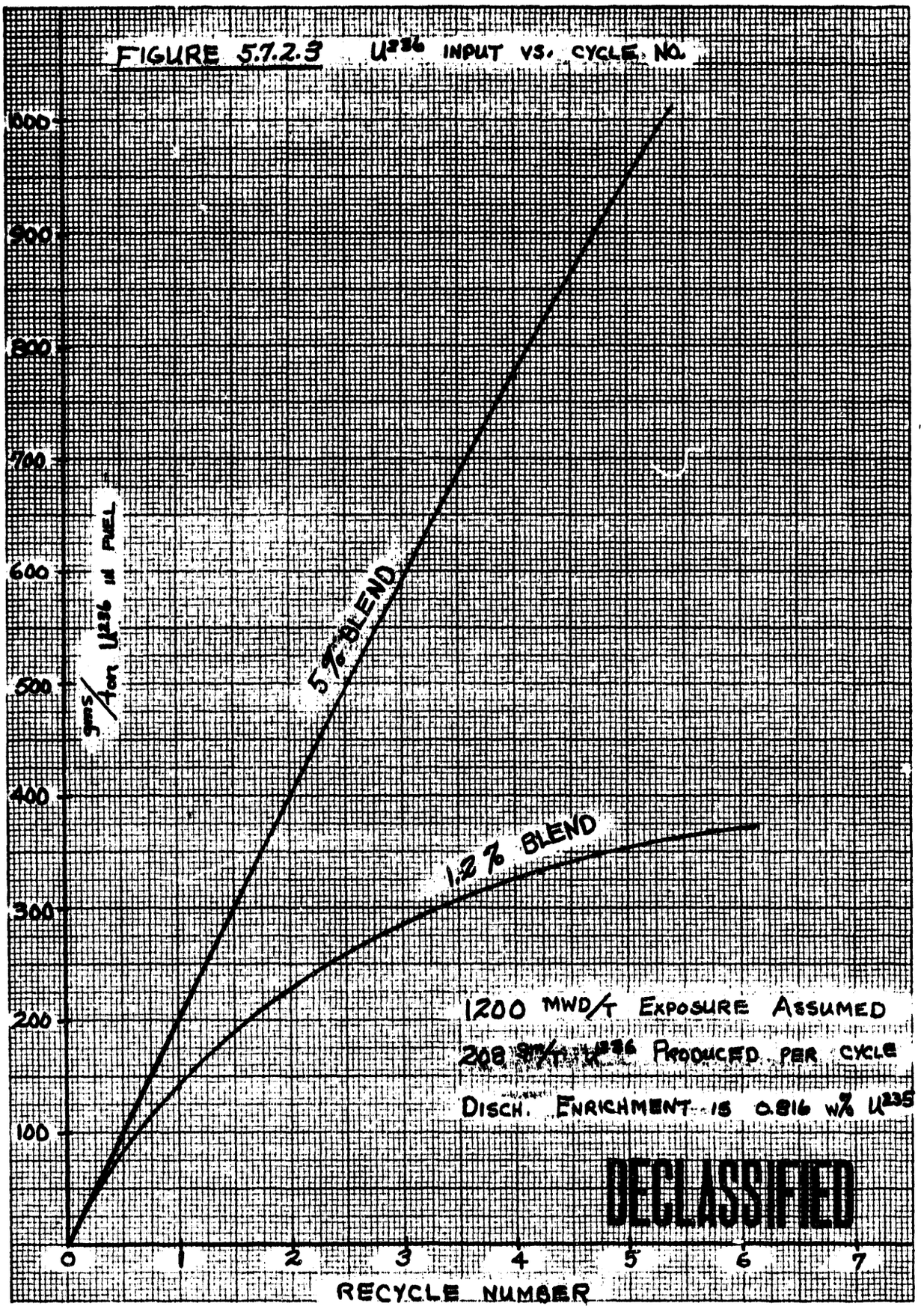

$$y = a_1\theta + a_2\theta + a_3\theta^3 + \ldots \tag{5.8.1}$$

$$\bar{y} = \frac{1}{V}\int_0^V y\,dV, \tag{5.8.2}$$

where V is the total uranium volume in a column. Therefore,

$$\bar{y} = \frac{a_1}{V}\int_0^V \theta\,dV + \frac{a_2}{V}\int_0^V \theta^2\,dV + \ldots \tag{5.8.3}$$

The parameter θ is a function of axial position in the column, radial position from the axis of the fuel and irradiation time, t. One can write

$$\theta = \theta_1(\ell)\,\theta_2(r)\,\theta_3(t), \tag{5.8.4}$$

where

ℓ = distance from front to rear in a column ,

r = radial distance from axis of fuel element .

The first integral in 5.8.3 becomes

$$\frac{a_1 t}{V}\int_0^L\int_{R_{11}}^{R_{12}} 2\pi r\,\theta_1(\ell)\,\theta_2(r)\,dr\,d\ell + \int_0^L\int_{R_{21}}^{R_{22}} 2\pi r\,\theta_1(\ell)\,\theta_2(r)\,dr\,d\ell \ , \tag{5.8.5}$$

where $\theta_3(t) = t$ has been taken outside the integral since it is independent of r and ℓ. The limits in the integrations over r are the inner and outer radii of each part of the concentric tube fuel element; for example R_{22} is the outer radius of the outer fuel tube.

$\theta_1(\ell)$ can be expressed as a normalization factor times a flux function which will be assumed to be sinusoidal.

$$\theta_1(\ell) = \theta_{1,max} \sin\left[\frac{\pi(\ell + \lambda)}{L + 2\lambda}\right] = \theta_{1,max}\, \psi(\ell), \qquad (5.8.6)$$

where λ is the front and rear extrapolation length.

$\theta_2(r)$ can also be expressed by a normalization factor times a flux function.

$$\theta_2(r) = \theta_{2,max}\, \beta(r). \qquad (5.8.7)$$

The function $\beta(r)$ must be obtained from the solution to the transport equation. For the N Reactor fuel geometry $\beta(r)$ cannot be simply expressed.

The first integral can then be written

$$\frac{a_1}{V}\int_0^V \theta dV = \frac{a_1\theta_{max}}{V}\left\{\int_0^L \psi(\ell)\, d\ell\left[\int_{R_{11}}^{R_{12}} 2\pi r\, \beta(r)\, dr + \right.\right.$$

$$\left.\left.\int_{R_{21}}^{R^{22}} 2\pi r\, \beta(r)\, dr\right]\right\} . \qquad (5.8.8)$$

$$= a_1\, \theta_{max}\, w_1^{\ell}\, w_1^{r} = a_1\, \theta_{max}\, w_1$$

where

$$w_1^{\ell} = \frac{1}{L}\int_0^L \psi(\ell)\, d\ell ,$$

$$w_1^r = \frac{L\,2\pi}{V}\left[\int_{R_{11}}^{R_{12}} \rho(r)\,r\,dr + \int_{R_{21}}^{R_{22}} \rho(r)\,r\,dr\right], \text{ and}$$

$$w_1 = w_1^r + w_1^{\ell}.$$

By similar techniques, for any term of the series (5.8.3),

$$w_n^{\ell} = \frac{1}{L}\int_0^L \psi^n(\ell)\,d\ell\,,$$

$$w_n^r = \frac{2\pi L}{V}\left[\int_{R_{11}}^{R_{12}} \rho^n(r)\,r\,dr + \int_{R_{21}}^{R_{22}} \rho^n(r)\,r\,dr\right], \text{ and}$$

$$w_m = w_m^r + w_m^l\,.$$

Therefore,

$$\bar{y} = a_1 w_1 \theta_{max} + a_2 w_2 \theta^2_{max} + \ldots . \qquad (5.8.9)$$

6. Reactivity Transients

6.1 Introduction

The sources of the reactivity variations over a normal operating cycle, including shutdown and startup, in N Reactor are similar to those in the other Hanford reactors. However, higher power levels, higher temperatures, higher fuel exposures and the undermoderated nature of the N lattice act to increase the normal reactivity variations of the Hanford-type reactor and to introduce new sources of reactivity variations not present in the older Hanford reactors.

6.2 Temperature Coefficients of Reactivity

The temperature-dependent sources of reactivity variations in N Reactor include, in addition to the usual fuel and graphite heating effects (which are nuclear) one associated with coolant heating (which is both nuclear and physical). The fuel temperature and coolant temperature coefficients of reactivity are negative; the graphite temperature coefficient is positive. Other temperature-associated physical effects, such as fuel expansion, are too small to produce any significant reactivity coefficient.

Except for the Doppler coefficient (in a dry lattice) there are no experimental determinations of the N-Reactor temperature coefficients. In most cases the calculational techniques are extensions of approximate methods which have been fairly successfully used in the old Hanford reactor calculations. There is perhaps no other area of physics which is more uncertain than the graphite and coolant temperature coefficients; the information presented here is therefore the best information available prior to startup and may after further investigations change somewhat. However, the gross effects to be described are felt to be fairly correct and any differences should occur in the details.

For an actual operating reactor, the calculation of the over-all temperature coefficient is complicated by the fact that the temperatures will vary over the reactor. It is simpler for discussion purposes to describe the temperature coefficient in terms of average temperatures which are properly weighted from a full pile reactivity standpoint. The simplest temperature weighting is by the square of the neutron flux.

$$\bar{T}_{pile} = \int_{pile} \phi^2(\vec{r})\, T(\vec{r})\, dr \Big/ \int_{pile} \phi^2(\vec{r})\, d\vec{r}, \qquad (6.2.1)$$

where $\phi(\vec{r})$ and $T(\vec{r})$ are the spatially-dependent temperature and macroscopic flux. In N Reactor an average fuel, graphite and coolant temperature must be thus calculated.

The temperature coefficients of N Reactor are most simply obtained by using the various IBM-7090 physics programs described earlier.[6] The average graphite temperature coefficient, for example, can be determined by computing k for an initial graphite temperature T_g and for a higher graphite temperature $(T_g + \Delta T_g)$ and dividing the difference by the change in temperature ΔT_g.

$$\overline{\frac{1}{k}\frac{\Delta k}{\Delta T_g}}\Bigg)_{T_w,\,T_f} = \frac{k\,(T_g) - k\,(T_g + \Delta T_g)}{k\,(T_g)\,\Delta T_g}\Bigg)_{T_w,\,T_f} \qquad (6.2.2)$$

The other temperatures are held fixed in such a calculation. The average temperature coefficient can be approximated (correct to first order) as a sum of average temperature coefficients of the individual lattice parameters.

$$\overline{\frac{1}{k}\frac{\Delta k}{\Delta T}} = \overline{\frac{1}{\eta}\frac{\Delta \eta}{\Delta T}} + \overline{\frac{1}{f}\frac{\Delta f}{\Delta T}} + \overline{\frac{1}{\epsilon}\frac{\Delta \epsilon}{\Delta T}} + \overline{\frac{1}{p}\frac{\Delta p}{\Delta T}}$$

$$- B^2\left(\frac{\overline{\Delta \tau}}{\Delta T} + \frac{1}{1 + L^2B^2}\,\frac{\overline{\Delta L^2}}{\Delta T}\right). \qquad (6.2.3)$$

Equation (6.2.3) is exact in the limit $\Delta T \to 0$ and is sufficiently accurate for temperature changes in the N Reactor to be useful. Equation 6.2.3 can be then written for each temperature, where only the constants which vary significantly with each temperatures are included.

$$\overline{\frac{1}{k}\frac{\Delta k}{\Delta T_g}}\Bigg)_{T_w,T_f} = \overline{\frac{1}{\eta}\frac{\Delta \eta}{\Delta T_g}} + \overline{\frac{1}{f}\frac{\Delta f}{\Delta T_g}} - B^2\left(\frac{\overline{\Delta \tau}}{\Delta T_g} + \frac{1}{1+L^2B^2}\,\frac{\overline{\Delta L^2}}{\Delta T_g}\right), \qquad (6.2.4)$$

$$\overline{\frac{1}{k}\frac{\Delta k}{\Delta T_w}}\Bigg)_{T_f,\,T_g} = \overline{\frac{1}{\eta}\frac{\Delta \eta}{\Delta T_w}} + \overline{\frac{1}{f}\frac{\Delta f}{\Delta T_w}} + \overline{\frac{1}{\epsilon}\frac{\Delta \epsilon}{\Delta T_w}} + \overline{\frac{1}{p}\frac{\Delta p}{\Delta T_w}} \qquad (6.2.5)$$

$$- B^2\left(\frac{\overline{\Delta \tau}}{\Delta T_w} + \frac{1}{1 + L^2B^2}\,\frac{\overline{\Delta L^2}}{\Delta T_w}\right),$$

$$\overline{\frac{1}{k}\frac{\Delta k}{\Delta T_f}}\Bigg)_{T_w,\,T_g} = \overline{\frac{1}{p}\frac{\Delta p}{\Delta T_f}}\,. \qquad (6.2.6)$$

The total temperature coefficient cannot be easily stated since none of the separate temperatures (graphite, fuel and coolant) are representative of a single reactor temperature (as would be the case in a homogeneous reactor). The temperatures are all related to the power of the reactor, however, (assuming constant coolant flow and inlet coolant temperature) and it is sometimes useful to define a power coefficient of reactivity as follows:

$$\frac{1}{k}\frac{dk}{dP} = \frac{1}{k}\frac{\partial k}{\partial T_g}\frac{dT_g}{dP} + \frac{1}{k}\frac{\partial k}{\partial T_w}\frac{dT_w}{dP} + \frac{1}{k}\frac{\partial k}{\partial T_f}\frac{dT_f}{dP} \qquad (6.2.7)$$

The power coefficient is more convenient to use in reactor operation since the power is measured directly whereas the individual temperatures are often not measured. Usually, the power coefficient is determined from operational experience in the reactor and once known can be correlated with the temperature coefficient if the temperature-power relationships are known.

6.2.1 Graphite Temperature Coefficient of Reactivity

The average graphite temperature coefficient is given in Equation 6.2.4. The terms involving η, f and L^2 involve variations in thermal cross sections of the various reactor materials with neutron energy. Since the graphite is the principal moderator in the reactor its physical temperature determines to a large degree the temperatures of the thermal neutrons in the reactor. (As is shown later the coolant temperature also plays an important role in determining the neutron temperature). For the simplest model, then, of a Maxwellian thermal flux distribution, a characteristic neutron temperature can be defined which is a function of T_g (and T_w).

$$T_n = T_n\,(T_g,\ T_w) \qquad (6.2.1.1)$$

In general, the neutron temperature will vary over the lattice and its calculation is exceedingly complex. The approximation used in the MOFDA and FLEX physics programs has been described earlier (See Section 2.).

The η- coefficient is simplest to calculate since it involves at most only two regions of the lattice cell (the two fuel regions). The following equations illustrate the form of the η -coefficients for the simple case where U^{235} is the only thermally-fissionable isotope present.

$$\eta = \frac{\nu_5 N_5 \sigma_{f5}}{N_5 \sigma_{a5} + N_8 \sigma_{a8}} = \frac{\nu_5}{1 + \alpha_5 + \frac{N_8}{N_5}\frac{\sigma_{a8}}{\sigma_{f5}}} \qquad (6.2.1.2)$$

$$\frac{1}{\eta}\frac{\partial \eta}{\partial T_g} = \frac{1}{\eta}\frac{\partial \eta}{\partial T_n}\frac{\partial T_n}{\partial T_g}\Bigg)_{T_w} = \frac{1}{\eta}\frac{T_\eta}{T_6}\Bigg)_{T_w}\left(\frac{\partial \eta}{\partial \alpha_5}\frac{d\alpha_5}{dT_n} + \frac{\partial \eta}{\partial \sigma_{a8}}\frac{d\sigma_{a8}}{dT_n}\right.$$

(6.2.1.3)

$$\left. + \frac{\partial \eta}{\partial \sigma_{f_5}}\frac{d\sigma_{f_5}}{d\,T_n}\right).$$

ν_5 is assumed independent of energy. The Westcott cross sections defined earlier can be used to obtain the variations of the cross sections with neutron temperature. (The use of Westcott cross sections in η has the effect of taking into account epithermal absorptions as well as thermal absorptions in all isotopes (in U^{238} only 1/v-law absorptions are included).

The averaged η -coefficient, $\overline{1/\eta\ \Delta\eta/\Delta\ T_g}$, as determined from MOFDA calculations averaged over a graphite temperature range of 20 to 550 C and with equilibrium coolant temperature and density (232 C and 0.82 gm/cm^3) is -1.0×10^{-5}/°C in the reactor with green fuel and -5.4×10^{-6}/°C in the reactor with an average fuel exposure of 700 MWD/T. The coefficient is less negative for the exposed fuel due to the positive temperature coefficient of the plutonium part of .

The f-coefficient is not amenable to a simple calculation since the knowledge of the neutron temperature and flux in each part of the lattice cell is required. The calculation of the fine flux structure across the cell requires the solution to the Boltzman transport equation. (The FLEX and MOFDA codes employ the P_3 approximation to the transport equation.) The same is true for the L^2-coefficient.

The averaged f-coefficient, $\overline{1/f\ \Delta f/\Delta\ T_g}$, as determined from MOFDA calculations under the same conditions as for the η -coefficient, is $+6.4 \times 10^{-5}$/°C in the green reactor and $+6.2 \times 10^{-5}$/°C in the 700 MWD/T reactor.

The averaged L^2-coefficient, $-B^2\ \frac{\overline{\Delta L^2}}{\Delta\ T_g}\ \frac{1}{1 + L^2 B^2}$ is -7.5×10^{-7}/°C in the green reactor and -5.9×10^{-7}/°C in the 700 MWD/T reactor.

The variation in the Fermi age, τ , with graphite temperature arises from the fact that the neutrons have to slow down over a smaller energy range as the neutron temperature increases. The coefficient is small and positive and for a hetereogeneous reactor is difficult to calculate. For these reasons it can be neglected.

The graphite coefficients are summarized in Table 6.2.1.1.

Table 6.2.1.1

Average Graphite Temperature Coefficient Over 20 - 550 C
(For Equilibrium Coolant Conditions)

	Green Fuel	700 MWD/T Average Exposure
$\overline{1/\eta \ \Delta\eta/\Delta T_g}$	$-1.0 \times 10^{-5}/^{\circ}C$	$-5.4 \times 10^{-6}/^{\circ}C$
$\overline{1/f \ \Delta f/\Delta T_g}$	$+6.4 \times 10^{-5}/^{\circ}C$	$+6.2 \times 10^{-5}/^{\circ}C$
$-B^2 \ \overline{\Delta\tau/\Delta T_g}$	negligible	negligible
$-B^2/(1 + L^2B^2) \ \overline{\Delta L^2/\Delta T_g}$	$-7.5 \times 10^{-7}/^{\circ}C$	$-5.9 \times 10^{-7}/^{\circ}C$
$\overline{1/k \ \Delta k/\Delta T_g}$	$+5.3 \times 10^{-5}/^{\circ}C$	$+5.6 \times 10^{-5}/^{\circ}C$

It is of interest to note that the exposure dependence of the graphite coefficient in the NPR is not as pronounced as that observed in the earlier Hanford reactors. This result is due of course to the higher U^{235} enrichment which tends to lessen the plutonium effect, at least at the exposures considered here.

The graphite coefficient is not a linear function of graphite temperature. At low temperatures the coefficient is considerably larger than the averages given in Table 6.2.2.1 and at higher temperatures the coefficient is less. The integral graphite temperature reactivity effect is shown in Figure 6.2.1.1. (See Figure C-4 of HW-71408 VOL2) as a function of local graphite temperature. The slope of the curves is the differential coefficient $1/k \ dk/dT_g$.

6.2.2 Coolant Temperature Coefficient of Reactivity

The coolant coefficient is given in Equation 6.2.5. The term involving ϵ is related to the coolant density variation. The terms involving η, f, L^2, p and τ are related to both the coolant density and temperature variations.

The ϵ -coefficient is simplest to compute. Basically, what is involved is a reduction in the shielding effect of the water within the fuel element to the interaction of fast neutrons between the concentric fuel tubes. The calculation of ϵ is made by homogenizing the fuel, cladding and coolant internal to the fuel assembly, and calculating the collision probabilities for the three fast neutron groups described in Section 2.5.2 on the fast effect calculation. In equation 2.5.1 for ϵ, the quantities δ, N_A, N_B, N_C and J_A are all dependent on the collision probabilities and hence the coolant density. The complete total

Figure 6.2.1.1 is a plot of the integral graphite temperature coefficient and is identical to Figure C-4 of HW-71408 VOL2.

differential is not repeated here but the general expression for the ϵ -part of the coolant temperature coefficient is functionally as follows.

$$\frac{1}{\epsilon}\frac{d\epsilon}{dT_w} = \frac{1}{\epsilon}\frac{d\epsilon}{d\rho_w}\frac{d\rho_w}{dT_w} = \frac{1}{\epsilon}\frac{d\rho_w}{dT_w}\left(\frac{\partial\epsilon}{\partial\delta}\frac{d\delta}{d\rho_w} + \frac{\partial\epsilon}{\partial N_A}\frac{dN_A}{d\rho_w} + \cdots\right) . \quad (6.2.2.1)$$

There is no exposure-dependence on the ϵ -coefficient. The theoretical value of the average value of this coefficient over the coolant temperature range is $\sim$ $+ 4 \times 10^{-6}/^{\circ}C$.

The p-coefficient is also fairly straightforward, and again the effect is related to the water density change primarily, although there is a slight effect associated directly with the water temperature, which is connected with the Doppler effect.

There are two distinctive water density effects on the resonance escape probability. Firstly, the reduction of the water density makes the lattice even more under-moderated and thus increase the importance of resonance capture. Secondly, the reduction of water density in the coolant internal to the fuel element decreases the effective resonance integral (lower surface-to-mass ratio) and thus decreases the importance of resonance capture. Thus, the two effects are opposite in sign; the former effect is dominant so the net coolant temperature coeffient of p is negative.

The coefficient can be written in functional notation as follows:

$$\frac{1}{p}\frac{\partial p}{\partial T_w} = \frac{1}{p}\frac{\partial p}{\partial\rho_w}\frac{d\rho_w}{dT_w} = \frac{1}{p}\frac{d\rho_w}{dT_w}\left(\frac{\partial p}{\partial RI}\frac{\partial RI}{\partial\rho_w} + \frac{\partial p}{\partial\Sigma_{sw}}\frac{\partial\Sigma_{sw}}{\partial\rho_w}\right), \quad (6.2.2.2)$$

or $$\frac{1}{p}\frac{\partial p}{\partial T_w} = \left(\frac{1}{p}\frac{\partial p}{\partial T_w}\right)_A + \left(\frac{1}{p}\frac{\partial p}{\partial T_w}\right)_B, \text{ where}$$

$$\left(\frac{1}{p}\frac{\partial p}{\partial T_w}\right)_A = \frac{1}{p}\frac{d\rho_w}{dT_w}\frac{\partial p}{\partial RI}\frac{\partial RI}{\partial\rho_w}, \text{ and}$$

$$\left(\frac{1}{p}\frac{\partial p}{\partial T_w}\right)_B = \frac{1}{p}\frac{d\rho_w}{dT_w}\frac{\partial p}{\partial\Sigma_{sw}}\frac{\partial\Sigma_{sw}}{\partial\rho_w} .$$

The coefficient is quite insensitive to fuel exposure and is not linear over the operating water density range in the N Reactor. The theoretical value of $1/p\Delta p/\Delta T_w$ is $-7.8 \times 10^{-5}/C$. The coefficient is seen to be quite large which is indicative of a fairly undermoderated lattice.

The behavior of the thermal utilization on coolant temperature variation is much more complex then either that for ϵ and p. There are several distinct effects:

1) Reduction of water density removes poison from the lattice and decreases the cell disadvantage factor*

2) Reduction of water density reduces the cooling effect of the water on the neutron temperature in the fuel which also decreases the cell disadvantage factor.

3) Increasing the water temperature increases the neutron temperature in the fuel more than in the graphite. This reduces the absorptiveness of the uranium to thermal neutrons which also decreases the cell disadvantage factor.

4) Increasing the water temperature and reducing the density increases the neutron temperature in the water which reduces the poisoning effect of the water and also decreases the cell disadvantage factor.

Effect 1) and 4) are positive and effects 2), and 3) are negative.

Since the calculation of f first requires a calculation of the neutron flux distribution across the lattice cell (disadvantage factor) and then a computation of the relative absorptions in each cell region (See Equation 2.5.4.1) and both these parts of the calculations depend on the cross sections, the functional dependence of f on the water temperature ultimately reduces to just one of cross section dependence which in turn depend on the coolant temperature and density. As a first approximation, only the uranium and coolant cross sections need be considered as changing enough to contribute to the coolant temperature coefficient of f. In functional notation each of the four effects can be identified. Defining T_w and ρ_w as the physical temperature and density of the coolant, respectively, and Θ_u and Θ_w as the neutron temperatures in the uranium and coolant, respectively, the functional dependencies can be written as follows:

* For a simple uranium-graphite lattice the cell disadvantage factor is defined as the ratio of the average flux in the graphite to the average flux in the fuel. For the N lattice the concept of a cell disadvantage factor can be carried over to represent the average flux in a homogenized region external to the fuel element to the average flux in a homogenized region internal to the outer diameter of the fuel element. Thus, decreasing the cell-disadvantage factor can be pictured as a flattening effect on the microscopic flux distribution across a lattice cell.

$$f = f\,(\Sigma_{au}, \Sigma_{aw}, \ldots.),$$

$$\Sigma_{au} = \Sigma_{au}\,(\theta_u, \ldots),$$

$$\Sigma_{aw} = \Sigma_{aw}\,(\rho_w, \theta_w \ldots), \qquad (6.2.2.3)$$

$$\theta_u = \theta_u\,(T_w, \rho_w, \ldots),$$

$$\theta_w = \theta_w\,(T_w, \rho_w, \ldots).$$

Then, the total differential is

$$\frac{df}{dT_w} = \left\{\frac{\partial f}{\partial \Sigma_w}\ \frac{\partial \Sigma_w}{\partial \rho_w}\ \frac{d\rho_w}{dT_w}\right\}_1 + \left\{\frac{\partial f}{\partial \Sigma_u}\ \frac{\partial \Sigma_u}{\partial \theta_u}\ \frac{\partial \theta_u}{\partial \rho_w}\ \frac{d\rho_w}{dT_w}\right\}_2 + \qquad (6.2.2.4)$$

$$\left\{\frac{\partial f}{\partial \Sigma_u}\ \frac{\partial \Sigma_u}{\partial \theta_u}\ \frac{\partial \theta_u}{\partial T_w}\right\}_3 + \left\{\frac{\partial f}{\partial \Sigma_w}\ \frac{\partial \Sigma_w}{\partial \theta_w}\left(\frac{\partial \theta_w}{\partial T_w} + \frac{\partial \theta_w}{\partial \rho_w}\ \frac{d\rho}{dT_w}\right)\right\}_4.$$

where subscripts on the curly braces refer to the four effects described earlier.

The coolant temperature coefficient of f is a function of fuel exposure since plutonium and uranium have different temperature dependences in these cross sections. Also, the coolant temperature coefficient of f is dependent on the graphite temperature. For cold graphite and green fuel the theoretical average coolant temperature coefficient $1/f\ \frac{\Delta f}{\Delta T_w}$ is $+1.3 \times 10^{-5}/^{\circ}C$.

The behavior of η with coolant temperature is connected solely with the effects on the neutron temperature in the fuel, thus

$$\eta = \eta\,(\theta_u),$$

$$\theta_u = \theta_w\,(T_w, \rho_w, \rho_1 \ldots.) \qquad (6.2.2.5)$$

$$\frac{d\eta}{dT_w} = \frac{\partial \eta}{\partial \theta_u}\left(\frac{\partial \theta_u}{\partial T_w} + \frac{\partial \theta_u}{\partial \rho_w}\frac{d\rho_w}{dT_w}\right). \qquad (6.2.2.6)$$

The coolant temperature coefficient of η is also exposure-dependent and a function of graphite temperature. For cold graphite and green fuel the theoretical value of $\overline{1/\eta \; \Delta\eta/\Delta T_w}$ is $-4.9 \times 10^{-5}/^{o}C$.

The variation in τ, with coolant temperature is linked with the decreased moderating effect as the coolant density is reduced. Thus, the age will increase as the coolant is heated. There is also the same effect discussed earlier with respect to graphite temperature, and that is that as the water temperature is raised, the general neutron temperature is raised and hence the neutrons have to slow down over a smaller range to reach thermal equilibrium. This latter effect is negligible, however. The calculated τ-coefficient $\overline{-B^2 \; \Delta\tau/\Delta T_w}$ for cold graphite and green fuel is $-5.6 \times 10^{-6}/^{o}C$.

The variation of L^2 with coolant temperature arises from both a reduction in coolant density which removes neutron absorbers from the lattice and an elevating of the general neutron temperature which reduces the over-all absorption cross sections and allows the neutrons to diffuse longer. The calculated average value of $\overline{-B^2(1 + L^2B^2)^{-1} \; \Delta L^2/\Delta T_w}$ for cold graphite and green fuel is $-3 \times 10^{-6}/^{o}C$.

The green fuel, cold graphite coolant coefficients are summarized in Table 6.2.2.1.

Table 6.2.2.1

Theoretical Average Coolant Temperature Coefficient

Over 20 - 230 C

(For Cold Graphite, Green Fuel)

$\overline{\frac{1}{\eta}\frac{\Delta\eta}{\Delta T_w}}$	$-4.9 \times 10^{-5}/^{o}C$
$\overline{\frac{1}{\epsilon}\frac{\Delta\epsilon}{\Delta T_w}}$	$-4 \times 10^{-6}/^{o}C$
$\overline{\frac{1}{p}\frac{\Delta p}{\Delta T_w}}$	$-7.8 \times 10^{-5}/^{o}C$
$\overline{\frac{1}{f}\frac{\Delta f}{\Delta T_w}}$	$+1.3 \times 10^{-5}/^{o}C$
$\overline{-B^2\frac{\Delta\tau}{\Delta T_w}}$	$-5.6 \times 10^{-6}/^{o}C$
$\overline{-B^2(1 + L^2B^2)^{-1}\frac{\Delta L^2}{\Delta T_w}}$	$-3 \times 10^{-6}/^{o}C$
$\overline{\frac{1}{k}\frac{\Delta k}{\Delta T_w}}$	$-11.7 \times 10^{-5}/^{o}C$

The total coolant coefficient can be expressed as a sum of two terms one relating to temperature alone and one relating to density alone. This allows a comparison with an experimental determination of the coolant density coefficient[12]. The theoretical breakdown for the green fuel, cold graphite, coolant coefficient is

$-9.1 \times 10^{-5}/C$ (Temp. only), and

$+3.1 \times 10^{-2}/g\text{-}cm^3$ (Density only).*

The experimental coolant density measurements[12] indicate $+4.6 \times 10^{-2}/g\text{-}cm^3$ (Density only)

Assuming the experimental result is closer to being correct than the theoretical result, the total coefficient in terms of the temperature variable (making no correction on the temperature-alone part) becomes $-13 \times 10^{-5}/^{o}C$ for the cold graphite, green fuel case instead of $-11.7 \times 10^{-5}/^{o}C$.

6.2.3 Doppler Coefficient of Reactivity

The Doppler coefficient has been measured for a prototypical N fuel element in the dry lattice[24]. The temperature range of the experiment was 297 K to 1241 K (24 C to 968 C). The measured change in k_{∞} was (T in ^{o}K).

$$\Delta k_{\infty}(T) = -(1 \pm 0.06)10^{-3}\Big\{ (1.790 \pm 0.006)(T_1^{1/2}-T_o^{1/2}) + 0.810 \pm 0.003\, U\,(T_i - 960)+(0.569 \pm 0.002)U(T_i-1090)\Big\} \qquad (6.2.3.1)$$

The unit functions $U(T_i-T_j) = \begin{matrix} 0, & T_i \leq T_j \\ 1, & T_i > T_j \end{matrix}$

are introduced to describe the change observed in k_{∞} due to the volume expansions when the $\alpha \rightarrow \beta$ and $\beta \rightarrow \gamma$ phase transformations were passed through. These are not part of the true Doppler effect.

Over the N-Reactor fuel temperature range of 20 - 380 C, one can obtain from the above expression and the experimental value of p for the dry lattice (0.717) the temperature coefficient of the resonance integral RI.

$$\left[\frac{1}{RI_o}\ \frac{d(RI)}{dT}\right]_{ave} = 1.24 \times 10^{-4}/C \qquad (6.2.3.2)$$

* Note that the sign of the density-only coefficient is given as positive; the density coefficient is negative, however, since the water density decreases with increasing temperature.

Assuming that the resonance integral temperature dependence is not grossly changed in the wet lattice and using the wet lattice p values, one obtains

$$\frac{1}{k}\frac{dk}{dT_f} = -5 \times 10^{-4} (T + 273)^{-1/2}/^{o}C \quad (T \text{ is } ^{o}C). \qquad (6.2.3.3)$$

The integral of 6.2.3.3 is plotted in Figure 6.2.3.1. The average coefficient over the range 20 - 360 C is -2.3×10^{-5}/C.

6.2.4 Operating Reactor Temperature Coefficients

A separate description of the temperature coefficients in terms more meaningful to the operator of the reactor is given below. The temperature coefficients are separated as follows:

a) Moderator Temperature Coefficient related only to effect produced by a change in graphite temperature. Most usefully defined for coolant and fuel already at equilibrium temperatures.

b) Water Temperature Coefficient related only to the effect of a change in inlet water temperature. Includes effect of metal heating (Doppler) caused by the water temperature change, the effects due to any density changes associated with the water temperature change and the neutron spectrum effects associated with changing water temperature.

c) Power Coefficient related to effect of additional fuel heating as reactor is brought to power and effect of increasing the average water temperature through the reactor - in other words, the corresponding change in water ΔT.

Theoretical differential coefficients (MOFDA) are given in Table 6.2.4.1 for cold and hot conditions. Complete curves are shown in Figures 6.2.3.1, 6.2.4.1, 6.2.4.2 and 6.2.4.3.

Table 6.2.4.1

N Reactor Temperature Coefficients - Operational

Coefficient	Green		700 MWD/T	
	Cold	Hot	Cold	Hot
Moderator (mk/C)	+0.105	+0.023	+0.105	+0.031
Water (mk/C)	-0.150	-0.150	-0.120	-0.130
Power (mk/MW)	-0.003	-0.003	-0.00265	-0.00265

The curves in Figure 6.2.4.1 depict the reactivity behavior with coolant temperature which would be characteristic during a reactor startup. Under zero power conditions the coolant inlet temperature is equal to the average coolant temperature. The curves in Figure 6.2.4.2 are representative of the reactivity effect of varying the coolant inlet at full reactor power, and in this case the average coolant temperature would be approximately the mean of the inlet and outlet temperatures, the outlet being 105 C hotter than the inlet.

* See Figure ~~6-7~~ of ~~HW-71408~~ VOL2.

Figure 6.2.3.1 is a plot of the integral Doppler coefficient and is identical to Figure C-7 of HW-71408 VOL2.

Figure 6.2.4.1 is a plot of the integral coolant temperature coefficient for zero power and is identical to Figure C-5 of HW-71408 VOL2.

Figure 6.2.4.2 is a plot of the integral coolant temperature coefficient for full power and is identical to Figure C-6 of HW-71408 VOL2.

6.3 Exposure-Dependent Effects

The reactivity effects associated with exposure include the effects of U^{235}-depletion, Pu^{239}, Pu^{240} and Pu^{241}-formation, and fission product formation. The net reactivity effect of U^{235}-burnout and plutonium formation is positive in spite of a less-than-one-for-one replacement of fissionable atoms by the conversion process. This increase results from the higher fission cross section and neutron yield of Pu^{239} compared to U^{235}. The net exposure effect, including fission products, is negative, however. The following sections deal with the various exposure-dependent effects on reactivity.

6.3.1 Long Term Gain (Cold)

The effects of plutonium formation, U^{235}-burnout and fission product formation (other than xenon and samarium) are for present purposes combined into one effect, called the long term gain. The long term gain is given most simply for the cold reactor, since it is usually convenient also to include exposure effects in the temperature coefficients.

Based on observation of long-term reactivity effects in the present Hanford reactors, the cold long term effect is positive in natural uranium fuel up to an exposure of 550 MWD/T. In N Reactor, the higher fuel enrichment will tend to decrease the long term gain, but the harder neutron spectrum will be a compensating factor. Calculations based on U^{235}-depletion and plutonium formation and assuming an average cross section of 50 barns for fission products (other than xenon and samarium), indicate a cold, long term reactivity gain to an average exposure of 700 MWD/T of $\sim 2 \times 10^{-3}$.

6.3.2 Xenon Poisoning

After a reactor startup, xenon poisoning reaches its equilibrium value after an incremental exposure of 30 MWD/T (2.5 days). After reactor shutdown, the xenon poisoning initially increases, due to the decay of the precursor iodine-135, then decreases and eventually decays to zero. A typical startup and shutdown xenon transient is shown in Figure 6.3.2.1* for an average fuel exposure of 700 MWD/T. The exposure dependence of the operating xenon poisoning is shown in Figure 6.3.2.2.** The equilibrium xenon in N Reactor will be worth 2.7 to 3.1% Δ k/k.

6.3.3 Samarium Poisoning

Samarium-149 poisoning reaches an equilibrium value of about 6.5×10^{-3} Δ k/k at 100 MWD/T exposure. After each reactor shutdown, the samarium poisoning increases due to the decay of its precursor promethium-149. The equilibrium value is regained by the time an additional exposure of 100 MWD/T is reached after each startup. The equilibrium samarium is shown in Figure 6.3.2.2 as a function of fuel exposure. The cold reactor samarium defect is 6.7×10^{-3} Δ k/k.

6.3.4 Neptunium Holdup

Calculations of the reactivity gains in a reactor due to plutonium buildup usually assume instantaneous formation of plutonium. The fact that the formation of plutonium-239 is delayed through the 2.33 day, beta-decay of neptunium-239 makes it necessary to correct the calculated reactivity gains. This is most conveniently done by assigning a reactivity "loss" for the neptunium

* Figure C-8 of HW-71408 VOL2.
** Figure C-9 of HW-71408 VOL2.

Figure 6.3.2.1 is a plot of the xenon transient and is identical to Figure C-8 of HW-71408 VOL2.

Figure 6.3.2.2 is a plot of Fission Product poisoning and neptunium holdup in N Reactor and is identical to Figure C-9 of HW-71408 VOL2.

holdup effect. The neptunium holdup reactivity defect at equilibrium is about 4×10^{-3}. The equilibrium neptunium holdup effect is shown in Figure 6.3.2.2 as a function of exposure.

6.3.5 Over-all Long Term Reactivity Effects

For additional clarity, two set of curves are given of the total exposure-dependent reactivity variation. (See Figures 6.3.5.1 and 6.3.5.2)* Neptunium holdup, samarium poisoning, other fission product poisoning, U^{235} burnout and plutonium buildup are all included. The exposure dependence of xenon poisoning is included, but not the initial, green 3.1 per cent $\Delta k/k$ loss. The curves give essentially the reactivity transient the reactor would experience after a startup and equilibrium xenon and temperature had been reached. Figure 6.3.5.1 is for a uniform exposure. Figure 6.3.5.2 is for a "mixed" exposure – that is exposures running uniformly from zero to goal. The abscissas in the figures are to be interpreted as follows: in the uniform exposure case, the goal exposure is equal to the pile-average exposure. In the mixed exposure case, the pile-average exposure is assumed to be about half of the goal exposure. The latter probably more closely represents the most likely charging and discharging scheme. The hot-pile, over-all, long term effects are also given in Figures 6.3.5.1 and 6.3.5.2 thus indicating the exposure-dependence of the net temperature coefficients.

6.4 Over-all Reactivity Changes

The preceding discussion in Sections 6.2 and 6.3 enables an estimate of the reactivity requirements and transients to be made. The estimated breakdown for the green reactor and the reactor with an average fuel exposure of 700 MWD/T are shown in Table 6.4.1.

Table 6.4.1

Estimated Reactivity Breakdown[a]

	Fuel Exposure (Average)	
	0 MWD/T	700 MWD/T
Xenon	-3.1%	-2.8%
Samarium (cold)	0	-0.67%
Neptunium (cold)	0	-0.38%
Long Term Gain (cold)	0	+0.2%
Temperature Coefficients		
Doppler	-0.8%	-0.8%
Coolant	-2.8%	-2.3%
Moderator	+2.8%	+3.0%
k, Cold (Xenon-Free)	1.059	1.050
Δ k/k, Cold to Hot	-0.8%	-0.1%
k, Equilibrium	1.020	1.021

[a] Δ k/k unless otherwise indicated.

*See Figures C-10 and C-11 of HW-71408 VOL2.

[redacted]

Figure 6.3.5.1 is a plot of the over-all long term transient for uniform exposures and is identical to Figure C-10 of HW-71408 VOL2.

6.5 Operational Reactivity Transients

The various temperature and exposure reactivity contributions have been combined to determine typical reactor startup and shut down reactivity transients.

6.5.1 Reactor Startup Transients

Typical reactor startup reactivity transients are shown in Figure 6.5.1.1 for the green reactor and the reactor with an average fuel exposure of 700 MWD/T. The curves are for an "infinite"outage. The green, infinite-outage startup transient should represent the most extensive case insofar as excess reactivity is concerned during a startup.

The startup procedure assumes operation at ten per cent power (400 MW) for the first two hours in order to bring the coolant inlet temperature up to the design value of 185 C. Thus, the initial negative transient is due to water and uranium heating. It is anticipated that the rise to full power will be accomplished at a rate of about 100 MW/min. Further uranium and coolant heating plus graphite heating and xenon buildup contribute to the transient durig this period. A peak power level, called turnaround, is reached approximately five hours after startup. At this time the full temperature effect has been attained, and the reactivity loss beyond turnaround is due to further xenon buildup.

The infinite-outage startup transient curves indicate that the maximum excess reactivity during the startup and operation is the cold, xenon-free reactivity. This differs from the present Hanford reactors where the "turnaround" level for an infinite-outage startup is higher than the initial cold, clean reactivity level.

Even if the reactor were scrammed at "turnaround", the immediate reactivity effect associated with cooling down of the fuel and coolant would not result in an excess reactivity beyond that for the cold reactor.

6.5.2 Normal Shutdown Transient

Typical reactivity shutdown transients are given in Figure 6.5.2.1 for the reactor loaded with green fuel and fuel at an average exposure of 600 MWD/T. The initial equilibrium reactivities shown are those expected with 0.947 per cent enriched fuel – actually the reactivity carried in control rods at equilibrium (equilibrium excess reactivity) will be nearer one per cent, so the entire set curves can be moved down about one per cent. To be consistent with startup transient (Figure 6.5.1.1) the reactivites are shown as they are expected to be with the full 0.947 per cent enrichment.

The assumed power reduction in Figure 6.5.2.1 is 2-1/2 per cent per minute. The initial small reactivity peak is due to the initial cooling of the fuel and coolant. Following the initial rise in reactivity is a decrease for about an hour as the graphite cools and xenon builds up. During this period the primary coolant system pressure is reduced and the average coolant temperature is held constant at about 338 F. Further cooling of the coolant and graphite to shutdown temperature (100 F) and further xenon buildup produces the transient shown between 1-1/2 hours and ten hours after starting down. After ten hours, the xenon decay becomes predominant and the reactivity increases to the cold pile valuesof 5.9 and 5.0 per cent respectively for the green and ripe cases.

Figure 6.3.5.2 is a plot of the over-all long term transient for mixed exposures and is identical to Figure C-11 of HW-71408 VOL2.

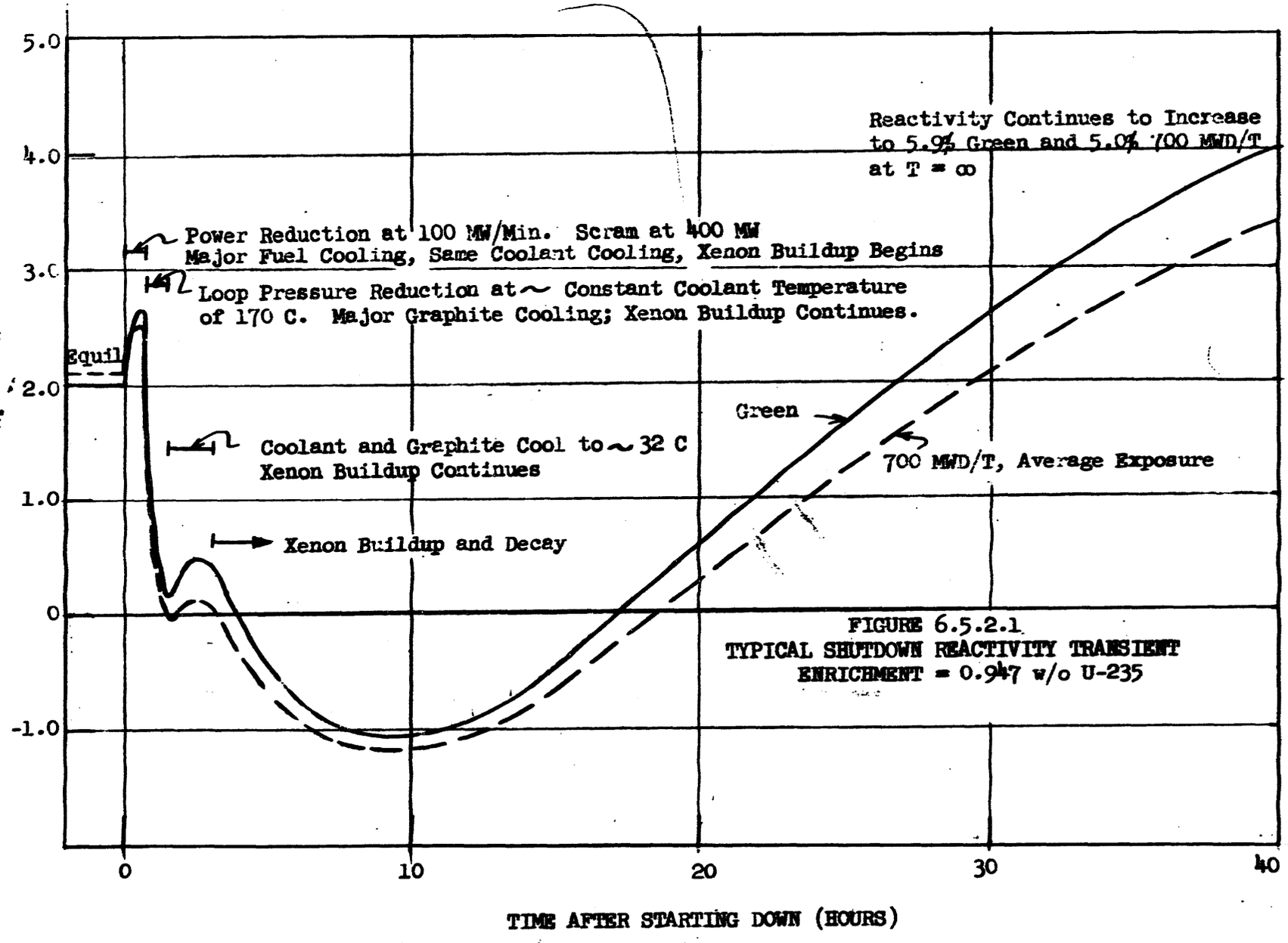

FIGURE 6.5.2.1
TYPICAL SHUTDOWN REACTIVITY TRANSIENT
ENRICHMENT = 0.947 w/o U-235

Figure 6.5.3.1 is a scram transient and is identical to Figure C-13 in HW-71408 VOL2.

6.5.3 Scram Transient

If the reactor is shut down from equilibrium by the scramming of the horizontal safety rods, the short-time behavior of the reactivity transient depends on the strength of the rods inserted. Several scram transient curves are given in Figure 6.5.3.1 (See Figure C-13 of HW-71408 VOL2). The rise following the initial reactivity decrease in each case is due to cooling of the fuel and coolant. The curves in Figure 6.5.3.1 (unlike the other transient curves) are plotted in terms of the reactivity of the reactor – that is the sum of the lattice reactivity and the reactivity effect of the rods. It is seen that nearly the full worth of the rods is obtained at about 1.3 seconds after the time the master safety circuit breaker operates.

6.6 Accidental Reactivity Changes

6.6.1 Loss-of-Coolant Reactivity Effect

The N-Reactor lattice is fail-safe upon loss of coolant. That is, the dry lattice is less reactive than the wet lattice. The primary loop coolant-loss reactivity effects for the green and ripe reactor are given in Table 6.6.1.1. The value for the cold, green reactor is an experimental value[12]; the others are theoretical values normalized to the experimental value.

Table 6.6.1.1

Loss of Coolant Reactivity Effect ($\Delta k/k$)

Condition	Zero Exposure	700 MWD/T
Cold Lattice	-6.0%	-6.1%
Hot Lattice	-7.5%	-7.3%

6.6.2 Lattice Flooding

The NPR has an undermoderated lattice, and as just discussed, loss of coolant results in a reactivity loss. Conversely, addition of more moderator to the lattice may result in an increase in reactivity. The effect of core-flooding has been analyzed theoretically[25]. In the analysis, the lattice was progressively flooded with water in a favored (low thermal flux) position and the maximum reactivity increase determined. Such an investigation should establish an upper bound for the effect. The calculated maximum $\Delta k/k$ for flooding under various lattice conditions are given in Table 6.6.2.1.

Table 6.6.2.1

Flooding Reactivity Effect (Maximum)

Condition (All for Green Fuel)	$\Delta k/k$
Cold Graphite, Hot Uranium and Water	+ 0.25%
Equilibrium Power	+ 2.2 %

AIIM

Association for Information and Image Management

1100 Wayne Avenue, Suite 1100
Silver Spring, Maryland 20910

301/587-8202

Centimeter

mm

Inches

MANUFACTURED TO AIIM STANDARDS
BY APPLIED IMAGE, INC.

2 of 2

6.6.3 Cold Water Reactivity Effect

The N lattice will gain reactivity when the density of the coolant water is increased. This reactivity effect has been calculated to be a maximum of 3.6 per cent in the hot reactor lattice at equilibrium power and for green fuel[25]. Values for other reactor conditions are given in Table 6.6.3.1.

Table 6.6.3.1

Cold Water Reactivity Effects (Maximum)

Condition (All for Green Fuel)	$\Delta k/k$
Zero Power (Cold graphite, hot uranium and water)	+ 3.1%
Equilibrium Power	+ 3.6%

7. Reactor Control

7.1 Introduction

In contrast to previous Hanford reactors, N Reactor has only one rod system, combining safety and control functions. The rod system is horizontal. Because of higher power levels, higher graphite temperatures and design flexibility characteristics, all requiring additional control strength and adjustability, more rods are provided at N than at the older reactors and, because of space limits, the rods will enter the reactor from both sides. Also, the recirculation or primary coolant, at high temperatures and pressures, makes the use of temporary poison columns highly inconvenient thereby creating an additional demand on control rod strength and flexibility over previous reactors.

The backup control system in the N Reactor is a vertical ball system. This system is independent of the horizontal rod system and provides capacity to control any credible operating or disaster reactivity situation.

7.2 Control Philosophy

The philosophy of reactor control and safety in the Hanford reactors had its origin in the days of the Manhattan Project. The original philosophy has satisfactorily stood the test of time and has carried on through the years with few changes. It was only natural, then, that the initial thoughts with respect to reactor control and safety for the NPR followed closely the traditional Hanford philosophy.

7.2.1 Operational Control Criteria

The operational control system must meet the following requirements:

1. Adequate strength to maintain the reactor subcritical under all normal operating and shutdown conditions.

2. Adjustment at rates fast enough to override all normal, operational reactivity transients and to minimize delays at startup. However, the system must be limited to its withdrawal rate to that rate which, in coincidence with simultaneous failure of the Primary Safety System, would not result in fuel melting.

3. Precision positioning and movement to permit establishing and maintaining the reactor power level within desired limits.

4. Adequacy of geometrical coverage and flexibility to permit attaining adequate power-flattening efficiencies and satisfactory control over spatial power cycling.

7.2.2 Safety Control Criteria

There must be two safety control systems. One of the systems, depending on the nature of the accident, is to provide the primary protection; the other, then, will function as a backup. The safety control systems must meet the following requirements:

1) Both primary and backup system must have adequate strength to maintain the reactor subcritical for all credible* accidents at least until the reactor is damaged beyond repair as a result of the causative accident. Beyond this point the inserted safety control system or systems are required to maintain control only to the extent that the consequences of the incident are no worse than those which would result from the causative accident alone.

2) The primary system must have speed of control insertion adequate to (a) limit a power excursion from credible accidents which would in themselves result in damage, (loss of coolant, for example,) to one of a magnitude such that the ultimate consequences of the excursion are no worse than those which would have resulted from the causative accident alone, or (b) limit a power excursion from other credible accidents (such as fast rod withdrawal) to one of a magnitude such that no damage beyond mild fuel stressing will result.

The backup system must satisfy criterion (2) except it is required to prevent fuel melting instead of fuel damage.

7.2.3 Backup Philosophy

The purpose of a backup safety system is to provide safety protection in the event of a failure in the primary system. There shall be no intent in design to permit the removal of one or part of one of the safety systems from service on the premise that the backup system is in service and will act if necessary.

* Credible accidents exclude acts-of-war, sabotage, and large falling objects; earthquakes which are severe enough to prohibit entry of poison from both safety systems are also considered incredible.

Each safety system must back up the other system for as many failure and accident conditions as possible. There may be certain accidents, such as a severe earthquake, in which one system is disabled, rendering it useless in either a primary or backup capacity. Therefore, the two systems shall be different in design, if possible, to reduce the probability of both systems being disabled by one accident.

Both safety systems shall be activated by automatic trips as well as by manual trips. The two safety systems shall have independent drives. It is desirable that they also take their activating signals from independent circuits. If common sensors or common circuits are used in the two safety systems, the reliability of these common elements must be high enough to yield an operational fault rate which is commensurate with that obtainable under a wholly-independent arrangement.

The degree to which the control systems meet these criteria is discussed in later portions of this section.

7.3 Horizontal Control Rods

The worth of individual control rods and the strength of the entire HCR system in N Reactor will only be known accurately after reactor startup tests have been completed. However, laboratory measurements of the N rod system in various configurations and theoretical calculations of the rod strengths have been made[12,24]

7.3.1 Control Strengths

The experimental determinations for the N Reactor control strengths consisted of determining the cold-reactor, control effectiveness of a single rod and of six rods arranged in the proper spacing in an exponential pile. Using the same theoretical methods which were used to calculate the control strengths in the N Reactor, itself, the exponential pile results were correlated with theory. The observed relationship between calculated and experimental values in the exponential pile was then used to establish most probable values for the control strengths in N Reactor under various operating conditions. The results of this normalization are listed in Table 7.3.1. The calculations are described in Reference 26.

The local control strengths of the control rods included in the table are defined as the change in buckling of a region with a cross sectional area of 1150 in.^{2} (32 in. x 36 in.). The migration areas listed are those used to derive the reactivity effect by the relationship $\Delta k/k = \Delta B^2 M^2$. The full-pile strengths are lower than the local strengths due to incomplete coverage of the reactor core with control rods. The lower values in each case represent an extrapolation from the six-rod exponential measurement, whereas the higher values are derived from the single-rod exponential measurement. The difference is probably due to the difficulty in exactly duplicating boundary conditions in calculating the effect in the reactor; the true value probably lies nearer to the lower value.

Table 7.3.1

Most Probable Control Strengths
(Horizontal Rods)

Reactor Condition	Local Control Strength[a] ΔB^2 (μb)	Full Reactor Strength Most Probable[a] ΔB^2 (μb)	M^2 (cm^2)	$\Delta k/k$ (%)	Theoretical $\Delta k/k$ (%)
Cold Reactor	170-213	120-133	640	7.7-8.5	7.0-8.3[d]
Hot Reactor	165-205	118-131	710	8.4-9.3	7.7-9.1
Cold Reactor Flooded[b]	205-245	131-140	409	5.4-5.7	5.1-5.6
Hot Reactor Flooded[b]	200-238	130-138	479	6.2-6.6	5.9-6.5
Hot Reactor-Cold Water	170-213	120-133	647	7.8-8.6	7.1-8.4
Maximum Accident[c]	205-245	131-140	416	5.4-5.8	5.2-5.7

(a) Lower value represents extrapolation from six-rod exponential pile measurements; higher value from single-rod exponential pile measurement.

(b) Flooded to extent that maximum reactivity is achieved. Rod strengths (full reactor will continue to decrease beyond "optimum" flooding but poisoning due to water exceeds the loss in control strength beyond point of optimum flooding.

(c) Optimum flooding combined with cold water injection in hot reactor.

(d) Lower value calculated with streaming correction on neutron free path; higher value with no streaming correction.

7.3.2 Maximum Worth of Single Rods or Groups of Rods

One-dimensional, three-group diffusion theory calculations have been made to determine the worst flux distortion under which rods may be withdrawn[26]. Two separate cases were studied. In each case, all rods were assumed inserted except for a single bank of rods (in N Reactor there are 11 rod banks). Withdrawing an entire center bank (nine rods) would result in an increase of about three per cent $\Delta k/k$. Withdrawal of an entire outermost rod bank (six rods) would result in an increase of 2.5% $\Delta k/k$. Withdrawing two adjacent banks theoretically could result in reactivity increases of six per cent and 4.3 per cent for central and outer rods, respectively. With normal hydraulic system action, the maximum reactivity withdrawal rate is 4 per cent per minute which corresponds to pulling two adjacent outer rod banks (12 rods) at the maximum rate.

7.3.3 Struck Rod Limit

In order to determine a failed (or stuck, or OFF) rod limit, it is necessary to first define the maximum reactivity condition which the rod system alone is expected to control. This is defined as the condition attained either under hot graphite, xenon-free, optimum-flooded conditions, or under hot graphite, xenon-free, cold-water-injection conditions, but not both.

The calculation of a failed-rod limit was simplified by conservatively assuming that the failed rods were centrally located, adjacent to each other, and in the region of maximum flux. A one-energy group, multiregional buckling calculation was used to determine the lattice material buckling at which the reactor would be just-critical with various numbers of rods out of service. It was found that three adjacent rods could be removed from service while maintaining the reactor subcritical under either accident assumption. The failed-rod limit, has, therefore, been set at three. If four or more rods fail to reach their 75 per cent limit switch within 1.5 seconds after a safety circuit trip, these failed rods are backed up by an automatic drop of balls in the rows in front of and behind each failed rod.

7.4 Ball 3X System

7.4.1 Control Strengths

Exponential pile measurements and calculations have been performed to determine the strength of the Ball (3X) Safety System using techniques similar to those used for determining rod strengths.[26] The results are given in Table 7.4.1.

Table 7.4.1

Most Probable Control Strengths
(Ball 3X)

Reactor Condition	Local Control Strength[a] ΔB^2(μb)	Full Reactor Strength[a] ΔB^2(μb)	M^2(cm^2)	Δk/k(%)
Cold Reactor	117-138	104-120	640	6.7-7.7
Hot Reactor	108-132	96-116	710	6.8-8.2
Cold Reactor Flooded[b]	144-165	125-140	409	5.1-5.7
Hot Reactor Flooded[b]	135-159	118-135	479	5.6-6.5
Hot Reactor Cold Water	117-138	104-120	647	6.7-7.8
Maximum Accident[c]	144-165	125-140	416	5.2-5.8

a Lower value represents extrapolation from six-channel exponential pile measurement; higher value from single-channel exponential pile measurement.
b Flooded to extent that maximum reactivity is achieved.
c Optimum flooding combined with cold water injection in hot reactor.

7.4.2 Inoperable Ball Column Limit

An "out-of-service Ball 3X hopper limit" has been determined in the same way as the failed-rod limit. A total of four ball hoppers may be locked out while still maintaining Ball (3X) Safety System Capacity to drive the reactor subcritical under either the cold water or flooding accident conditions.

[redacted]

7.5 Total Control Considerations

The operational control criteria and part of the safety control criteria are re-statements of the Hanford Total Control Criterion. As far as the operational control criteria are concerned, the horizontal control rods have adequate strength in the operating reactor (minimum of 7.7 per cent $\Delta k/k$ cold) to control any foreseeable transient. The cold, clean, green reactivity with 0.947 per cent enriched fuel is 5.9 per cent. For ripe fuel, the cold, clean reactivity is 5.0 per cent. Thus, the cold reactor shutdown margin with the control rods is at a minimum 1.8 per cent $\Delta k/k$. Actually, the reactor fully enriched with 0.947 per cent U^{235} fuel is expected to have an excess reactivity at equilibrium about one per cent higher than needed (if the temperature coefficients are correct), and an effective enrichment reduction by the use of natural uranium columns will then be employed which will reduce the cold excess reactivity of 4.9 per cent. This would serve to increase further the shutdown margin.

The more restrictive criterion is the one dealing with adequacy of control over various accident conditions. The first safety control criterion states that either control system must be able to maintain the reactor subcritical for all credible accidents*.

The shutdown margins for both the horizontal rod and Ball 3X systems for a number of reactivity states are given in Tables 7.5.1 and 7.5.2.

It is seen that either safety system is able to maintain the reactor subcritical under all credible conditions. A simultaneous cold water accident and optimum flooding incident resulting in a five per cent increase in reactivity (which is considered incredible) would result in a reactivity state outside of the strength of the horizontal rods. However, assuming a just-critical state prior to the postulated accident, the shutdown margin of the Ball 3X system would be positive even for this accident.

7.6 Speed-of-Control Considerations

The second safety control criterion is a restatement of the Hanford Speed-of-Control Criterion. Since the water-loss accident in N Reactor does not result in a rapid increase in reactivity as is the case in the present reactors, the accident

* The qualifying clause "at least until the reactor is damaged beyond repair, etc." is included to make it unnecessary to maintain subcriticality beyond the point when the consequences of the accident would not be increased significantly even if the reactor did go supercritical. Such is the case in the present Hanford reactors for the water-loss accident. When the reactor has heated sufficiently from fission product decay heat to render it no longer possible to re-establish cooling, there is no real point in being concerned about a delayed-critical state since a meltdown is inevitable. Going supercritical would only hasten the meltdown with no significant increase in fission product inventory or fission product release probability. The situation at the N Reactor is slightly more complicated. Even if flow cannot be re-established in the process tubes, accident severity is minimized by operation of the moderator cooling system. Supercriticality during operation of this system would increase severity of consequences.

Table 7.5.1

Shutdown Margin - Horizontal Rod System

Reactor Condition	Excess Lattice Reactivity %[a]	Minimum Probable Rod Strength %	Shutdown Margin %[b]
Cold, Clean, Green	4.9	7.7	2.8
Hot (Turnaround)[c]	3.3	8.4	5.1
Hot (Turnaround)[c] Plus Cold Water	6.9	7.8	0.9
Hot (Turnaround)[c] Plus Flooding	5.5	6.2	0.7
Hot (Equilibrium)	1.0	8.4	7.4
Hot (Equilibrium) Plus Cold Water	4.6	7.8	3.2
Hot (Equilibrium) Plus Flooding	3.2	6.2	3.0

a Adjusted to give one per cent excess reactivity at equilibrium.
b Assuming no other control poison in the reactor.
c Ripe - 700 MWD/T average exposure.

Table 7.5.2

Shutdown Margins - Ball 3X System

Reactor Condition	Excess Reactivity %[a]	Minimum Probable Ball 3X Strength (%)	Shutdown Margin[b]
Cold, Clean, Green	4.9[c]	6.7	1.8
Hot (Turnaround)	0[d]	6.8	6.8
Hot (Turnaround) Plus Cold Water	3.6[d]	6.7	3.1
Hot (Turnaround) Plus Flooding	2.2[d]	5.6	3.4
Hot (Equilibrium)	0[d]	6.8	6.8
Hot (Equilibrium) Plus Cold Water	3.6[d]	6.7	3.1
Hot (Equilibrium) Plus Flooding	2.2[d]	5.6	3.4
Hot (Scram Recovery)	5.1[e]	6.8	1.7

a Adjusted to give ~ one per cent excess reactivity at equilibrium.
b Assuming no shadowing due to control rods already inserted. Assuming no rods already inserted are ejected.
c Lattice excess reactivity. No control rods or other poisons inserted.
d Pile excess reactivity. Sufficient control rods in reactor to maintain reactor just critical at equilibrium or turnaround.
e Assumes all horizontal rods are withdrawn to make a scram recovery, reactor is scrammed with Ball 3X and cools to xenon-free state.

governing the response of the safety systems is one associated with rod-withdrawal. Since the horizontal rods combine both operational and safety functions, the limitation on withdrawal rate specified in the operational control criteria can also be included in this discussion.

There are two degrees of accidents involved and the allowable consequences differ for each. Firstly, there is the case where the control rods are withdrawn so as to result in the maximum possible reactivity ramp and the reactor is automatically shut down by a safety rod scram (primary system). In this case, the speed of shutdown should be fast enough to limit any damage to mild fuel stressing only – definitely no boiling or fuel melting should occur.* This may at first appear to be a much more demanding requirement on the primary safety system than is required in the older Hanford reactors. However, the possible reactivity insertion rates (poison withdrawal rates) in N Reactor are so much smaller than that possible from coolant loss in the older reactors that a "no-boiling criterion actually is less restrictive than the no-melting criterion in effect in the speed-of-control interpretation in the present reactors. (As will be seen later, the major factor in this result is the strongly-negative prompt temperature coefficient in the NPR).

Secondly, there is the case where the control rods are withdrawn at their maximum rate (or reactivity is added by some other means – cold water accident, for example) and the primary safety system (safety rods) fail to enter the reactor. This is a more improbable accident (two failures or accidents are required), and the requirement that the backup system response must meet is set at no fuel melting. No fuel melting in this case means no uranium melting.

In order to assess the degree to which the safety systems meet both these speed-of-control requirements, it is first necessary to consider the sources and magnitudes of the reactor excursions. Then, particular excursions are examined to determine whether the criteria are indeed satisfied.

7.6.1 Reactivity Sources

The principal accidental sources of positive reactivity are 1) core flooding, 2) cold water insertion during equilibrium reactor operation and 3) excessive control rod withdrawal rates. There are two types of failures or errors which must be considered in any discussion on withdrawal of control rods. The two failures or errors are 1) increased rod withdrawal speeds due to inadvertent admission of air or gas into the hydraulic systems, and 2) steeper ramps resulting from maximum strength rods being involved in the rod withdrawal.

---

* From a reactor efficiency standpoint, any power transient should not stress the fuel elements to the point where a rupture rash would occur. Procedural rod withdrawal rates will be less than these maximumly possible and will undoubtedly be governed by fuel rupture considerations.

7.6.1.1 Control Rod Withdrawal

The control system is designed so the maximum rate at which horizontal control rods can be withdrawn depends on the pumping capacity of the oil pumps serving the rod hydraulic systems. The possibility of air or some other gas leaking into the hydraulic lines has been considered since rod speeds could be increased by the presence of gas in the hydraulic system. The maximum reactivity ramp due to such a failure in the hydraulic system is believed to be 0.04 per cent per second. This compares to the 0.025 per cent per second maximum ramp for a normally-working hydraulic system.

The situation in which the particular rods chosen to be withdrawn together are the maximum-worth rods will also result in a reactivity ramp larger than 0.025 per cent per second. If the twelve rods in one end of the reactor (rear or front) were ganged together and withdrawn at the maximum speed (assuming normal operation of the hydraulic system) the reactivity ramp would be 0.062 per cent per second. Such a ganging will be prohibited by mandatory Process Standards and the occurrence is very unlikely. After operating experience is gained, the control rods will probably be grouped in permanent gangs and thus the flexibility of unlimited combination will only exist during the initial operating period of the reactor. Any permanent ganging of control rods before startup is considered unwise since the best control rod patterns can only be determined after some reactor operation has been achieved.

Assuming a combination of the two circumstances, both hydraulic system failure (gas in the lines) and a withdrawal of the strongest rods at one time at full speed, would result in an average ramp of 0.10 per cent $\Delta k/k$ per second. This ramp is only half of that currently possible in the present Hanford reactors from the simultaneous withdrawal of all vertical safety rods at their maximum speed.

7.6.1.2 Cold Water Addition

The time when cold water addition would produce a maximum reactivity increase is when the reactor is at equilibrium. The average coolant density at operating conditions is about 0.82 gm/cm^3 and the average temperature is about 230 C. An increase to near unity density and near river temperature in the coolant by the substitution of cold emergency cooling water will produce a theoretical full-pile reactivity increase of about 3.6 per cent.[25]

Results of detailed studies on how fast cold water can be injected into the reactor have shown that in the case of a primary coolant system dump, cold raw water may start to reach the reactor in approximately 30 seconds and may fill all coolant channels in an additional 30 seconds. Thus, the reactivity ramp during the time cold water is replacing the normal coolant in the reactor is about 0.12 per cent per second.

7.6.1.3 Core Flooding

The rupture of a process tube during reactor opeation will admit high temperature water into the graphite stack. If it is assumed that the water does not flash to steam but remains in a saturated state at low pressure in the hot stack and collects in the graphite in such a manner that the maximum

reactivity effect is achieved (around 10 to 15 per cent of the available voids filled – those closest to the process tubes), an increase in reactivity of 2.2 per cent is calculated.[25] The rate at which water could fill the stack to this amount from a single process tube leak (assuming a critical flow rate of 200 pounds/second*) is about 150 seconds. Thus, the average reactivity ramp from such a break would be about 0.015 per cent per second. A faster addition of water to the stack could only come from a multiple tube break which is considered highly improbable.

7.6.1.4 Summary of Reactivity Ramps

For convenience a graphic summary of the possible positive reactivity ramps is shown in Figure 7.6.1.4. (See Figure A-1 of HW-71408 VOL2).

7.6.2 Excursion With Scram

The safety philosophy requires that the primary safety control system have a response which is fast enough to limit any credible power excursion to one of a magnitude such that no damage beyond mild fuel stressing will result. Since the magnitudes of the credible reactivity ramps in N Reactor are considerably smaller than in the older Hanford reactors, speed of control in N Reactor is not so severe a problem as it is in the present reactors. Nevertheless, the scram speed of the horizontal rods is very high; the rods reach 90 per cent effectiveness from their full-out position in about 1.2 seconds. A plot of the reactivity characteristic curve for the horizontal safety rods is given in Figure 7.6.2.1 (See Figure A-2 of HW-71408 VOL2). The initial delay includes instrument and circuit delays as well as the time required for the rods to enter the active zone of the reactor from their full-out position.

To test the meeting of the criterion on primary safety system response, reactor kinetic calculations have been made under a variety of assumptions. The scram response of the horizontal rods is shown to be more than adequate to shut down the reactor from any credible excursion before any boiling occurs. A plot of a startup excursion due to a reactivity ramp of 0.10 per cent per second (which is equivalent to the maximum reactivity insertion rate due to rod withdrawal) is shown in Figure 7.6.2.2. (See Figure A-3 of HW-71408 VOL2). As shown, the excursion is characterized by a sharp initial peak which, in this case, is turned around at about 26,000 MW (reactor power) by the combined action of the scram rods and the negative temperature coefficients. The scram signal is assumed to be given by the high-level neutron flux monitor (set to initiate a trip at 4400 MW, 110 per cent of equilibrium level**). The scram rods continue to drive the power and temperatures down as shown in the figure. The peak fuel temperature is 383 F and the outlet coolant temperature peaks well below 300 F. Half-coolant flow is assumed in the startup excursion calculations; the loop pressure is 300 psia and the reactor is initially 4.3 per cent $\Delta k/k$ subcritical. At the startup pressure of 300 psia boiling would begin at 410 F.

* Only 130 pounds is liquid water.

** This would be the last nuclear trip in the safety circuit. In other words, the calculation has assumed that all lower period, power-rate and level trips failed.

[redacted]

Figure 7.6.1.4 is a graphical summary of N-Reactor reactivity ramps and is same as Figure A-1 of HW-71408 VOL2.

Figure 7.6.2.1 is a plot of the scram rod characteristic and is identical to Figure A-2 of HW-71408 VOL2.

Figure 7.6.2.2 is a plot of a startup excursion with normal HSR scram and is identical to Figure A-3 of HW-71408 VOL2.

Figure 7.6.2.3 (See Figure A-4 of HW-71408 VOL2) illustrates the case in which the excursion is assumed to occur at equilibrium level. The assumed reactivity ramp rate in this case is 0.05 per cent per second, which corresponds to control rod withdrawal in excess of the simultaneous movement of the maximum number of control rods together with gas in each hydraulic system so that the rods come out faster than normal. A balanced-flux is assumed, however. The power variation in Figure 7.6.2.3 is that for a nominal central tube operating initially at 4400 kw. The temperature increases are mild even though there is about a ten per cent increase in tube power. Boiling would occur at an outlet temperature of about 585 F.

It is conceivable, but highly improbable, that the Primary Safety System (horizontal rods) would fail and the excursion would have to be terminated by the Ball (3X) Safety System. The Ball 3X system is required to be able to shut down the reactor from any credible excursion before fuel melting occurs.

Tests using actual hoppers have indicated that the Ball 3X insertion rate is about 7.84 lb/second. The mechanical construction of the hoppers and entry valves determines the release rate; furthermore, the time required to fill the ball channels is longer than formerly expected due to the time required to fill the exit piping. The full-pile reactivity effect of Ball 3X insertion is, therefore, first characterized by an initial poisoning effect (about 30 per cent of the total Ball 3X system worth) due to the "grey" streams of falling balls during the period of filling the exit piping. This is followed by a gradually-increasing poisoning effect as the columns fill up. About 50 seconds are required to achieve the full effectiveness of the Ball 3X poisoning. A plot of the expected scram characteristic curve of the Ball 3X system is given in Figure 7.6.2.4 (See Figure A-5, HW-71408 VOL2).

The kinetic calculations show that in spite of the slow-acting nature of the Ball 3X system, the initial partial poisoning effect is strong enough to adequately shut down the reactor from any credible excursion if the primary system fails. A 1.5 second time from a 1X trip has been assumed for the circuitry of the Ball 3X system to sense failure of the rods to scram properly. The results of the calculations are shown in Figures 7.6.2.5 and 7.6.2.6 (See Figures A-6 and A-7 of HW-71408 VOL2). It is seen that peak fuel temperature achieved in the equilibrium excursion case is about 680 F. In fact, the outlet coolant temperature is held about 10 F below the boiling point (585 F). Thus no fuel melting is fairly well assured for this case. The fact that the assumptions made are for the most part extremely conservative adds weight to this conclusion.

[redacted]

Figure 7.6.2.3 is a plot of an excursion during equilibrium with normal HSR scrams identical to Figure A-4 of HW-71408 VOL2.

Figure 7.6.2.4 is a plot of the characteristic scram curve of the Ball 3X system and is same as Figure A-5 of HW-71408 VOL2.

Figure 7.6.2.5 is a plot of a startup excursion with Ball 3X scram identical to Figure A-6 of HW-71408 VOL2.

Figure 7.6.2.6 is a plot of an equilibrium excursion with Ball 3X scram and is identical to Figure A-7 of HW-71408 VOL2.

[redacted]

The major reason the relatively slow-acting Ball 3X system has time to adequately shut down the reactor is that the reactor, itself, has a powerful shutdown mechanism, the prompt negative fuel and coolant temperature coefficients. Thus, as soon as the reactor enters the significant power-producing range in the excursion, the reactivity-damping effects due to fuel and coolant heating are sufficient in themselves to prevent a runaway power excursion. Therefore time is provided during a subsequent, slower-acting, potential excursion resulting from a continuation of the ramp (combined with reactor heating) to permit the entry of Ball 3X balls and the termination of the power rise before boiling occurs. Figure 7.6.2.5 (the startup case) clearly illustrates this behavior. The initial excursion is turned around solely by the prompt temperature coefficients.

7.7 Ultimate Shutdown Mechanism

Figures 7.7.1 and 7.7.2 (See Figures A-8 and A-9 of HW-71408 VOL2) illustrate the consequences of a nuclear excursion with failure of both automatic scram systems. The ultimate shutdown mechanism (if the reactor is not manually scrammed) in this case is the negative void coefficient after boiling commences. Whether there would be alternate boiling and condensation in the post-boiling period is not known - additional studies including two-phase flow and heat transfer considerations are necessary. However, eventual loss of all coolant (with all controls out of the reactor) and continued heating of the reactor should result in a just-critical reactor (based on conservative calculations) at the melting point of zirconium, 1900 C. Eventual flow of molten fuel into the graphite will render the reactor permanently subcritical.

It is reassuring that a simultaneous failure of all automatic shutdown devices during a maximum startup excursion leaves about 15 seconds after the initial power turnaround by the temperature coefficients to manually scram the reactor, before boiling commences.

7.8 Reactor Kinetics

The non-equilibrium, short-time behavior of the reactor is described by the conventional reactor kinetics equations

$$\frac{dN}{dt} = \frac{(\delta k - \beta) N}{\ell} + \sum_{i=1}^{6} \lambda_i C_i , \qquad (7.8.1)$$

$$\frac{dC_i}{dt} = \frac{\beta_i N}{\ell^*} - \lambda_i C_i , \qquad (7.8.2)$$

Figure 7.7.1 is a plot of a startup excursion with no scram. Same as Figure A-8 of HW-71408 VOL2.

Figure 7.7.2 is a plot of an equilibrium excursion without scram. Same as Figure A9 of HW-71408 VOL2.

where

N = neutron density,

C_i = concentration of delayed neutron precursor, group i,

β_i = fraction of delayed neutrons in group i,

$\delta_k = \frac{k_{eff} - 1}{k_{eff}} \simeq k_{eff} - 1$,

ℓ^* = mean neutron lifetime (prompt),

λ_i = decay constant of delayed neutron precursor, group i, and

$\beta = \Sigma \beta_i$.

The delayed neutron constants have been computed for various exposure conditions in N Reactor[27]. Table 7.8.1 gives the various constants for several reactor conditions.

The delayed neutron fraction is .693 for green fuel. The fraction decreases with exposure (Pu^{239} has a smaller delayed neutron fraction than U^{235}) in the manner shown in Figure 7.8.1. The reactor period in seconds is plotted in Figure 7.8.2 as a function of δk for green and 2000 MWD/T fuel.

In the solution of the reactor kinetics equations for short term transients there are two prompt reactivity feedback effects. These are related to the uranium and coolant temperature coefficients. Xenon variation and graphite heating have too long a time constant to affect the short-time kinetics calclations.

The temperature equations can be written for single-phase flow.

$$\frac{dT_m}{dt} = K_1 Q - K_2 (T_m - T_w), \tag{7.8.3}$$

$$\frac{dT_o}{dt} = K_3 \left[2 T_m - (T_o + T_{in}) \right] - K_4 \left[T_o - T_{in} \right], \tag{7.8.4}$$

where

T_m = fuel temperature, °C,

T_o = outlet coolant temperature, °C,

T_{in} = inlet coolant temperature, °C,

Q = tube power, kw, and

T_w = average coolant temperature, °C.

The constants K_1, K_2, etc. include heat transfer coefficients, specific heats, flow rates, etc. The numerical values are given below for N Reactor.[28]

	Half-Flow (Startup)	Full-Flow (Equilibrium)
K_1	0.01731	0.01731
K_2	0.7898	0.7898
K_3	0.6985	0.6985
K_4	0.7353	1.4705

Instrumentation trips and shut down rod functions are also necessary in the kinetic calculations as are any reactivity effects associated with the accident - ramp rate, etc.

The prompt neutron lifetime in N Reactor is about half that in a conventional graphite moderated reactor. The value is $\sim 5.4 \times 10^{-4}$ seconds.[28]

7.9 Xenon Oscillations

The combination of a large core (in comparison to the neutron migration distance) and the relatively high power density in N Reactor results in a complication in the dynamic behavior of the reactor which is associated with the formation and destruction of xenon.

Xenon instability can persist only above a threshold flux which depends both on the size of the reactor and the flux distribution in the reactor. The over-all temperature coefficient also influences the oscillatory tendency; a negative over-all coefficient raises the threshold flux whereas a positive coefficient has the opposite effect - thus acting as an additional driving agent for the oscillation.

A comparison of parameters and characteristics which are important in the assessment of xenon instability is given in Table 7.9.1 for both N Reactor and the K Reactors. The information in the table is for a radial oscillation of the first mode which is the most prevalent mode in the Hanford reactors — i.e., has the lowest threshold.* The threshold fluxes are given for two degrees of radial flattening efficiency; the zero per cent flattening efficiency corresponds to the unflattened radial distribution whereas the 80 per cent flattening efficiency is representative of radial flattening efficiencies in the Hanford reactors.

The parameter "A" listed in the table is a measure of the severity of the disturbance. It is the ratio of the peak local power obtained in a free oscillation to the minimum local power. Amplitude ratios of the magnitudes indicated have never been obtained in any of the Hanford reactors chiefly because the cycling periods are long (on the order of 25-30 hours) thereby allowing adequate time to either damp out the oscillation by proper control action or to shut down the reactor if control action is not successful.

* Due to the increase length of N Reactor, the threshold for axial oscillation is also attainable assuming a zero, net temperature coefficient (See Table 7.9.1).

Table 7.8.1

NPR Delayed Neutron Constants

Exposure (MWD/T) - Cold

	0	500	1000	1500	2000
β_1	0.0210%	0.0196%	0.0185%	0.0176%	0.0169%
β_2	.1443	.1363	.1302	.1252	.1211
β_3	.1328	.1243	.1179	.1127	.1083
β_4	.2729	.2536	.2390	.2272	.2172
β_5	.0896	.0836	.0790	.0754	.0722
β_6	.0319	.0294	.0286	.0274	.0265
β_T	.6926	.6468	.6132	.5856	.5622
λ_1	0.0125	0.0125	0.0125	0.0125	0.0125
λ_2	.0306	.0306	.0306	.0306	.0306
λ_3	.1138	.1144	.1149	.1153	.1157
λ_4	.3081	.3086	.3096	.3104	.3111
λ_5	1.189	1.191	1.194	1.196	1.198
λ_6	3.180	3.178	3.174	3.171	3.168

Exposure (MWD/T) - Hot

	0	500	1000	1500	2000
β_1	Same as zero - exposure, cold	0.0193%	0.0180%	0.0170%	0.0162%
β_2		.1343	.1272	.1215	.1170
β_3		.1223	.1147	.1088	.1040
β_4		.2489	.2317	.2183	.2073
β_5		.0821	.0768	.0726	.0692
β_6		.0296	.0279	.0266	.0255
β_T		.6364	.5962	.5649	.5392
λ_1		0.0125	0.0125	0.0125	0.0125
λ_2		.0306	.0306	.0306	.0306
λ_3		.1146	.1152	.1157	.1162
λ_4		.3090	.3101	.3111	.3120
λ_5		1.192	1.195	1.198	1.200
λ_6		3.177	3.172	3.168	3.165

$$\beta_T = \sum_i \beta_i$$

The information in Table 7.9.1 can be summarized by asying that N Reactor should experience a considerably smaller tendency towards xenon-instability than do the K Reactors. Furthermore, the much more flexible control system in N Reactor will make oscillation-control much easier. N Reactor, by virtue of its net negative over-all temperature coefficient, will tend to self-damp oscillations if they start. The threshold fluxes given in the table are computed for a zero temperature coefficient. The net positive temperature coefficient in the K Reactors will therefore lower the threshold quoted in these reactors.

The chief factors then contributing to N Reactor's better stability against xenon oscillationsare as follows:

1) The ratio of equilibrium flux to threshold flux is low compared to the K Reactors.

2) The net temperature coefficient is slightly negative.

3) Greater control flexibility exists: 87 control rods in N Reactor compared to 20 in the K Reactor.

Table 7.9.1

Parameters Important to Radial Xenon Instability[a]
A Comparison Between N and K Reactors

Parameter	K	N
Average Thermal Flux at 4000 Mw[b]	3.3×10^{13}	2.8×10^{13}
Equilibrium Xenon	2.6 per cent $\Delta k/k$	3.0 per cent $\Delta k/k$
Threshold Flux (0 per cent flattening)	2.2×10^{13}	4.4×10^{13}
Threshold Flux (30 per cent flattening)	9.5×10^{12}	1.4×10^{13}
A (0 per cent flattening)	6	1
A (80 per cent flattening)	20	10
Migration Area, M^2	600 cm^2	650 cm^2
Reactor Length H	946 cm	1160 cm

a For typical operating flattening efficiencies, the axial oscillations are also attainable in N-Reactor. For example, for a 20 per cent axial flattening efficiency, the threshold flux for axial oscillations is 2.1×10^{13} n/cm^2-sec and the value of A is 5.

b Conventional flux in fuel, averaged over the reactor.

The only factor acting to increase the cycling tendency is the greater length of N Reactor as compared to the K Reactors.

7.10 System Stability

The dynamic performance of the N-Reactor system has been analyzed in considerable detail.[29, 30, 31]

The most significant aspect of the reactor is that it is relatively fast compared to the total loop. The time constants of the fuel element and coolant transport time through the reactor are on the order of one and one-half seconds, whereas the total coolant transport time is 60 seconds and the effective time constant of the heat exchanger is 20 seconds. Furthermore, there is a very tight loop in the reactor kinetics in the form of the two prompt, negative, temperature-coefficient feedbacks from the coolant water and fuel. These two coefficients produce a power coefficient of reactivity of -2.6×10^{-6} per Mw.

The relatively slow driving functions which can be applied to the reactor through primary coolant temperature changes are followed almost exactly by the reactor. In responding to changes in reactor coolant inlet temperature, the combination of the fuel and coolant temperature coefficients of reactivity is such that changes in inlet temperature are attenuated to approximately one-third their value, and appear at the reactor outlet with the opposite sign.

The significant feature of the heat exchanger is that, at rated power operation, any changes in inlet temperature are attenuated by approximately a factor of four when they appear at the primary coolant outlet of the heat exchanger. The transport time through the primary side of the heat exchanger is three seconds. Therefore, with a heat exchanger time constant of 20 seconds, it is found that changes in the inlet temperature to the heat exchanger appear much more rapidly at the outlet than do changes in secondary steam flow. In the control of the heat exchanger, it is found that the time constant of the steam flow valve will be an important parameter in the control loop.

The analysis also showed that there can be changes in reactor power level (due to various system disturbances) some of which will be of a transient nature and others which will maintain a steady state deviation from the nominal value. The analysis indicated that operator action to bring the power level back to its original level will be relatively unimportant in the over-all performance of the primary loop. The main feature of operation noted is that if there is a power disturbance, the action of the operator would tend to bring the power back to the nominal value immediately, whereas, in the case of no operator action, there will be a delay for the temperature effects to get around the loop and bring the power level back to the operating value. From the limited amount of work done to date on the effect of operator action on over-all loop performance, it appears that there are no detrimental effects of normal operator action on the over-all loop performance.

8. Criticality

The enrichment level of N-Reactor fuel elements is high enough so that a critical condition can be obtained with light water as a moderator. Since irradiated fuel elements are stored under water, and since flooding of other storage areas can never be absolutely ruled out as an incredible event, care in the storage configurations and amounts must be exercised to prevent inadvertant attainments of critical masses.

8.1 Criteria for Safe Storage

Procedures and safeguards which have proven successful in preventing the attainment of critical masses with enriched fuel in the older Hanford reactors have been based on the following criteria.

1) The handling, shipping and storage of unirradiated, enriched uranium shall be such that both an error or accident in the physical arrangement or mass of fuel and water inundation is required to achieve a critical mass.

2) The handling, shipping and storage of irradiated fuel (where handling, shipping and storage under water is required for cooling and radiation protection) shall be such that a critical arrangement is prohibited by physical means in every situation possible and by procedures in only those situations not subject to prevention by physical means.

3) In cases where control over configuration or shape is not possible, the allowed mass or volume of enriched uranium will be 2/3 of the value for the uranium-to-water volume ratio which yields the minimum critical mass or volume and will be calculated for the optimum shape (sphere).

4) In cases where control over configuration or shape is possible, the same criterion as 3 will apply except the allowed mass or volume will be calculated for the actual shape or configuration.

8.2 Basic Data

Material bucklings have been measured in an exponential assembly for prototypical N-Reactor fuel elements enriched to 1.0C % U^{235} [32]. Water lattices of both the complete tube-in-tube assembly and outer tube alone were measured. The measured bucklings were correlated to the one-group critical equation and critical masses and geometries were calculated for enrichments up to 1.10% U^{235}. The results are given in Tables 8.2.1 and 8.2.2.

Table 8.2.1

Maximum Bucklings - N-Reactor Fuel in Light Water

Uranium Enrichment % U^{235}	Maximum B^2, 10^{-6} cm^{-2}		
	Inner Tube	Outer Tube	Tube-in-Tube
0.95	2090	2280	1825
1.00	2680	2900	2480
1.05	3250	3500	3060
1.10	3790	4100	3660

Table 8.2.2

Minimum Critical Masses - N-Reactor Fuel in Light Water

Uranium Enrichment % U^{235}	Minimum Critical Mass, K_g U		
	Inner Tube	Outer Tube	Tube-in-Tube
0.95	5820	4300	7620
1.00	3820	2800	4500
1.05	2700	2000	3100
1.10	2040	1500	2270

These data have been translated into the critical mass, volume and fuel densities shown in Table 8.2.3 for both the unirradiated enrichment level of 0.947 w/o U^{235} and an effective discharge enrichment level of 1.0 w/o U^{235}.

Table 8.2.3

Criticality Data - NPR Fuel Elements in Light Water

UNIRRADIATED FUEL - 0.95% U^{235}

(All buckling values are $\pm$ 3 x 10^{-4} cm^{-2})

	Tube-in-Tube	Outer Tube Only	Inner Tube Only
Maximum Material Buckling	0.001825 cm^{-2}	0.002280 cm^{-2}	0.002090 cm^{-2}
Minimum Critical* Mass	7620 Kg U (380 elements)	4300 Kg U (310 tubes)	5820 Kg U (870 tubes)
Minimum Critical* Volume	1180 liters	825 liters	945 liters
Minimum Critical ∞-Cylinder Diameter	38.0 inches	33.5 inches	35.5 inches
Minimum Critical** Mass Per Unit Area	740 lbs U/ft^2 (17 elements/ft^2)	520 lbs U/ft^2 (17 tubes/ft^2)	656 lbs U/ft^2 (44 tubes/ft^2)
Minimum Critical ∞-Slab Thickness	22.6 inches	19.9 inches	20.8 inches

* Spherical geometry.

** ∞-Slab geometry.

IRRADIATED FUEL - 1.0% U^{235}

	Tube-in-Tube	Outer Tube Only	Inner Tube Only
Maximum Material Buckling	.002480 cm^{-2}	.002900 cm^{-2}	.002680 cm^{-2}
Minimum Critical* Mass	4500 Kg U (225 elements)	2800 Kg U (211 tubes)	3820 Kg U (570 tubes)
Minimum Critical* Volume	705 liters	546 liters	620 liters
Minimum Critical oo - Cylinder Diameter	31.7 inches	28.1 inches	30.4 inches
Minimum Critical** Mass Per Unit Area	610 lbs U/ft^2 (14 elements/ft^2)	430 lbs U/ft^2 (14 elements/ft^2)	545 lbs U/ft^2 (36 elements/ft^2)
Minimum Critical oo - Slab Thickness	18.5 inches	16.9 inches	17.8 inches

* Spherical geometry.
** oo Slab geometry.

8.3 Procedures and Safeguards

The procedures and safeguards for the handling, shipping, and storage of N-Reactor fuel elements can be drived from the criteria and basic data. Detailed procedures will be given in the N-Reactor Process Standards. Assessment of the safety of procedures and storage arrangements are discussed in detail in the NPR Hazards Review.[33]

9. Heat Generation

Of importance are the various sources of nuclear heat generation in the reactor and as well the geometrical distribution of such sources. The heat generation during equilibrium reactor operation and after shutdown are both of interest and must be considered.

9.1 Equilibrium Heat Generation (Total)

The total heat generation has been calculated for the 21.6 lb/ft startup element.[34]

9.1.1 Energy Sources

The nuclear sources of energy can be divided into primary and secondary sources. The primary sources are those directly associated with the fissioning event and these are listed in Table 9.1.1 (From Reference 35). The data refer to U^{235}.

Table 9.1.1

Primary Energy Sources From Fission

Source	Energy Release Per Fission
Fission Fragments	$E_k = 168 \pm 2$ Mev
Prompt Neutrons	$E_n = 4.87 \pm 0.6$ Mev
Prompt Gamma Rays	$E\gamma = 7.2 \pm 0.8$ Mev
Delayed Neutrons	$E_n = (FP) = 0.0068 \pm 0.0003$ Mev
Isomeric Gamma Rays	$E\gamma\ (I) = 0.24$ Mev
Fission Product Gammas	$E\gamma(FP) = 5.7 \pm 0.8$ Mev
Fission Product Betas	$E\beta\ (FP) = 8.0 \pm 0.7$ Mev
Fission Product Anti-Neutrinos	$E\nu\ (FP) = 10.5 \pm 0.8$ Mev

The isomeric gamma rays occur 5×10^{-8} to 10^{-6} seconds after fission. All but the anti-neutrinos provide sensible heat. The total energy emission per fission is seen to be 204.5 ± 2.5 Mev, with 194.0 Mev of it appearing as sensible heat in the reactor. The secondary energy sources in the reactor are those associated with various neutron interactions. These energy sources are given in Table 9.1.2. The specific energies depend on the reactor.

The total, primary plus secondary, sensible heat generated per fission is detailed in Tables 9.1.3 and 9.1.4 for the 21.6 lb/ft tube-in-tube element for two different reactor conditions. The first illustration represents the equilibrium energy generation after the reactor had been in operation at full power for one day. The second illustration represents the equilibrium energy generation after an exposure of 1000 MWD/T had been attained. Differences arise principally from the change in the proportion of fissions in the various fissionable isotopes and from the time dependences of decaying fission products (including Np^{239}).

9.2 Equilibrium Heat Generation (Fractional)

The calculations have been made for the 21.6 lb/ft startup fuel element[34].

9.2.1 Heat Generation in Fuel

The major fraction of the energy of fission appears as heat in the fuel element. The total kinetic energy of the fission fragments, fission and decay beta particles is absorbed in the uranium due to the short ranges of these particles (only a very small surface fraction would escape the fuel). Also, a large fraction of the neutron kinetic energy is absorbed through inelastic scattering, fast capture and fast fission in the fuel. Of the various gamma radiations, an appreciable fraction will also be absorbed in the fuel due to the high Z of the uranium.

Table 9.1.2

Secondary Energy Sources From Fission

Source	Net Energy Per Event[a]
Radiative Neutron Capture	
U^{235}	6.41 Mev γ
U^{238}	4.63 Mev γ
Pu^{239}	6.39 Mev γ
Pu^{240}	5.65 Mev γ
Pu^{241}	6.11 Mev γ
Graphite	5.0 Mev γ
Water	2.24 Mev γ
Zirconium	8.0 Mev γ
O^{16} (n,p) N^{16}	1 Mev γ
Capture Product Decay	
U^{239}	0.074 Mev γ, 0.45 Mev β
Np^{239}	0.284 Mev γ, 0.15 Mev β
Zirconium	0.065 Mev γ, 0.02 Mev β
Fast Fission in U^{238}	194.0 Mev Sensible

a Beta particle energies are estimated from the end point energies and assuming an allowed spectrum.

Table 9.1.3

Total Energy Release 21.6 lb/ft Element
(Reactor Operating One Day at Full Power)

Event	Events/Fission	Net Energy Release/Event (Mev)				Energy/Fission (Mev)
		FP	n	β	γ	
n-cap. in graph.	0.0334				4.95	0.165
n-cap. in PT	0.0450				7.95	0.358
n-cap in H_2O	0.0855				2.24	0.192
n-cap in Clad.	0.0077				7.95	0.061
Outer Fuel Tube						
U^{235} fission	0.6709	168	4.87	7.23	13.49	129.880
U^{238} fission	0.0420	168	3.2	7.23	13.49	8.061
U^{235} capture	0.1409				6.41	0.903
U^{238} capture	0.6829				4.63	3.162
U^{239} decay	0.6829			0.45	0.074	0.359
Np^{239} decay	0.1755			0.15	0.284	0.084
Inner Fuel Tube						
U^{235} fission	0.2660	168	4.87	7.23	13.49	51.495
U^{238} fission	0.0211	168	3.2	7.23	13.49	4.050
U^{238} capture	0.0567				6.41	0.363
U^{238} capture	0.2510				4.63	1.163
U^{239} decay	0.2510			0.45	0.074	0.132
Np^{239} decay	0.0645			0.15	0.284	0.031
Total Mev/Fission						200.5 Mev

Table 9.1.4

Total Energy Release 21.6 lb/ft Element
(Reactor Operating to Exposure of 1000 MWD/T)

Event	Events/Fission	Net Energy Release/Event (MW)				Energy/Fission (MW)
		FP	n	β	γ	
n-cap. in graph.	0.0319				4.95	0.158
n-cap. in PT	0.0426				7.95	0.339
n-cap. in H_2O	0.0791				2.24	0.177
n-cap. in clad	0.0072				7.95	0.057
Outer Fuel Tube						
U^{235} fission	0.5442	168	4.87	7.55	13.9	105.770
U^{238} fission	0.0424	168	3.2	7.55	13.9	8.168
Pu^{239} fission	0.1321	168	5.8	7.55	13.9	25.793
Pu^{241} fission	0.0017	168	5.8	7.55	13.9	0.332
U^{235} capture	0.1153				6.41	0.739
U^{238} capture	0.6542				4.63	3.029
Pu^{239} capture	0.0736				6.39	0.470
Pu^{240} capture	0.0146				5.65	0.082
Pu^{241} capture	0.0007				6.11	0.004
U^{239} decay	0.6542			0.45	0.074	0.343
Np^{239} decay	0.6542			0.15	0.284	0.314
Inner Fuel Tube						
U^{235} fission	0.2200	168	4.87	7.55	13.9	42.759
U^{238} fission	0.0206	168	3.2	7.55	13.9	3.969
Pu^{239} fission	0.0390	168	5.8	7.55	13.9	7.614
Pu^{241} fission	negl.	168	5.8	7.55	13.9	negl.
U^{235} capture	0.0474				6.41	0.304
U^{238} capture	0.2393				4.63	1.109
Pu^{239} capture	0.0215				6.39	0.137
Pu^{240} capture	0.0040				5.65	0.023
Pu^{241} capture	negl.				6.11	negl.
U^{239} decay	0.2393			0.45	0.074	0.125
Np^{239} decay	0.2393			0.15	0.284	0.115
Total Mev/Fission						201.9 Mev

9.2.2 Heat Generation in Process Tube

The zirconium process tubes are sufficiently thick in the N Reactor to stop an appreciable fraction of gamma radiation from sources both inside the tube and outside the tube (n, γ capture in the graphite). Energy losses due to neutron interactions in the process tubes are negligible.

9.2.3 Heat Generation in Graphite Moderator

The graphite moderator receives energy from gammas escaping the fuel process tube and coolant, by fast neutron moderation and from neutron capture gamma rays from the carbon. Neutron scattering in the coolant water must be considered in determining the neutron kinetic energy remaining for energy transfer to the graphite. Neutrons which do interact with the water can be assumed to do so only once while their kinetic energy is still significant to be considered as an important energy source.

9.2.4 Summary of Heat Generation Fractions

The total heat generation fractions for the 21.6 lb/ft startup fuel geometry are given in Table 9.2.4.1.

Table 9.2.4.1

Summary of Heat Generation Fractions
(Equilibrium - 21.6 lb/ft Element)

Exposure	Inner Fuel & Clad	Outer Fuel & Clad	H_2O	P.T.	Graphite
0 (1 Day)	27.63%	67.41%	0.21%	0.44%	4.31%
1000 MWD/T	27.06%	67.87%	0.22%	0.46%	4.37%

9.3 Shutdown Heat Generation

The generation of heat after reactor shutdown must be known for many reasons. Sufficient heat is generated for a considerable time after fissioning ceases (due to the decay of radioactive fission products) so that cooling of the reactor must be maintained for sometime. The shape of the power decay curve during the actual shutdown process and immediately afterward is also important in the N Reactor since the heat removal system must be programmed to respond properly. However, the shape of the heat decay curve during shut down is dependent on the rate control poison is added, the conditions imposed on flow and/or outlet temperature, etc. Delayed neutron fissioning also affects the shutdown transient and will vary somewhat according to the proportion of fissionable isotopes present.

The fractional heat generations will differ considerably after fissioning ceases. The greater proportion of penetrating energy carriers (gamma rays) after cessation of fissioning will mean that a greater fraction of heat will "appear" in the graphite than did during equilibrium reactor operation. Also, the time-dependent energy variation of the fission-product gamma rays, will vary the fuel-to-graphite heat generation fraction with time.

9.3.1 Shutdown Heat Generation Transient

Early analysis of the shut down heat transient in N Reactor were made for several simplifying assumptions [36]. These calculations should be brought up to date at an early date. For the present they will be reported.

9.3.1.1 Assumptions and Model

1. Constant reactor inlet temperature.
2. N-Reactor fuel element simulated by solid rod element.
3. Constant over-all heat transfer coefficient for fuel element.
4. One-second time constant between scram signal and 75% rod insertion.

The heat transfer and neutron kinetics equations were standard. (See Section 7.8). Delayed neutron constants were characteristic of fuel exposed to 1000 MWD/T. Safety rod strengths of 20, 40 and 60 x 10^{-3} $\Delta k/k$ were considered. Results for two cases are given in Figure 9.3.1.1 and 9.3.1.2. In the first set of curves a constant tube outlet temperature was assumed and in the second set constant flow was assumed. The power for constant outlet temperature is seen to decay faster than for constant flow due to the absence of the positive reactivity effect from cooling down the coolant in the constant-outlet-temperature case.

9.3.2 Heat Generaton After Shutdown (Total)

The principle sources of energy in irradiated fuel for times greater than 100 seconds after a reactor shutdown are beta and gamma decay of fission products and beta and gamma decay of U^{239} and Np^{239}. Recent compilations of gamma and beta decay rates from 123 isotopes from thermal fission of U^{235} have been reported by Perkins and King [21] for reactor operation times from one to 1000 hours and as a function of time after shutdown from 100 to 10^8 seconds. Knabe and Putnam [37] combined the experimental results of Maienschain, etal [38] and the computed Perkins-King data to determine an accurate time dependence of the fission product decay gamma activity for times between one and 10^8 seconds after reactor shutdown. Beta decay energy release rates for the same times were also determined by Knabe and Putnam from the Perkins-King compilation and other sources of data. Smith [39] has programmed the equations of Knabe and Putnam and curves for Smith's report are given in Figure 9.3.2.1.

The contributions from U^{239} and Np^{239} must be treated separately. The energy emissions per disintegration of U^{239} and Np^{239} are as follows: [40]

$$E_{29}(\beta) = 0.45 \text{ Mev/dis},$$

$$E_{29}(\gamma) = 0.074 \text{ Mev/dis},$$

$$E_{39}(\beta) = 0.15 \text{ Mev/dis},$$

$$E_{39}(\gamma) = 0.284 \text{ Mev/dis}.$$

The energy ($\beta + \gamma$) decay rates of U^{239} and Np^{239} (for T > 1000 hours, where T is time of reactor operation) are

$$E_{29}(t) = 1.51 \times 10^{10}\ e^{-\lambda_{29} t}\ \text{Mev/watt-sec},$$
$$E_{39}(t) = 1.25 \times 10^{10}\ e^{-\lambda_{39} t}\ \text{Mev/watt-sec}, \qquad (9.3.2.1)$$

where λ_{29} and λ_{39} are the decay constants for U^{239} and Np^{239}, respectively.

The beta and gamma heat generation rates after shutdown are plotted in Figure 9.3.2.2 and 9.3.2.3 [34] for 1000 hour NPR operation. The total heat generation rates are shown in Figures 9.3.2.4 and 9.3.2.5 for 1000 hour NPR operation. The scram strength assumed in Figure 9.3.2.4 is 40 cmk.

9.3.3 Heat Generation After Shutdown (Fractional)

The fractional heat generation in the NPR has been calculated for several times after shutdown[34]. The results are presented in Table 9.3.3.1.

Table 9.3.3.1

Fractional Heat Generation After Shutdown

Time After Shutdown (Seconds)	Per Cent Heat Generation		
	Outer Fuel[a]	Inner Fuel[a]	Graphite[b]
10^2	61.0%	26.1%	8.9%
10^3	61.7%	26.2%	7.8%
10^4	62.4%	26.4%	6.6%
10^5	63.5%	26.7%	5.5%
10^6	61.0%	26.0%	9.5%
10^7	61.4%	26.4%	6.7%

a Does not include cladding.
b Remaining heat would be roughly distributed in the ratio 1:2:4 for water, clad and process tube respectively.

The significant peak in the fraction of heat generated in the graphite at 10^6 seconds after reactor shut down is due to an increase in the average energy of the fission product decay gammas at these times. However, at 10^6 seconds after shut down the total heat generation rate is only one per cent of the equilibrium reactor power, so the peaking in the graphite fraction at 10^6 seconds is of no concern.

FIGURE 9.3.2.2

BETA AND GAMMA ENERGY RELEASE RATES
AFTER SATURATION (10 = 10^{11} SEC)
(1000 HRS OPERATING TIME)
(NORMALIZED TO POWER LEVEL OF 1 WATT)

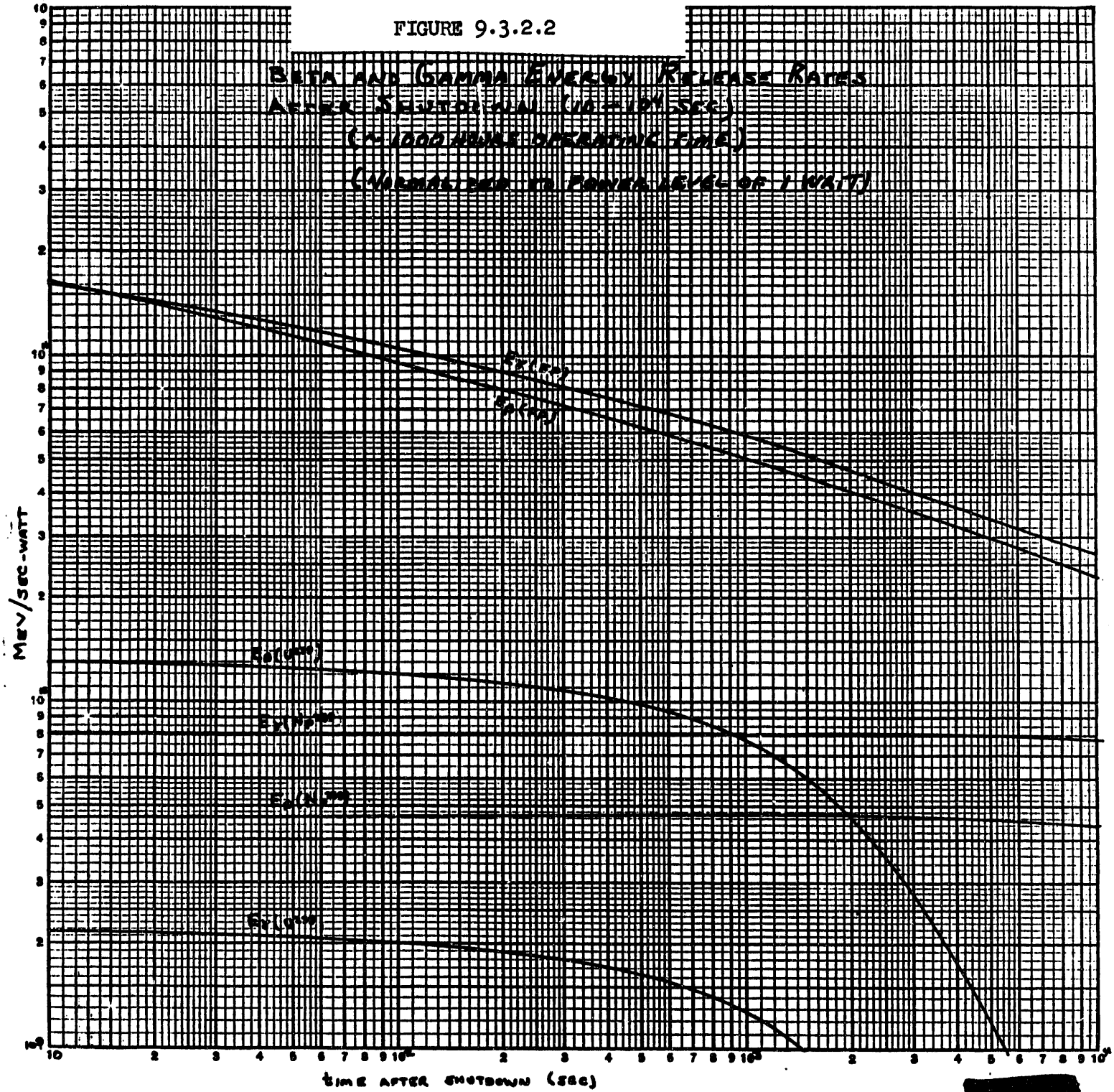

FIGURE 9.3.2.3

BETA AND GAMMA ENERGY RELEASE RATES
AFTER SHUTDOWN (10^4 - 10^7 SEC)
(~ 1000 HOURS OPERATING TIME)
(NORMALIZED TO POWER LEVEL OF 1 WATT)

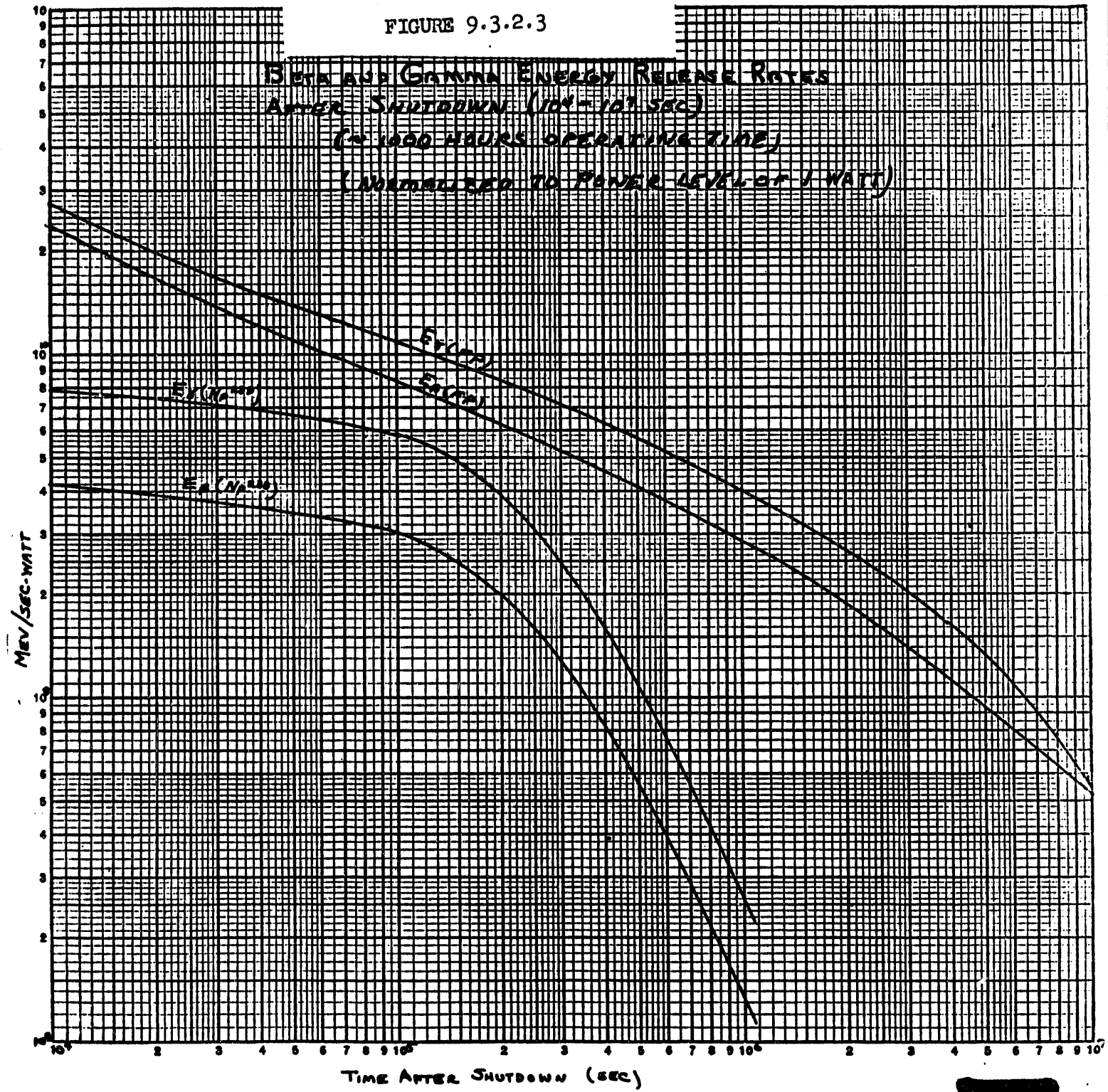

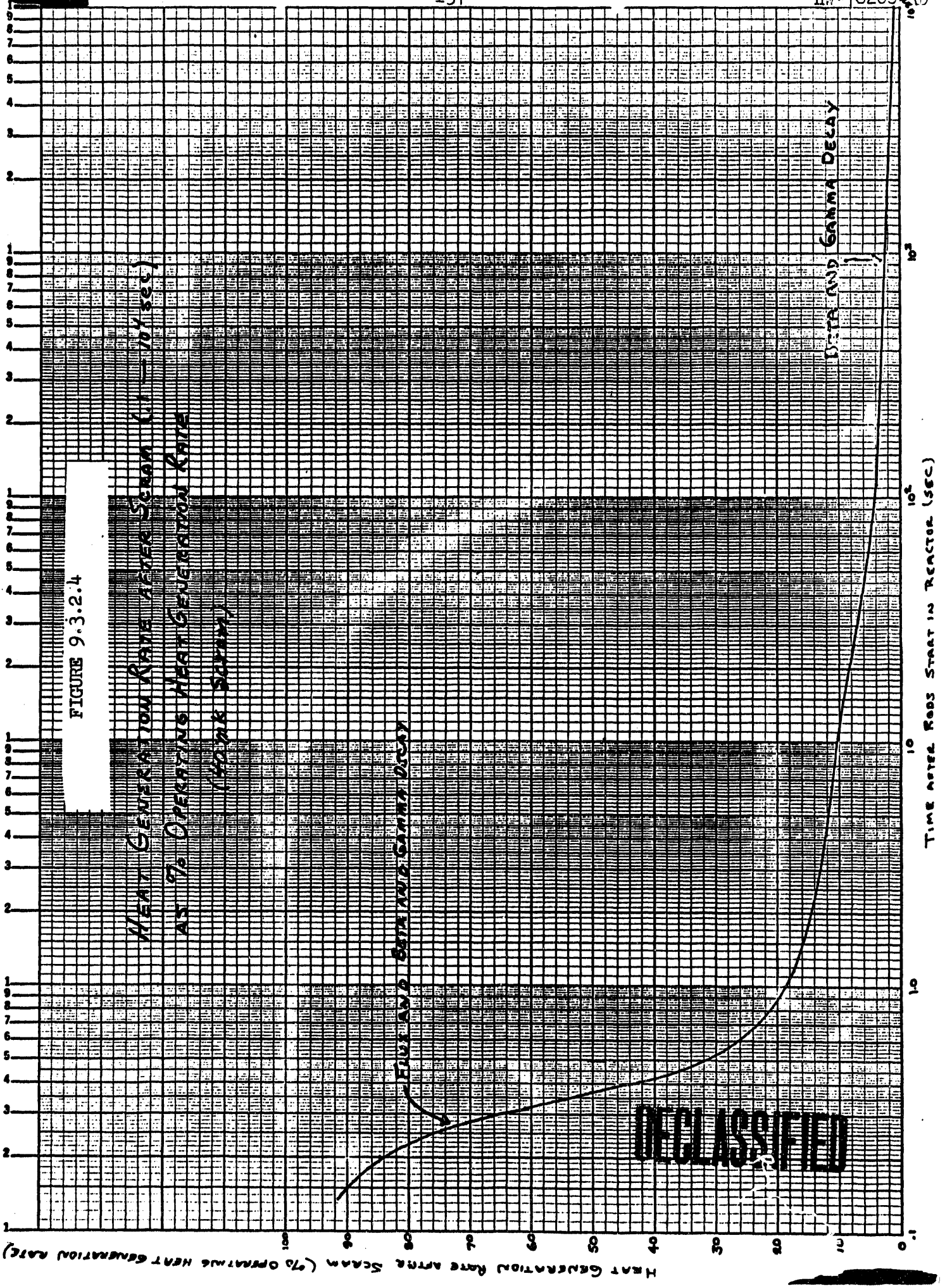

FIGURE 9.3.2.4

HEAT GENERATION RATE AFTER SCRAM (1 — 10⁷ sec)
AS % OPERATING HEAT GENERATION RATE
(HANFORD)

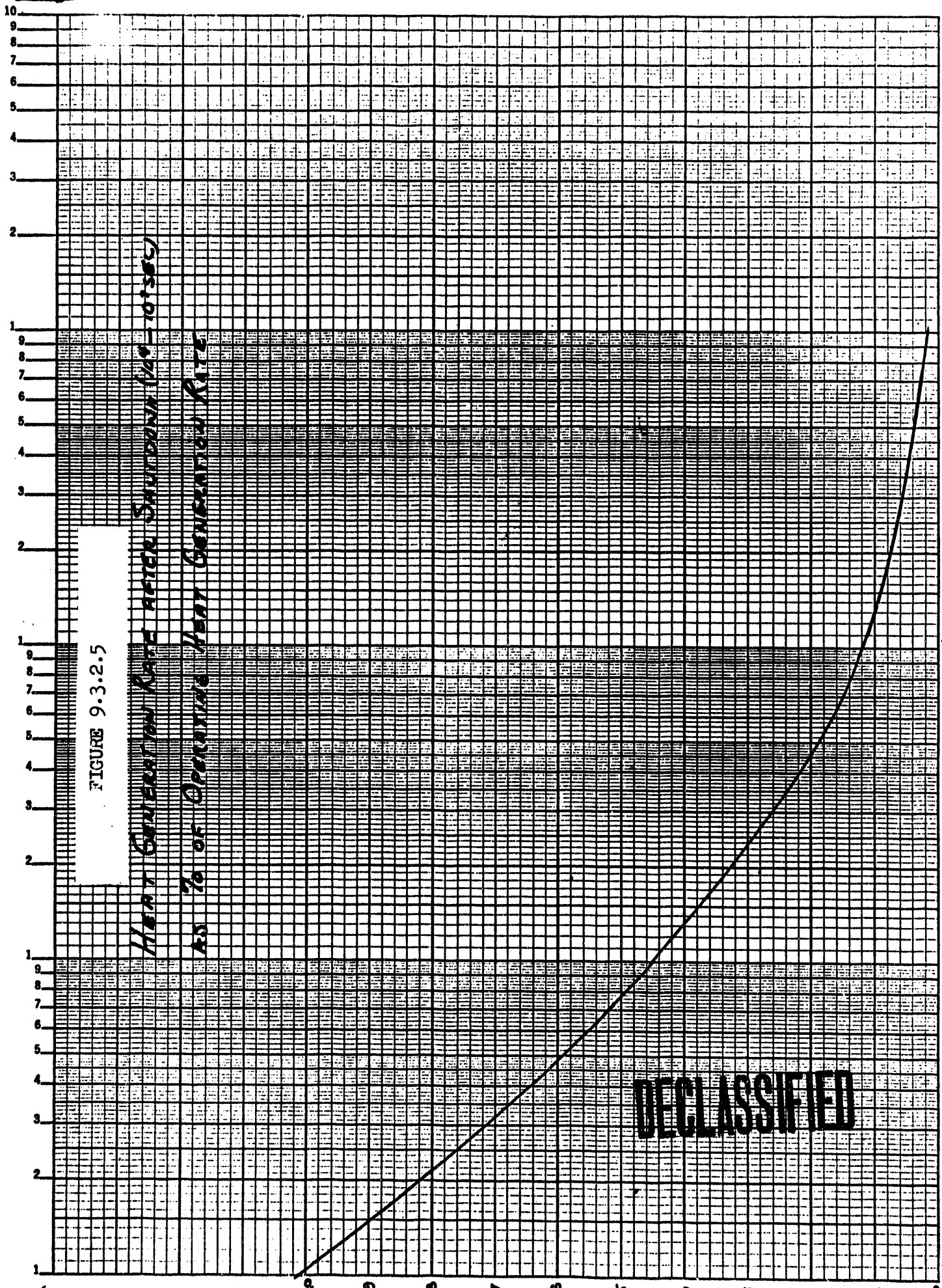
Heat Generation Rate After Shutdown (Btu - 10³ sec)
As % of Operating Heat Generation Rate
Time After Shutdown (sec)
Heat Generation Rate Area Shutdown (% Operating Heat Generation Rate)
DECLASSIFIED

FIGURE 9.3.2.5

REFERENCES

1. Westcott, C. H. Effective Cross Section Values for Well-Moderated Thermal Spectra, CRRP-960 ED3 Rev. November 1, 1960.

2. Cranberg, L., G. Frye, N. Nereson, and L. Rosen, "Fission Neutron Spectrum of U^{235}", Phys. Rev. 103:662.1956.

3. Fleishman, M. R. and H. Soodak. "Methods and Cross Sections for Calculating the Fast Effect," Transactions of ANS 1, No. 2: 153: 1958. Nuclear Sci. and Eng. 7:217.1960.

4. Hellstrand, E. and G. Lundgren. "The Resonance Integral for Uranium Metal and Oxide," Nuclear Sci., and Eng. 12: 435. 1962.

5. Joanou, G. D. Notes on Lattice Parameter Calculations, HW-60422 REV. October 6, 1960.

6. FLEX is an Engineering physics survey code written by R. J. Shields. MOFDA is an engineering physics survey code written by R. O. Gumprecht.

7. Conveyou, R. R., R. R. Bate and K. K. Osburn. "Effect of Moderator Temperature Upon Neutron Flux in Infinite Capturing Medium," J. Nuclear Energy 2: 153. 1956.

8. Westcott, C. H., W. A. Walker and T. K. Alexander. "Effective Cross Sections and Cadmium Ratios for the Neutron Spectra of Thermal Reactors," Proc. 2nd Intern. Conf. Peaceful Uses Atomic Energy, Geneva 16: 70. 1958.

9. Sher, R. and J. Felberbaum. Least Squares Analysis of the 2200 m/sec Parameters of U^{233}, U^{235}, and Pu^{239}, BNL-722. June, 1962.

10. Spinrad, B. I., "Fast Effect in Lattice Reactors," Nucl. Sci. and Eng. 1: 455. 1956. (See also Reference 3).

11. Pershagen, B., G. Anderson, and I. Carlvik, "Calculation of Lattice Parameters for Uranium Rod Clusters in Heavy Water and Correlations With Experiments," Proc. 2nd Intern. Conf. Peaceful Uses Atomic Energy, Geneva 12: 341. 1958.

12. Wood, D. E. and D. L. Johnson. Lattice Parameter Measurements for N Reactor, HW-72096. To be issued. (Secret).

13. Simpson, D. E. NPR Three-Group Flux Distribution, HW-64501. March 31, 1960. (Confidential).

14. Behrens, D. J. The Migration Length of Neutrons in a Reactor, AERE TR-877. 1956.

15. Elyckert, W. A. Increase of the Diffusion Length of Neutrons in N Reactor Due to Voids, HW-76125, January 7, 1963. (Unclassified).

[redacted]

16. Wilkinson, C. D. NPR Moderator Stack Purity Test - Description, Analysis and Results, HW-72654 PT3. June 8, 1962. (Secret).

17. Nechodom, W. S. NPR Reactivity Parameters As a Function of Fuel Element Weight. HW-64693-RD. January 19, 1960. (SECRET ROUGH DRAFT)

18. Bowers, C. E., Private Communication.

19. Cohen, E. R. and R. H. Sehnert. Long Term Irradiation of Nuclear Fuels, NAA-SR-1012. September 15, 1954. (Secret).

20. Nilson, R. The Effective (n,2n) Cross Section for U^{238}, HW-58817. January 9, 1959 (Secret).

21. Perkins, J. F. and R. W. King. "Energy Release from the Decay of Fission Products, Nuclear Sci. and Eng. 3: 726. 1958.

22. Johnson, D. L. ACTICAY Fission Product Decay Program, HW-71984. December 10, 1961.

23. Richey, C. R. Technical Description of the New SS Accountability Program on the IBM-709, HW-63159. January 7, 1960. (Secret).

24. Smith, R. I. The variation of k_∞ With Fuel Temperature for the NPR, HW-69343. April 21, 1961. (Confidential).

25. Allen, C. W. N-Reactor Hazards Review of Cold Water, Flooding and Startup Accidents, HW-64755. April 25, 1960. (Secret).

26. Bailey, G. F. Review of NPR Control System Capacities, HW-74470. To be issued. (Secret).

27. Allen, C. W. NPR Delayed Neutron Fractions and Decay Constants, HW-69751. May, 1961. (Secret).

28. Tiller, R. E., private communication.

29. Leiby, D. W., Development and Performance of NPR Reactor Analog Model, HW-66665. August 5, 1960. (Confidential).

30. Leiby, D. W., NPR Heat Exchanger and Load Control Analysis, HW-65544. May 10, 1960. (Confidential).

31. Leiby, D. W. NPR Primary Loop Performance Study, HW-68168. October 25, 1960. (Confidential).

32. Lloyd, R. C. and C. L. Brown. Exponential Measurements and Critical Parameter Calculations - NPR Fuel Elements in Light Water, HW-69399, July, 1961. (Confidential).

[redacted]

33. Miller, N. R. and R. E. Trumble. NPR Hazards Review (Phase I - Production Only), HW-71408 VOL1 REV. December 15, 1961. (Secret).

34. Meichle, R. H. NPR Heat Generation Rates - Startup Fuel Geometry, HW-76343. To be issued. (Secret).

35. Nilson, P. NPR Heat Generation Rates During Operation, HW-59075 REV. To be re-issued. (Secret).

36. Norwood, K., J. C. Peden and R. E. Tiller. N-Reactor Post-Scram Transients and Heat Exchange Thermal Shock Considerations, HW-64476. April 25, 1960. (Secret).

37. Knabe, W. E. and G. E. Putnam. The Activity of the Fission Products of U^{235}, AFEX-448. October 31, 1958.

38. Maienschein, F. C., R. W. Peelle, W. Zobel, and T. A. Love, "Gamma Rays Associated With Fission," Proc. 2nd Intern. Conf. Peaceful Uses of Atomic Energy, Geneva, 15: 366. 1956.

39. Smith, M. R. The Activity of the Fission Products of U^{235} (Program 408), XDC-60-1-57. December 10, 1959.

40. Nilson, R. and R. H. Meichle. Fractional Heat Generation Rates in Hanford Reactors After Shutdown, HW-69628, May 17, 1961. (Confidential).

DATE

FILMED

8/2/94

END